TA03

ENTEREL

Los Alamos
NATIONAL LABORATORY
EST. 1943

Environmental Programs
P.O. Box 1663, MS M991
Los Alamos, New Mexico 87545
(505) 606-2337/FAX (505) 665-1812

RECEIVED
JUN 2009
NMED Hazardous Waste Bureau

National Nuclear Security Administration
Los Alamos Site Office, MS A316
Environmental Restoration Program
Los Alamos, New Mexico 87544
(505) 667-4255/FAX (505) 606-2132

Date: May 30, 2009
Refer To: EP2009-0254

James P. Bearzi, Bureau Chief
Hazardous Waste Bureau
New Mexico Environment Department
2905 Rodeo Park Drive East, Building 1
Santa Fe, NM 87505-6303

Subject: Submittal of the Completion Report for Regional Aquifer Well R-44

Dear Mr. Bearzi:

Enclosed please find two hard copies with electronic files of the Completion Report for Regional Aquifer Well R-44.

If you have any questions, please contact Mark Everett at (505) 667-5931 (meverett@lanl.gov) or Nancy Werdel at (505) 665-3619 (nwerdel@doeal.gov).

Sincerely,

Michael J. Graham, Associate Director
Environmental Programs
Los Alamos National Laboratory

Sincerely,

David R. Gregory, Project Director
Environmental Operations
Los Alamos Site Office

31661

MG/DG/PH/ME/SW:sm

Enclosures: Two hard copies with electronic files – Completion Report for Regional Aquifer Well R-44 (LA-UR-09-3066)

Cy: (w/enc.)
Neil Weber, San Ildefonso Pueblo
Nancy Werdel, DOE-LASO, MS A316
Mark Everett, EP-LWSP, MS M992
RPF, MS M707 (with two CDs)
Public Reading Room, MS M992

Cy: (Letter and CD only)
Laurie King, EPA Region 6, Dallas, TX
Steve Yanicak, NMED-OB, White Rock, NM
Steve White, EP-LWSP, MS T005
Kristine Smeltz, EP-WES, MS M992
EP-LWSP File, MS M992

Cy: (w/o enc.)
Tom Skibitski, NMED-OB, Santa Fe, NM
Keyana DeAguero, DOE-LASO (date-stamped letter emailed)
Michael J. Graham, ADEP, MS M991
Alison M. Dorries, EP-WES, MS M992
Paul Huber, EP-LWSP, MS M992
IRM-RMMSO, MS A150 (date-stamped letter emailed)

LA-UR-09-3066
May 2009
EP2009-0254

Completion Report for Regional Aquifer Well R-44

Los Alamos
NATIONAL LABORATORY
EST. 1943

Prepared by the Environmental Programs Directorate

Los Alamos National Laboratory, operated by Los Alamos National Security, LLC, for the U.S. Department of Energy under Contract No. DE-AC52-06NA25396, has prepared this document pursuant to the Compliance Order on Consent, signed March 1, 2005. The Compliance Order on Consent contains requirements for the investigation and cleanup, including corrective action, of contamination at Los Alamos National Laboratory. The U.S. government has rights to use, reproduce, and distribute this document. The public may copy and use this document without charge, provided that this notice and any statement of authorship are reproduced on all copies.

LA-UR-09-3066
EP2009-0254

Completion Report for Regional Aquifer Well R-44

May 2009

Responsible project leader:

Mark Everett	Mark Everett	Project Leader	Environmental Programs	5-26-09
Printed Name	Signature	Title	Organization	Date

Responsible LANS representative:

Michael Graham	M Langeng	Associate Director	Environmental Programs	5/27/09
Printed Name	Signature	Title	Organization	Date

Responsible DOE representative:

David R. Gregory	David R Gregory	Project Director	DOE-LASO	5/28/09
Printed Name	Signature	Title	Organization	Date

EXECUTIVE SUMMARY

This well completion report describes the drilling, installation, development, and aquifer testing of Los Alamos National Laboratory's regional aquifer well R-44, which is located in a tributary of Mortandad Canyon, Technical Area 05 (TA-05) in Los Alamos County, New Mexico. This report was written in accordance with the requirements in Section IV.A.3.e.iv of the March 1, 2005, Compliance Order on Consent. The well was installed at the direction of the New Mexico Environment Department (NMED) to monitor groundwater quality and contaminant movement and to define the southern limit of chromium contamination in the vicinity of well R-28 (which has consistently shown elevated concentrations of chromium in the regional aquifer at the Laboratory). The well will also be used to monitor water levels within the regional aquifer and measure pumping effects from nearby water supply wells.

The R-44 borehole was drilled using dual-rotary air-drilling methods. Fluid additives used included potable water and foam. Foam-assisted drilling was used only in the vadose zone and ceased approximately 100 ft above the regional aquifer; no drilling-fluid additives other than small amounts of potable water were used in the regional aquifer. Additive-free drilling provides minimal impacts to the groundwater and the formation. The R-44 borehole was successfully completed to total depth using dual-rotary casing-advance and open-hole drilling methods.

A retractable 16-in. casing was advanced through the Bandelier Tuff, Guaje Pumice Bed and basaltic volcaniclastic sediments to a depth of 345.8 ft bgs. A 15-in. open borehole was advanced with fluid-assisted air-rotary methods with a downhole hammer bit through the Cerros del Rio basalt and into the Puye Formation to a depth of 765 ft bgs. Then 12-in. casing was advanced with an 11-5/8-in. tricone bit through the remainder of the Puye Formation, through Miocene pumiceous sediments, and through Santa Fe Group Miocene riverine gravels to a total depth of 1094 ft bgs.

Well R-44 was completed as a dual-screen well to evaluate water quality and measure water levels at two discrete depth intervals within the regional aquifer. Well screens will be separated by a packer, as part of the permanent dedicated sampling system, to ensure isolation of each groundwater bearing zone. The upper 10-ft long screened interval has the top of the screen set at 895 ft bgs and the lower 10-ft long screened interval has the top of the screen set at 985.3 ft bgs. Both screen intervals are within the Puye Formation. The composite depth to water after well installation and well development was 879.1 ft bgs.

The well was completed in accordance with an NMED-approved well design and was developed and met target water-quality parameters. Hydrogeologic testing indicated that monitoring well R-44 is highly productive and will perform effectively to meet the planned objectives. Water-level transducers will be placed in the upper and lower well screens in the R-44 well, and groundwater sampling will be performed as part of the facility-wide groundwater-monitoring program.

CONTENTS

1.0 INTRODUCTION 1

2.0 PRELIMINARY ACTIVITIES 1
2.1 Administrative Preparation 2
2.2 Site Preparation 2

3.0 DRILLING ACTIVITIES 2
3.1 Drilling Approach 2
3.2 Chronology of Drilling Activities 3

4.0 SAMPLING ACTIVITIES 4
4.1 Cuttings Sampling 4
4.2 Water Sampling 4

5.0 GEOLOGY AND HYDROGEOLOGY 5
5.1 Stratigraphy 5
5.2 Groundwater 7

6.0 BOREHOLE LOGGING 7
6.1 Video Logging 7
6.2 Geophysical Logging 7

7.0 WELL INSTALLATION 8
7.1 Well Design 8
7.2 Well Construction 8

8.0 POSTINSTALLATION ACTIVITIES 9
8.1 Well Development 9
8.1.1 Well Development Field Parameters 9
8.2 Aquifer Testing 10
8.2.1 Aquifer Testing Field Parameters 10
8.3 Dedicated Sampling System Installation 10
8.4 Wellhead Completion 11
8.5 Geodetic Survey 11
8.6 Waste Management and Site Restoration 11

9.0 DEVIATIONS FROM PLANNED ACTIVITIES 12

10.0 ACKNOWLEDGMENTS 12

11.0 REFERENCES 12

Figures

Figure 1.0-1 Regional aquifer well R-44 with respect to surrounding regional wells and PM-5 15
Figure 5.1-1 R-44 borehole stratigraphy 17
Figure 7.2-1 R-44 as-built well construction diagram 17
Figure 8.3-1a As-built schematic for regional well R-44 18
Figure 8.3-1b As-built technical notes for R-44 19

Tables

Table 3.1-1 Fluid Quantities Used during Drilling and Well Construction 21
Table 4.2-1 Summary of Groundwater-Screening Samples Collected during Drilling, Well Development, and Aquifer Testing of Well R-44 22
Table 6.0-1 R-44 Video and Geophysical Logging Runs 23
Table 7.2-1 R-44 Annular Fill Materials 23
Table 8.5-1 R-44 Survey Coordinates 24
Table 8.6-1 Summary of Waste Samples Collected during Drilling and Development of R-44 24

Appendixes

Appendix A Well R-44 Lithologic Log
Appendix B Groundwater Analytical Results
Appendix C Aquifer Testing Report
Appendix D Borehole Video Logging (on DVD included with this document)
Appendix E Schlumberger Geophysical Logging Report (on CD included with this document)

Acronyms and Abbreviations

µS/cm	microsiemens per centimeter
amsl	above mean sea level
BETCO	barometric and Earth tide correction
bgs	below ground surface
CNL	Compensated Neutron Log
Consent Order	Compliance Order on Consent
cu	capture unit
DO	dissolved oxygen
ECS	Elemental Capture Sonde
EES-14	Earth and Environmental Sciences Group
ENV-MAQ	Environmental Division–Meteorology and Air Quality Group

EP	Environmental Programs
gAPI	American Petroleum Institute gamma ray
GR	gamma ray
HNGS	Hostile Natural Gamma Spectroscopy
IC	ion chromatography
ICPMS	inductively coupled (argon) plasma mass spectrometry
ICPOES	inductively coupled (argon) plasma mass spectrometry
ID	identification
I.D.	inside diameter
ICPMS	inductively coupled (argon) plasma mass spectrometry
ICPOES	inductively coupled (argon) plasma optical emission spectroscopy
LANL	Los Alamos National Laboratory
lbf	pound force
MDA	material disposal area
mV	millivolt
NMED	New Mexico Environment Department
NTU	nephelometric turbidity unit
O.D.	outside diameter
ORP	oxidation-reduction potential
PVC	polyvinyl chloride
RPF	Records Processing Facility
SOP	standard operating procedure
SVOC	semivolatile organic compound
TA	technical area
TD	total depth
TLD	Triple Detector Litho-Density
TOC	total organic carbon
VOC	volatile organic compound
WCSF	waste characterization strategy form
WES-EDA	Waste and Environmental Services Division–Environmental Data and Analysis

1.0 INTRODUCTION

This completion report summarizes the site preparation, drilling, well construction, well development, and aquifer testing for regional aquifer well R-44. The report is written in accordance with the requirements in Section IV.A.3.e.iv of the March 1, 2005, Compliance Order on Consent (the Consent Order). Well R-44 was drilled from November 10, 2008 to December 8, 2008, and the well was completed from December 13, 2009, to January 15, 2009, at Los Alamos National Laboratory (LANL or the Laboratory) for the Environmental Programs (EP) Directorate Water Stewardship Program.

The R-44 project site is located in a small tributary of Mortandad Canyon in the vicinity of regional well R-13 within Technical Area 05 (TA-05), Los Alamos County, New Mexico (Figure 1.0-1). The purposes of the R-44 monitoring well are to monitor potential releases of contaminants from Mortandad and Sandia Canyon sources, assess the conceptual model for contaminant fate and transport of known chromium contamination in the vicinity of well R-28, monitor water levels within the regional aquifer, and measure pumping effects from water-supply well PM-5 and other wells in the vicinity.

The primary objective of the drilling activities at R-44 was to drill and install a dual-screen regional aquifer monitoring well in the uppermost part of the regional groundwater system. The two-screen approach was designed to determine the vertical extent of potential chromium contamination so that pathways and potential future impacts to regional groundwater may be assessed. Water-level transducers will be placed in upper and lower well screens to evaluate hydraulic connections between this monitoring well, other monitoring wells and nearby water-supply well PM-5. Secondary objectives were to collect drill-cutting samples, conduct borehole geophysical logging, and investigate potential perched groundwater zones.

The R-44 borehole was drilled to a total depth (TD) of 1094.0 ft below ground surface (bgs). A monitoring well was installed with two screens. Currently, a temporary packer is being used to isolate the two well screens until the permanent sampling system that is being built by an off-site contractor can be installed. The permanent sampling system will isolate the two screens with a packer when installed in the near future. The upper 10-ft long screened interval is between 895.0 and 905.0 ft bgs and the lower 10-ft long screened interval is between 985.3 and 995.2 ft bgs. The composite depth to water after well installation and well development was 879.1 ft bgs on December 9, 2008. Cuttings samples were collected at 5-ft intervals in the borehole from ground surface to TD. Post installation activities included well development, aquifer testing, surface completion, and a geodetic survey. Future activities include dedicated sampling system installation, site restoration, and waste management.

The information presented in this report was compiled from field reports and daily activity summaries. Records, including field reports, field logs, and survey information, are on file at the Laboratory's Records Processing Facility (RPF). This report contains brief descriptions of activities and supporting figures, tables, and appendixes completed to date associated with the R-44 project.

2.0 PRELIMINARY ACTIVITIES

Preliminary activities included preparing administrative planning documents and preparing the drill pad. All preparatory activities were completed in accordance with Laboratory policies and procedures and regulatory requirements.

2.1 Administrative Preparation

The following documents helped guide the implementation of the scope of work for well R-44: “Final Drilling Plan for Regional Aquifer Wells R-44 and R-45” (TerranearPMC 2008, 105083); “Integrated Work Document for Regional and Intermediate Aquifer Well Drilling” (LANL 2007, 100972); “Storm Water Pollution Prevention Plan Addendum” (LANL 2006, 092600); and “Waste Characterization Strategy Form for the R-38, R-41, R-44, R-45, and R-46 Regional Groundwater Well Installation and Corehole Drilling” (LANL 2008, 103916).

2.2 Site Preparation

Site preparation was performed by LANL staff several weeks prior to rig mobilization. Between November 8 and 9, 2008, activities included mobilizing the drill rig, air compressors, trailers, and support vehicles to the drill site and staging alternative drilling tools and construction materials at the Pajarito Road lay down yard.

Office supply trailers, generators, and general field equipment were moved on-site after mobilization of drilling equipment. Potable water was obtained from the Puye Road fire hydrant and a fire hydrant near the Los Alamos County landfill on East Jemez Road. Safety barriers and signs were installed around the borehole-cuttings containment pit and along the perimeter of the work area.

3.0 DRILLING ACTIVITIES

This section describes the drilling strategy and approach and provides a chronological summary of field activities conducted at monitoring well R-44.

3.1 Drilling Approach

The drilling methodology and selection of equipment, including drill casing sizes, for R-44 were designed to retain the ability to case off perched groundwater and ensure reaching TD with a sufficiently sized casing to allow well installation with the required 2-in. minimum annular filter pack thickness for a 5.56-in.-outside diameter (O.D.) well. It was anticipated that if perched groundwater was encountered at R-44, the perched zone would be isolated and sealed off either with casing or by cementing to avoid commingling perched groundwater with the regional aquifer.

Dual-rotary drilling methods using a Foremost DR-24HD drill rig were employed to drill the R-44 borehole. Dual-rotary drilling has the advantage of simultaneously advancing and casing the borehole. The Foremost DR-24HD drill rig was equipped with conventional drilling rods, tricone bits, downhole hammer bits, one deck-mounted 900 ft^3/min air compressor, and general drilling equipment. Auxiliary equipment included two Sullair 1150 ft^3/min trailer-mounted air compressors. Two sizes of A53 grade B flush-welded mild carbon-steel casing (16-in. and 12-in. inside-diameter [I.D.]) were used for the R-44 project. The dual-rotary technique used filtered compressed air and fluid-assisted air to evacuate cuttings from the borehole. Cuttings samples were collected at 5-ft intervals in the borehole from ground surface to TD to characterize the hydrostratigraphy of rock units encountered in the borehole.

Drilling fluids, other than air, used in the vadose zone included municipal water and a mixture of municipal water with Baroid AQF-2 foaming agent. The fluids were used to cool the bit and help lift cuttings from the borehole. Use of foaming agents was terminated at 780 ft bgs, approximately 100 ft above the predicted regional aquifer water table. No additives other than municipal water were used for drilling within the

regional aquifer. Total amounts of drilling fluids introduced into the borehole and those recovered are recorded and presented in Table 3.1-1.

3.2 Chronology of Drilling Activities

Mobilization of drilling equipment and supplies to the R-44 site occurred during November 8 and 9, 2008. The borehole was initiated the next day, at 0145 hours using dual-rotary methods with 16-in. casing and a 15-in. tri-cone, long-tooth carbide bit. After drilling and advancing 16-in. casing through the alluvium, Bandelier Tuff, and volcaniclastic sediments overlying the Cerros del Rio basalt, the 16-in. casing was landed at 345.8 ft bgs in the morning of November 12, 2008. In conjunction with preparation to start open-hole drilling the top-head drive developed a minor hydraulic leak which required replacing a seal.

Open-hole drilling resumed using a 15-in. hammer bit at the top of Cerros del Rio basalt at 1807 h on November 13, 2008. Drilling progressed smoothly through the basalt to the contact with underlying Puye Formation sediments, at 707.0 ft bgs (at 0400 h on November 16, 2008). Progress was slowed because of problems with one of the two auxiliary Sulair air compressors. However, open-hole drilling was eventually suspended at 765.0 ft bgs (within the Puye Formation sediments) due to borehole instability.

On November 17, 2008 the 16-in. casing was cut in order to detach the welded drive shoe at 344.0 ft bgs, prior to running the Laboratory's video and geophysical (gamma ray and induction) logging tools in the borehole. The video tool revealed water entering the borehole at 739 ft bgs. Two groundwater samples were collected from this depth using a bailer; however the exact depth of this water was suspect because there were "knots" in the logging wire line. Because of the lack of water at this depth during later monitoring, and based on chemical analysis of these samples, it was decided that the water was most likely drilling water and not perched groundwater.

The drive shoe and 20-ft sections of 12-in. casing were welded and installed in the hole from November 18 through 24, 2008. Several mechanical and hydraulic problems with the top-head drive required ordering replacement parts and servicing, which slowed progress. On December 2, 2008, dual-rotary drilling commenced with the 12-in. casing and an 11-5/8 in. tricone bit. Drilling was unusually slow in the soft Puye Formation sediments, and the bit was pulled on December 3, 2008, for inspection. Several carbide buttons were observed to be absent from the bit cones, but of particular note was the presence of heavy score marks on the bit just above the cones. The score marks were indicative of the bit cutting into the steel drive shoe due to the bit not being able to be advanced outside the bottom of the 12-in. casing. All signs pointed to a misalignment somewhere toward the bottom of the 12-in. casing string. The decision to remove the entire 12-in. casing string for inspection was determined to be imperative.

Once on the surface, the bottom 12-in. casing joint was found to be slightly bent and the drive shoe weld showed some cracking. A new drive shoe was then welded on to a new lead casing joint on December 3, 2008, and the 12-in. casing string was reinstalled in the borehole. Drilling with dual-rotary methods and 12-in. casing recommenced on December 6, 2008. Eleven groundwater samples were collected, by air-lifting, from the 920 to 1094 ft bgs interval on December 7 and 8, 2008. Significant water production in the borehole was noted beginning at about 990 ft bgs and some indication of formation heaving occurred at 1094 ft bgs. A total depth of 1094 ft bgs was reached on December 8, 2008 at 1735 h. The next day the drill string was tripped out of the hole in preparation for geophysical logging by Schlumberger on December 9, 2008. After logging concluded, a stable depth-to-water of 879.1 ft bgs was recorded the same day.

Twelve-in. (74.0 ft casing and shoe) and 16-in. (1.8 ft casing and shoe) drill casing were left in the borehole. The longer length of 12-in. casing was left in place to help control heaving. The 12-in. casing stub was buried in backfill and isolated by the lowermost bentonite seal and the 16 in. casing stub was set in bentonite to avoid unwanted impacts in future.

Before moving the drilling rig off the site, the 12-in. casing was cut on December 10, 2008, at 1020.0 ft bgs. The rig was moved off site early in the morning of December 11, 2008, to the next drilling location (R-46).

The field crews typically worked two 12-h shifts per day (24-h operation) and 7 d/wk. Daily activities progressed without weather delays throughout the duration of drilling. Only minor mechanical delays with the 12-in. casing shoe, top-head drive, and air compressors slowed drilling progress.

4.0 SAMPLING ACTIVITIES

This section describes the cuttings and groundwater sampling activities at well R-44. All sampling activities were conducted in accordance with applicable quality procedures.

4.1 Cuttings Sampling

Cuttings samples were collected from the R-44 borehole at 5-ft intervals from ground surface to the TD of 1094.0 ft bgs. At each interval, approximately 500 mL of bulk cuttings were collected from the discharge hose, placed in resealable plastic bags, labeled, and archived in core boxes. Sieved fractions (>#10 and >#35 mesh) were also collected from ground surface to bottom depth and placed in chip trays along with unsieved (whole rock) cuttings. Radiation control technicians screened cuttings before removal from the site. The core boxes and chip trays were delivered to the Laboratory's archive at the conclusion of drilling activities. All screening measurements were within the range of background values.

Drilling and sample collection methods used at R-44 did not retain a majority of the fine fraction (silt and clay) of the drill cuttings, and much of the fine material throughout the borehole was lost. The volume of compressed air and water required for circulation made catching samples difficult, and fines were selectively lost during sample collection. Site geologists manually collected samples with a wire mesh basket directly from the discharge hose, and discharge velocities commonly forced the fine fraction of sample through the basket. Recovery of the coarser fraction of the cuttings samples was successful in nearly 100% of the borehole. The borehole lithologic log for R-44 stratigraphy is summarized in section 5.1 and detailed in Appendix A.

4.2 Water Sampling

Groundwater-screening samples were collected from the drilling discharge hose at approximate 20-ft intervals starting at 739 ft bgs to evaluate a potential perched zone (see discussion in section 3.2) and continued through the top of the regional aquifer to the borehole's TD of 1094.0 ft bgs. Typically, upon reaching the bottom of a 20-ft run of casing, the driller would stop water circulation (if injecting water) and circulate air, and as the discharge cleared; a water sample was collected directly from the discharge hose. Not all depth intervals below the top of the regional groundwater table could be captured at the end of each casing run. Alternatively, some water samples were collected upon start-up of the next casing run after the borehole equilibrated. Refer to Table 4.2-1 for a summary of screening samples collected at well R-44.

Eleven groundwater-screening samples, from depths of 739.0 to 1094.0 ft bgs, were collected during drilling operations by bailing or air-lifting water samples through the drill string. Two of these samples represented waters collected while drilling through the vadose zone to evaluate the presence or absence of perched groundwater. Drilling screening samples were analyzed for anions and metals, and one sample was analyzed for tritium.

Four regional groundwater-screening samples were collected during well development; two from the upper screen interval (895–905 ft bgs) and two from the lower screen interval (985.3–995.2 ft bgs). Development screening samples were analyzed for anions, metals, and total organic carbon (TOC).

Twelve regional groundwater-screening samples were collected at regular intervals (approximately one sample per 4 h) during aquifer testing. Six of these screening samples were collected from the upper screen interval (895–905 ft bgs), and six samples were collected from the lower screen interval (985.3–995.2 ft bgs). The groundwater samples were collected from a stainless-steel riser pipe that was connected to the surface discharge line from the submersible pump. Aquifer-testing screening samples were analyzed for dissolved anions, metals and TOC.

Groundwater characterization samples were collected from the completed well in accordance with the Consent Order. The samples were analyzed for the full suite of constituents including radioactive elements; anions/cations; general inorganic chemicals; volatile and semi-volatile organic compounds; and stable isotopes of hydrogen, nitrogen, and oxygen. These groundwater analytical results will be reported in the annual update to the “Interim Facility-Wide Groundwater Monitoring Plan.”

5.0 GEOLOGY AND HYDROGEOLOGY

A brief description of the geologic and hydrogeologic features encountered at R-44 is presented below. The Laboratory’s geology task leader and site geologists examined cuttings and geophysical logs to determine geologic contacts and hydrogeologic conditions. Drilling observations, video logging, water-level measurements, and geophysical logs were used to characterize groundwater occurrences encountered at R-44.

5.1 Stratigraphy

The stratigraphy for the R-44 borehole is presented below in order of youngest to oldest geologic units. Lithologic descriptions are based on cuttings samples collected from the discharge hose. Cuttings and borehole geophysical logs were used to identify geologic contacts. Figure 5.1-1 illustrates the stratigraphy at R-44. A detailed lithologic log based on analysis of drill cuttings is presented in Appendix A.

Quaternary Alluvium, Qal (0–47 ft bgs)

Quaternary alluvium, consisting of unconsolidated tuffaceous silty sand to sandy silt with pebble gravels containing pumice and volcanic detritus, occurs from 0 to 47 ft bgs. No evidence of alluvial groundwater was observed.

Unit 1g of the Tshirege Member of the Bandelier Tuff, Qbt 1g (47– 70 ft bgs)

Unit 1g of the Tshirege Member of the Bandelier Tuff was encountered from 47 to 70 ft bgs as interpreted by natural gamma geophysical log analysis. Unit 1g is a poorly welded vitric ash-flow tuff that is pumiceous, generally crystal rich and lithic-poor, with abundant vitric ash matrix. The thin Tshirege Unit 1g section preserved in R-44 contains strongly weathered pumices, minor lithics of diverse volcanic lithologies and abundant quartz and sanidine crystals.

Cerro Toledo Interval, Qct (70–94 ft bgs)

The Cerro Toledo interval, a thin layer of poorly consolidated volcaniclastic sediments that occurs stratigraphically between the Tshirege and Otowi Members of the Bandelier Tuff, is present from 70 to 94 ft bgs based on natural gamma ray geophysical log interpretation. This unit consists of silty fine to

medium sands and gravels made up of detrital volcanic materials (dacites, obsidian, rhyodacite), generally weathered pumice fragments, and abundant quartz and sanidine crystal grains.

Otowi Member of the Bandelier Tuff, Qbo (94–296 ft bgs)

The Otowi Member of the Bandelier Tuff is present from 94 to 296 ft bgs as interpreted from natural gamma geophysical log data. The Otowi Member is a poorly welded, pumiceous, locally lithic-rich, ash-flow tuff. Abundant pumice lapilli are white to pale orange, glassy, fibrous-textured and quartz- and sanidine-phyric and are enclosed in a matrix of vitric ash. Locally abundant volcanic lithic fragments, or xenoliths (generally up to 15 mm in diameter), are commonly subangular to subrounded and of intermediate volcanic composition, predominantly gray and light pinkish gray hornblende-and biotite-phyric dacites.

Guaje Pumice Bed of the Otowi Member of the Bandelier Tuff, Qbog (296–313 ft bgs)

The Guaje Pumice Bed occurs from 296 to 313 ft bgs on the basis of natural gamma ray log interpretation. The Guaje is a pumice-rich, lithic- and crystal-poor fall deposit that contains abundant (97%–100% by volume) pristine-appearing vitric, phenocryst-poor pumice fragments and lapilli. Trace volumes of volcanic lithics, quartz and sanidine phenocrysts, and fine ash are present.

Basaltic Volcaniclastic Sediments, Unassigned (313–344 ft bgs)

A thin sedimentary layer of pinkish to orange-tan siltstone to silty fine- to medium-grained sandstone with pebble gravel was intersected from 313 to 344 ft bgs, based on natural gamma log interpretation. Locally abundant subrounded detrital clasts (up to 20 mm in diameter) consist of basalt, basaltic scoria, vitric pumice fragments, dacite, and minor quartzite. These basalt-rich sediments occur at a stratigraphic position regionally occupied by the Puye Formation but have not yet been assigned to a particular unit. Basaltic constituents in these sediments likely were derived from underlying Cerros del Rio basalt lavas.

Cerros del Rio Basalt, Tb4 (344–707 bgs)

The Cerros del Rio basalt, intersected from 344 to 707 ft bgs, is locally a sequence of basalt lava flows with interlayers of cinders and basaltic ejecta, and pumiceous and basaltic sediments, some of which suggest a possible hydromagmatic origin. The upper part of the Cerros del Rio section, from 344 to 505 ft bgs, is made up of three distinct clinopyroxene (cpx)-phyric and olivine-cpx basalt flows, each with a layer of cinders/ejecta at its base. Cuttings suggest that a basaltic tuff layer containing basalt cinders, glassy scoria, dacite, weathered pumice, minor quartzite and fragments of indurated volcaniclastic sandstone, from 505 to 535 ft bgs, may indicate a hydromagmatic event between effusive lava eruptions. A similar sequence of three olivine-bearing basalt flows, with intercalated thin sedimentary deposits containing basalt and pumice detritus, makes up the lower part of the Cerros del Rio section between 535 and 707 ft bgs.

Puye Formation, Tpf (707–1005 ft bgs)

Puye Formation volcaniclastic sediments encountered from 707 to 1005 ft bgs consist of texturally diverse, gray, grayish brown and pinkish tan, poorly sorted, fine to coarse gravels, gravelly sandstones and silty sandstones with gravel. Detrital constituents that make up these sediments are generally subangular to subrounded and represent a range of volcanic lithologies including olivine-basalt (present as detrital clasts mainly at the top of the section), abundant biotite- and hornblende-dacites (present as a major constituent in large volumes throughout the section), rhyodacite, weathered pumice, scoria and dark colored vitrophyre.

Miocene Pumiceous Sediments, Tjfp (1005–1088 ft bgs)

A section of pumice-rich volcaniclastic sediments occur from 1005 to 1088 ft bgs. These deposits are made up of fine- to coarse-grained sandstones with pebble gravels, locally with a silty matrix. White, glassy, phenocryst-poor detrital pumices generally make up a large percent (locally as much as 100% by volume) of granule and pebble-size clasts. Additional constituents include abundant subangular to subrounded dacites, lesser amounts of basalt and andesite, and locally trace occurrences of Precambrian quartzite.

Miocene Riverine Sediments, Tcar (1088–1094 ft bgs)

A brief interval of fine to coarse gravels with fine- to coarse-grained sandstones, representing axial-river deposits, was encountered from 1088 ft bgs to the total borehole TD of 1094 ft bgs. These distinctive sediments are characterized by rounded to well-rounded pebbles and coarser gravel clasts composed of diverse volcanic litholgies (i.e., dark colored fine-grained andesites, varieties of dacite and rhyolite) and locally abundant (up to 30% by volume) Precambrian granites and quartzites.

5.2 Groundwater

Possible groundwater was first encountered at approximately 739 ft bgs in the Puye Formation sediments on January 24, 2009. As discussed in section 6.1, video log interpretation and later water-level measurements suggested that this was water introduced during drilling (see Appendix B). Perched water was not present in R-44. After the well was drilled to final depth of 1094 ft bgs, the water level was measured at approximately 879.1 ft bgs in the borehole.

Groundwater-screening samples were collected during drilling, well development, and aquifer testing as discussed in section 4.2 and presented in Table 4.2-1. Groundwater chemistry and field water-quality parameters are discussed in Appendix B. Aquifer testing data and analysis are discussed in Appendix C.

6.0 BOREHOLE LOGGING

Several video logs and a limited suite of geophysical logs were collected during the R-44 drilling project using Laboratory-owned equipment. An additional suite of cased-hole geophysical logs was collected by Schlumberger Wireline Services. A summary of video and geophysical logging runs is presented in Table 6.0-1.

6.1 Video Logging

A video log was run in the uncased borehole to check for the presence of perched groundwater on November 17, 2008. Water was observed in the video log in the Puye Formation sediments at a depth of 739 ft bgs when the borehole was at 765-ft depth. However interpretation of the log indicated the actual depth of the observed water was uncertain because there was a “knot” in the wire line. The November 17, 2008, video log from the borehole is presented on a digital video disc as part of Appendix D included with this document. Table 6.0-1 provides details about the video logging run.

6.2 Geophysical Logging

A suite of Schlumberger geophysical logs was run inside the drill casing on December 9, 2008. At the time of logging, the terminations of the two casing strings in the borehole were located at the following depths: 16-in. casing at 344 ft bgs and the 12-in. casing at 1094 ft bgs. The geophysical suite included

natural gamma ray, Triple Litho-Density (TLD), Elemental Capture Sonde (ECS), and Compensated Neutron Log (CNL). Interpretation and details of the logging are presented on CD as part of Appendix E.

7.0 WELL INSTALLATION

R-44 well was installed between December 13, 2008, and January 15, 2009.

7.1 Well Design

The R-44 well was designed in accordance with the approved Drilling Work Plan. NMED approved the well design before installation. The well was designed with dual-screened intervals to monitor groundwater quality at two depths in the upper part of the regional aquifer within Puye Formation sediments.

7.2 Well Construction

The R-44 monitoring well was constructed of 5.0-in.-I.D./5.56-in.-O.D., type A304 stainless-steel beveled casing fabricated to American Society for Testing and Materials A312 standards. The two screened sections utilized 10-ft lengths of 5.0-in.-I.D. rod-based 0.020-in. wire-wrapped well screen. Welding, using compatible stainless-steel welding rods, was used to join all individual casing and screen sections. All casing and screens were steam and pressure washed on-site before installation. A 2-in. I.D. steel threaded/coupled tremie pipe string (decontaminated prior to use) was utilized for delivery of backfill and annular fill materials during well construction. The placement of annular materials typically had two components: installing materials, and retracting the drill casing and raising the tremie pipe. As each section of drill casing was cut off the string, it was picked up and laid down. During this part of the process, the well casing was hung under full tension on a wireline while the drill casing was supported by a ring and slips.

Two screened intervals were chosen for the R-44 well design, based on monitored water levels and indications of potentially productive full-saturation intervals in the Schlumberger geophysical logs. The lower nominal 10-ft long screened interval had the top of the screen set at 985.3 ft bgs, and the upper nominal 10-ft long screened interval had the top of the screen set at 895 ft bgs. A 20.8-ft stainless-steel sump was placed below the bottom of the lower well screen. Stainless-steel centralizers (four sets of four) were welded to the well casing approximately 2.1 ft above and below each screen. A Pulstar work-over rig was used for well construction activities. Figure 7.2-1 presents an as-built schematic showing construction details for the completed well.

Well construction materials were moved onto the R-44 site starting on December 11, 2008. The Pulstar rig was moved on location and decontamination of the stainless-steel well casing and screens took place the next day. Before running the well casing, 41 ft^3 of 10/20 silica sand was added to the borehole as backfill bringing the borehole bottom to 1024.7 ft bgs, which is roughly 5 ft below the 12-in. casing cut.

On December 13 the well casing was installed. Each joint was welded as it went into the borehole, using careful welding techniques and covering the borehole to avoid slag falling into the annular void. After hanging the well at 1016 ft bgs the process of installing annular materials began. Additional 10/20 silica sand (5.5 ft^3) was added to bring the top of the backfill to 1008.4 ft bgs. A lower bentonite seal composed of ¼-in. pellets (1.3 ft^3) followed by ⅜-in. chips (0.7 ft^3) was placed from 999.8 to 1008.4 ft bgs. The lower screen 10/20 silica sand filter pack was then installed, and surged to promote compaction, from 980.2–1008.4 ft bgs. This was capped by a finer 20/40 silica sand transition from 976.3 to 980.2 ft bgs on December 22, 2008. All fieldwork was suspended that day due to the Laboratory holiday shut-down and R-44 well construction recommenced on January 5, 2009, after the break.

A seal separating the two screened intervals was placed from 910.2–976.3 ft bgs and consisted of ¼-in. bentonite pellets (13.4 ft^3) followed by ⅜-in. bentonite chips (45.2 ft^3). The upper screen filter pack of 10/20 silica sand was then installed (and surged) from 890.3 to 910.2 ft bgs. The upper filter pack was then capped with a transition 20/40 silica sand from 887.6 to 890.3 ft bgs.

The well's upper bentonite seal (⅜-in. chips) was installed from 342.4 to 887.6 ft bgs from January 8 to January 12, 2009. A surface seal (mix of 97–98 wt% Portland cement with 2–3 wt% bentonite) was placed above the upper bentonite seal from 3–342.4 ft bgs; this marked well construction completion on January 15, 2009 (1030 h). Table 7.2-1 details volumes of all materials used during well construction.

8.0 POSTINSTALLATION ACTIVITIES

Following installation, the well was developed and aquifer pumping tests were performed. Total groundwater purged during well development and aquifer testing was 92,929 gal. The wellhead and surface pad was constructed and a geodetic survey performed. A dedicated dual-zone sampling system will be installed after receipt from the manufacturer. Site restoration activities will be completed following the final disposition of contained drill cuttings and groundwater, per the NMED-approved waste-decision trees.

8.1 Well Development

Well development was conducted between January 15 and January 20, 2009. Initially, the screened interval was bailed and swabbed to remove formation fines in the filter pack and well sump. Bailing and swabbing continued until water clarity visibly improved. Final development was accomplished using a submersible pump. The swabbing tool was a 4.5-in.-O.D. 1-in.-thick nylon disc attached to a weighted steel rod. The swabbing tool was lowered by wireline and drawn repeatedly in both directions across each screened interval. After bailing and swabbing, a 10-hp, 4-in.-Grundfos submersible pump was installed in the well for the final stage of well development. Approximately 16,005 gal. of groundwater was purged at R-44 during well development activities.

During the pumping stage of well development, turbidity, temperature, pH, dissolved oxygen (DO), oxygen-reduction potential (ORP), and specific conductance parameters were measured. In addition, water samples for TOC analysis were collected. The required values for TOC and turbidity to determine adequate well development are less than 2.0 ppm and less than 5 nephelometric turbidity units (NTUs), respectively.

A discussion of water removed during well development, field water-quality parameters, and analytical results for samples collected during development is summarized below in section 8.1.1 and detailed in Table B.1.2-1 of Appendix B.

8.1.1 Well Development Field Parameters

Field parameters were measured at well R-44 by collecting aliquots of groundwater from the discharge pipe without the use of a flow-through cell, allowing the samples to be exposed to the atmosphere. Results are provided here and in greater detail in Appendix B. This condition probably resulted in a slight variation of field parameters during well development and during the pumping test, most notably, temperature, pH, and DO.

Measurements of pH varied from 8.22 to 8.30 in the upper screened interval and from 8.19 to 8.29 in the lower screened interval. Measurements of temperature varied from 18.3°C to 18.56°C in the upper screened interval and from 17.47°C to 18.78°C in the lower screened interval. Concentrations of DO

varied from 9.70 to 10.66 mg/L in the upper screened interval and from 11.57 to 13.72 mg/L in the lower screened interval. Uncorrected ORP measurements varied from –135.1 to–129.7 millivolts (mV) in the upper screened interval and from –130.8 to –118.9 mV in the lower screened interval. These negative, uncorrected ORP values are not reliable and representative of known relatively oxidizing conditions characteristic of the regional aquifer beneath the Pajarito Plateau. Specific conductance ranged from 142 to 148 microsiemens per centimeter (μS/cm) in the upper screened interval and from 193 to 204 μS/cm in the lower screened interval. Values of turbidity measured at R-44 ranged from 0.0 to 0.1 NTU for the nonfiltered groundwater samples of the upper screen and from 0.0 to 55.8 NTUs for the lower screen samples.

8.2 Aquifer Testing

Aquifer pumping tests were conducted at R-44 from February 14 to February 17, 2009. Several short-duration tests with short-duration recovery periods were performed on the upper and lower screens in the well. A 24-h test followed by a 24-h recovery period completed the testing. The same 10-hp Grundfos pump used during well development was used to perform the aquifer tests. Approximately 76,924 gal. of groundwater was purged during aquifer testing activities.

During aquifer testing, turbidity, temperature, pH, DO, ORP, and specific conductance parameters were measured. In addition, water samples for TOC analysis were collected.

A discussion of water removed during well development, field water-quality parameters, and analytical results for samples collected during development is summarized below in section 8.2.1 and detailed in Table B.1.2-1 of Appendix B. Results of the R-44 aquifer test are presented in Appendix C.

8.2.1 Aquifer Testing Field Parameters

Measurements of pH varied from 7.80 to 8.04 in the upper screened interval and 8.31 to 8.67 in the lower screened interval at R-44. Measurements of temperature varied from 14.99°C to 19.08°C in the upper screened interval and 15.14°C to 20.31°C in the lower screened interval. Concentrations of DO varied from 7.95 to 9.30 mg/L in the upper screened interval and from 8.60 to 11.14 mg/L in the lower screened interval. Uncorrected ORP measurements varied from 117.3 to 204.4 mV in the upper screened interval and from 117.3 to 195.2 mV in the lower screened interval. The uncorrected ORP measurements are in general agreement with the DO values, suggesting that relatively oxidizing conditions were established during the aquifer performance testing at well R-44. Specific conductance ranged from 60 to 140 μS/cm in the upper screened interval and 173 to 154 μS/cm in the lower screened interval. Values of turbidity for the nonfiltered groundwater samples ranged from 0 to 2.8 NTUs in the upper screened interval and 1.6 to 5.9 NTUs in the lower screened interval.

8.3 Dedicated Sampling System Installation

A dedicated sampling system for the R-44 well was custom-designed based on the hydrogeologic data gathered during the aquifer tests. The sampling system is on order from the manufacturer and will be installed upon delivery. The system consists of Baski Inc.-designed stainless-steel plumbing and an inflatable isolation packer. The system will implement a shrouded 4-in, Grundfos submersible pump (environmentally retrofitted with Teflon) with a 4-in., 3-phase, 460-V, viton-fitted Franklin Electric submersible motor. The pump will draw water from discrete intervals via pneumatically actuated access port valves. An inflatable viton-covered packer will be supplied as a component of the dedicated system.

All materials that contact the groundwater will be constructed of stainless steel, Teflon, viton, or polyvinyl chloride (PVC). All components of the pump column will be new. The pump column will be constructed of 1-in. threaded/coupled stainless steel pipe with check valves installed in the pipe string every 200 ft. A weep hole will be installed at the bottom of the uppermost pipe joint to protect the pump column from freezing. To measure water levels in the well, two 1-in. I.D. schedule 80 PVC pipes will be installed to the top of the pump shroud in order to set dedicated transducers below the measured static water levels. The upper PVC transducer tube will be equipped with a 6-in. section of 0.010-in slot screen with a threaded end cap at the bottom of the tube. The lower PVC transducer tube will be equipped with a flexible nylon tube that will extend from a threaded end cap at the bottom of the PVC tube through the isolation packer to measure water levels in the lower screen interval. A weather-resistant pump control box will be installed next to the wellhead.

Post-installation construction and sampling system component installation details for R-44 are presented in Figure 8.3-2a. Figure 8.3-2b presents technical notes.

8.4 Wellhead Completion

A reinforced concrete surface pad, 10 ft × 10 ft × 6 in. thick, was installed at the wellhead. The pad will provide long-term structural integrity for the well. A brass survey pin was embedded in the northwest corner of the pad. A 10-in.-I.D. steel protective casing with a locking lid was installed around the stainless-steel well riser. The concrete pad was slightly elevated above the ground surface and crowned to promote runoff. Base course was graded around the edges of the pad. A total of four bollards, painted yellow for visibility, are set at the outside edges of the pad to protect the well from traffic. All of the four bollards are designed for easy removal to allow access to the well. Details of the wellhead completion are presented in Figure 8.3-1a.

8.5 Geodetic Survey

A New Mexico licensed professional land surveyor conducted a geodetic survey on February 10, 2009 (Table 8.5-1). The survey data collected conforms to Laboratory Information Architecture project standards IA-CB02, “GIS Horizontal Spatial Reference System,” and IA-D802, “Geospatial Positioning Accuracy Standard for A/E/C and Facility Management.” All coordinates are expressed as New Mexico State Plane Coordinate System Central Zone (NAD 83); elevation is expressed in feet above mean sea level (amsl) using the National Geodetic Vertical Datum of 1929. Survey points include ground-surface elevation near the concrete pad, the top of the brass pin in the concrete pad, the top of the well casing, and the top of the protective casing.

8.6 Waste Management and Site Restoration

Waste generated from the R-44 project includes drilling fluids, purged groundwater, decontamination water, drill cuttings, and contact waste. A summary of the waste characterization samples collected from the R-44 well is presented in Table 8.6-1.

All waste streams produced during drilling and development activities were sampled in accordance with “Waste Characterization Strategy Form for the R-38, R-41, R-44, R-45, and R-46 Regional Groundwater Well Installation and Corehole Drilling” (LANL 2008, 103916).

Fluids produced during drilling and well development are expected to be land-applied after a review of associated analytical results per the waste characterization strategy form (WCSF) and the EP-Directorate Standard Operating Procedure (SOP) 010.0, Land Application of Groundwater. If it is determined that drilling fluids are nonhazardous but cannot meet the criterion for land application, the drilling fluids will be

evaluated for treatment and disposal at one of the Laboratory's six wastewater treatment facilities. If analytical data indicate that the drilling fluids are hazardous/nonradioactive or mixed low-level waste, the drilling fluids will be disposed of at an authorized facility.

Cuttings produced during drilling are anticipated to be land-applied after a review of associated analytical results per the WCSF and ENV-RCRA SOP-011.0, Land Application of Drill Cuttings. If the drill cuttings do not meet the criterion for land application, they will be disposed of at an authorized facility. Decontamination fluid used for cleaning the drill rig and equipment is containerized. The fluid waste was sampled and will be disposed of at an authorized facility. Characterization of contact waste will be based upon acceptable knowledge, pending analyses of the waste samples collected from the drill cuttings, purge water, and decontamination fluid.

Site restoration activities will include removing drilling fluids and cuttings from the pit and managing the fluids and cuttings in accordance with SOP-010.06, removing the polyethylene liner, removing the containment area berms, and backfilling and regrading the containment area, as appropriate.

9.0 DEVIATIONS FROM PLANNED ACTIVITIES

Drilling, sampling, and well construction at R-44 were performed as specified in "Final Drilling Plan for Regional Aquifer Wells R-44 and R-45" (TerranearPMC 2008, 105083).

10.0 ACKNOWLEDGMENTS

Patrick Longmire wrote Appendix B, Groundwater Analytical Results.

Boart Longyear drilled the R-44 borehole and installed the well.

Los Alamos National Laboratory personnel ran downhole video equipment.

Schlumberger Wireline Services performed the final geophysical logging of the borehole.

Right Bit Services and Equipment Repair welded the stainless well screen and casing.

TerranearPMC provided oversight on all preparatory and field-related activities.

11.0 REFERENCES

The following list includes all documents cited in this report. Parenthetical information following each reference provides the author(s), publication date, and ER ID. This information is also included in text citations. ER IDs are assigned by the Environmental Programs Directorate's Records Processing Facility (RPF) and are used to locate the document at the RPF and, where applicable, in the master reference set.

Copies of the master reference set are maintained at the NMED Hazardous Waste Bureau and the Directorate. The set was developed to ensure that the administrative authority has all material needed to review this document, and it is updated with every document submitted to the administrative authority. Documents previously submitted to the administrative authority are not included.

LANL (Los Alamos National Laboratory), March 2006. "Storm Water Pollution Prevention Plan for SWMUs and AOCs (Sites) and Storm Water Monitoring Plan," Los Alamos National Laboratory document LA-UR-06-1840, Los Alamos, New Mexico. (LANL 2006, 092600)

LANL (Los Alamos National Laboratory), October 4, 2007. “Integrated Work Document for Regional and Intermediate Aquifer Well Drilling (Mobilization, Site Preparation and Setup Stages),” Los Alamos National Laboratory, Los Alamos, New Mexico. (LANL 2007, 100972)

LANL (Los Alamos National Laboratory), November 2007. “Work Plan for Geochemical Characterization and Drilling for Fate and Transport of Contaminants Originating in Sandia Canyon,” Los Alamos National Laboratory document LA-UR-07-7579, Los Alamos, New Mexico. (LANL 2007, 099607)

LANL (Los Alamos National Laboratory), October 2008. Waste Characterization Strategy Form for the R-38, R-41, R-44, R-45, and R-46 Regional Groundwater Well Installation and Corehole Drilling, Los Alamos, New Mexico. (LANL 2008, 103916)

TerranearPMC, October 2008. “Final Drilling Plan for Regional Aquifer Wells R-44 and R-45,” plan prepared for Los Alamos National Laboratory, Los Alamos, New Mexico. (TerranearPMC 2008, 105083)

Map Data Sources for R-42 Completion Report Location Map

Point Feature Locations of the Environmental Restoration Project Database; Los Alamos National Laboratory, Waste and Environmental Services Division, EP2008-0109; February 28, 2008.

Hypsography, 100 and 20 Foot Contour Interval; Los Alamos National Laboratory, ENV Environmental Remediation and Surveillance Program; 1991.

Surface Drainages, 1991; Los Alamos National Laboratory, ENV Environmental Remediation and Surveillance Program, ER2002-0591; 1:24,000 Scale Data; Unknown publication date.

Paved Road Arcs; Los Alamos National Laboratory, KSL Site Support Services, Planning, Locating and Mapping Section; 06 January 2004; as published January 4, 2008.

Dirt Road Arcs; Los Alamos National Laboratory, KSL Site Support Services, Planning, Locating and Mapping Section; 06 January 2004; as published January 4, 2008.

Structures; Los Alamos National Laboratory, KSL Site Support Services, Planning, Locating and Mapping Section; 06 January 2004; as published January 4, 2008.

Technical Area Boundaries; Los Alamos National Laboratory, Site Planning & Project Initiation Group, Infrastructure Planning Division; September 19, 2007.

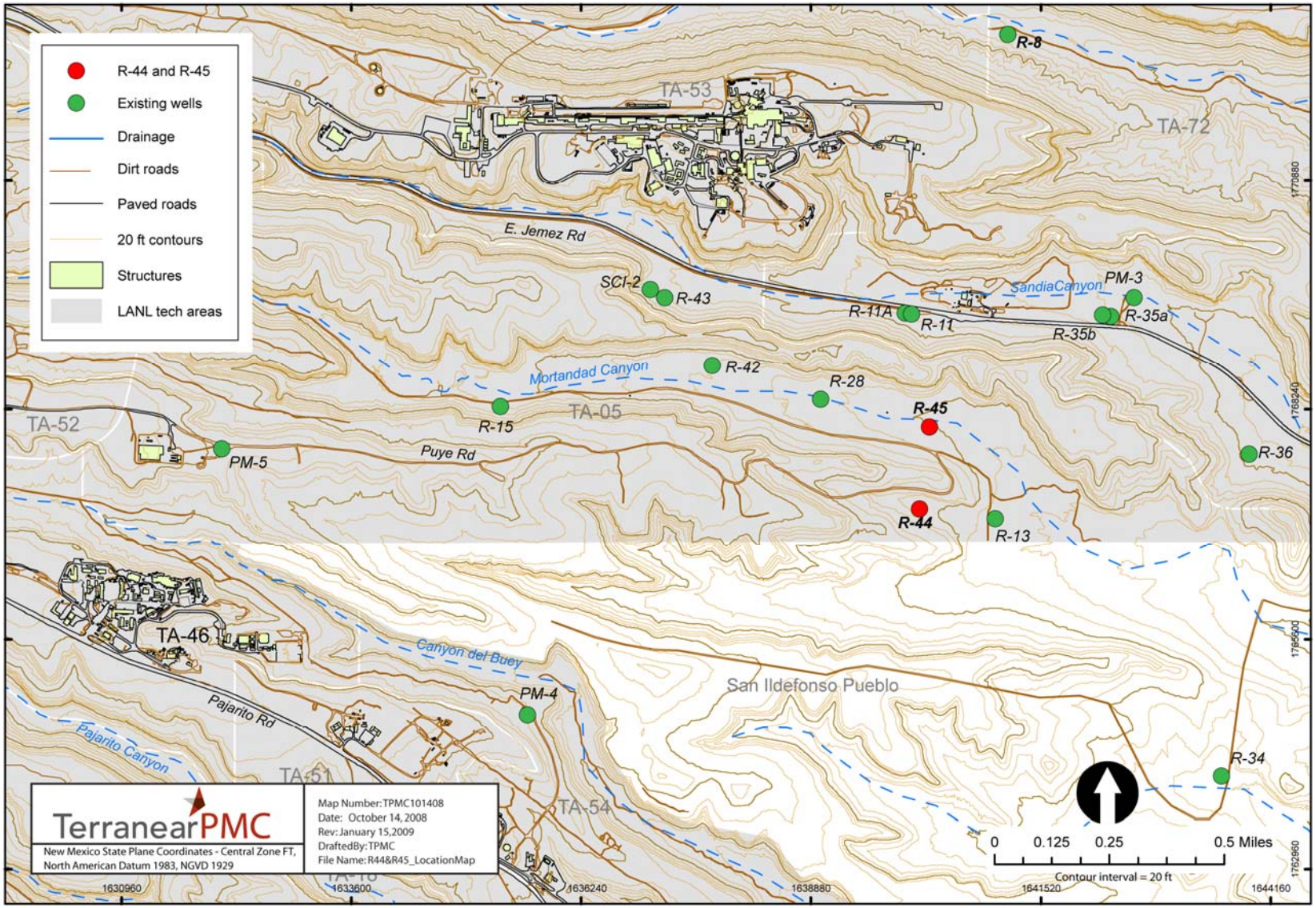

Figure 1.0-1 Regional aquifer well R-44 with respect to surrounding regional wells and PM-5

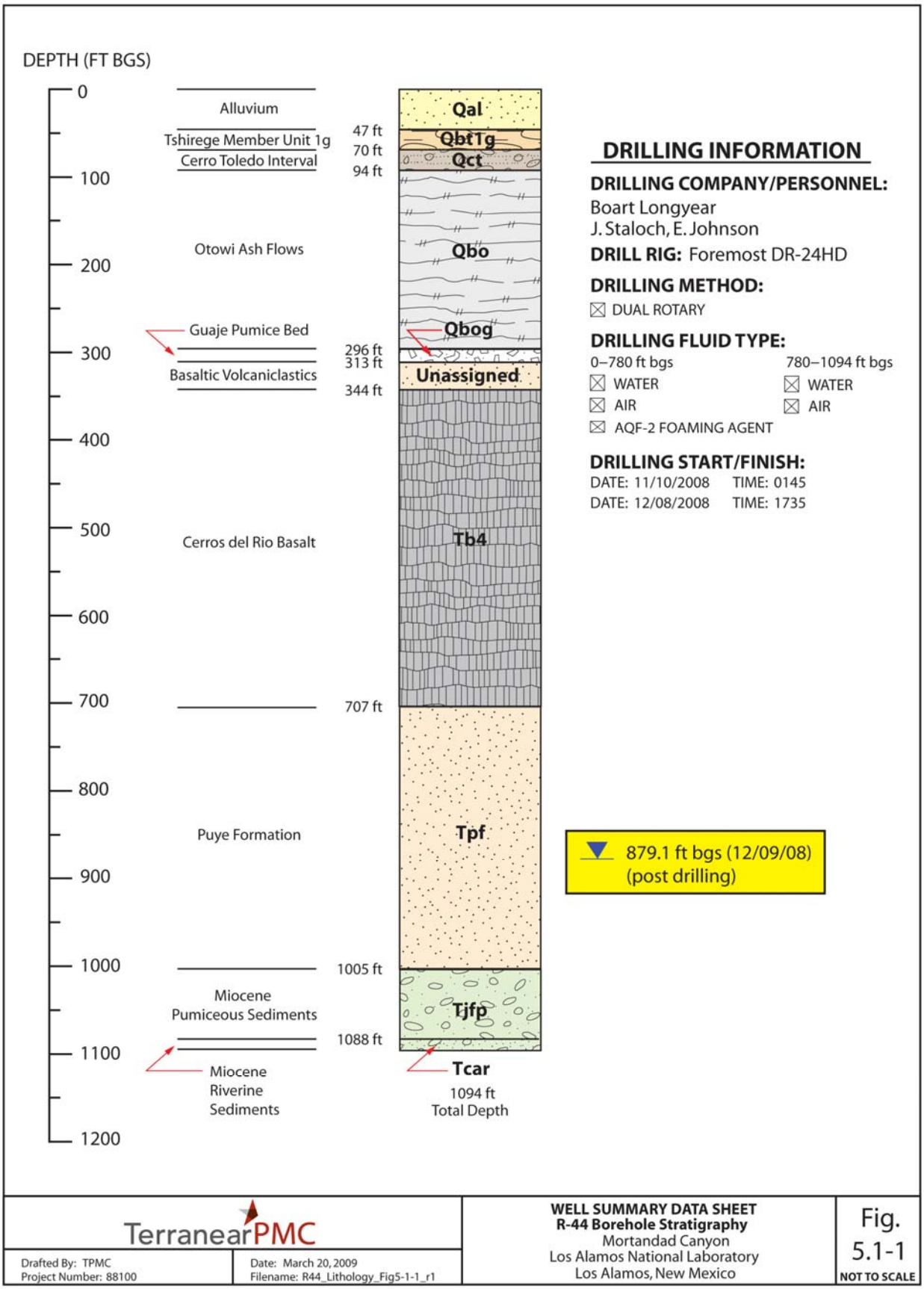
DEPTH (FT BGS)
0
100
200
300
400
500
600
700
800
900
1000
1100
1200
Alluvium
Tshirege Member Unit 1g
Cerro Toledo Interval
Otowi Ash Flows
Guaje Pumice Bed
Basaltic Volcaniclastics
Cerros del Rio Basalt
Puye Formation
Miocene
Pumiceous Sediments
Miocene
Riverine
Sediments
47 ft
70 ft
94 ft
296 ft
313 ft
344 ft
707 ft
1005 ft
1088 ft
Qal
Qbt1g
Qct
Qbo
Qbog
Unassigned
Tb4
Tpf
Tjfp
Tcar
1094 ft
Total Depth
DRILLING INFORMATION
DRILLING COMPANY/PERSONNEL:
Boart Longyear
J. Staloch, E. Johnson
DRILL RIG: Foremost DR-24HD
DRILLING METHOD:
DUAL ROTARY
DRILLING FLUID TYPE:
0–780 ft bgs
WATER
AIR
AQF-2 FOAMING AGENT
780–1094 ft bgs
WATER
AIR
DRILLING START/FINISH:
DATE: 11/10/2008 TIME: 0145
DATE: 12/08/2008 TIME: 1735
879.1 ft bgs (12/09/08)
(post drilling)
TerranearPMC
Drafted By: TPMC
Project Number: 88100
Date: March 20, 2009
Filename: R44_Lithology_Fig5-1-1_r1
WELL SUMMARY DATA SHEET
R-44 Borehole Stratigraphy
Mortandad Canyon
Los Alamos National Laboratory
Los Alamos, New Mexico
Fig.
5.1-1
NOT TO SCALE

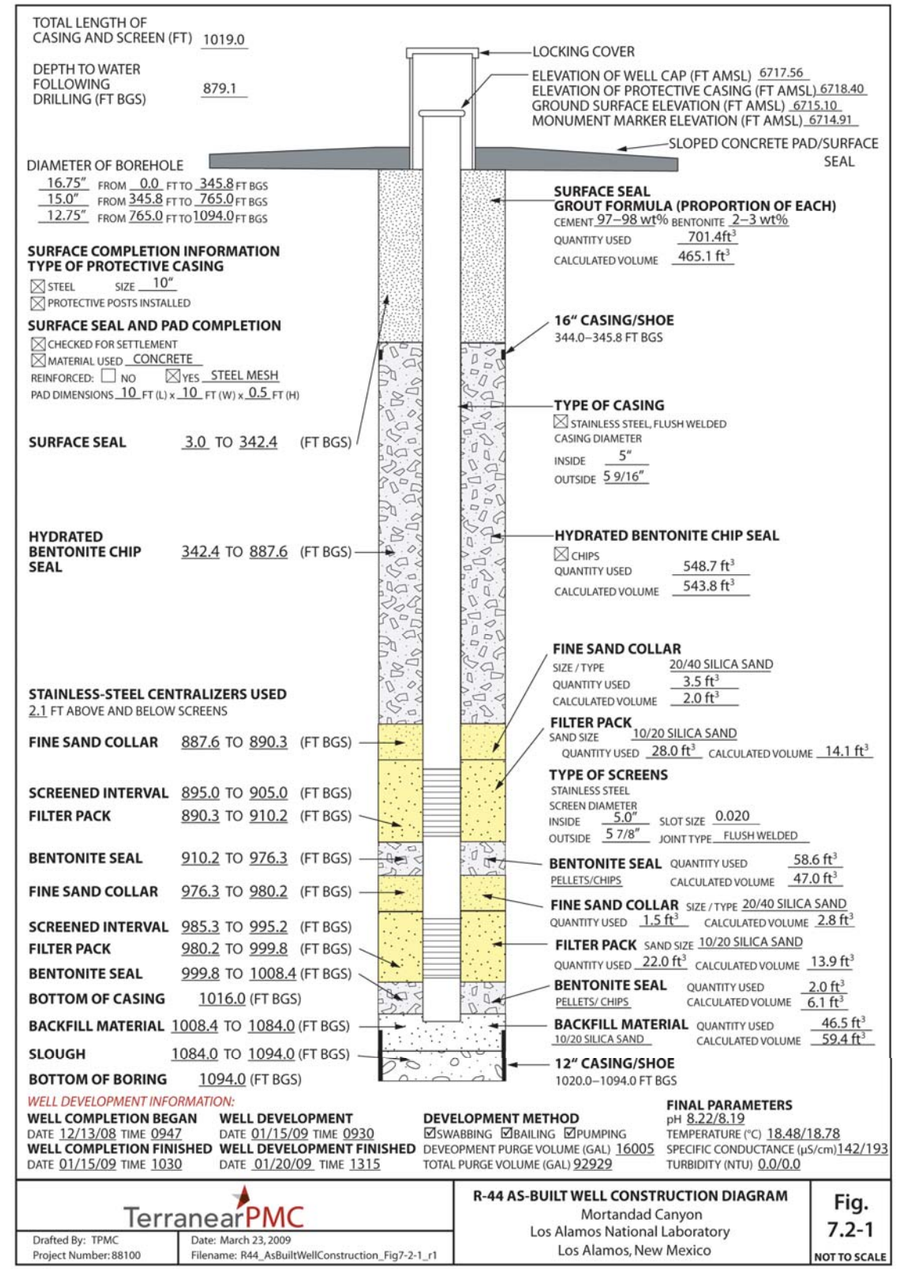

Figure 7.2-1 R-44 as-built well construction diagram

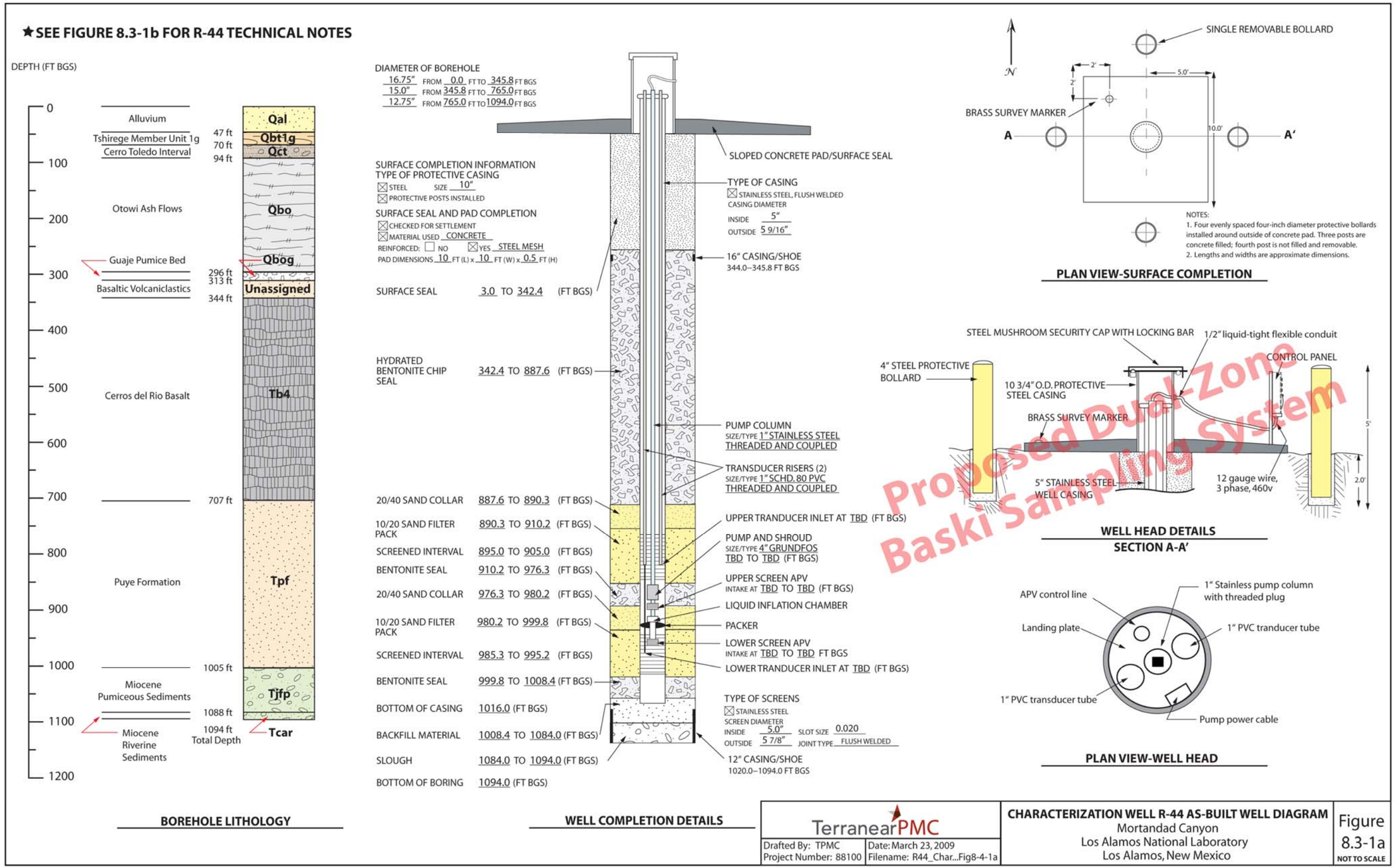

Figure 8.3-1a As-built schematic for regional well R-44

R-44 TECHNICAL NOTES: [1]

SURVEY INFORMATION[2]

Brass Marker

Northing:	1767109.8527 ft
Easting:	1640061.3389 ft
Elevation:	6714.91 ft AMSL

Well Casing (top of stainless steel)

Northing:	1767104.3569 ft
Easting:	1640063.4865 ft
Elevation:	6717.56 ft AMSL

BOREHOLE GEOPHYSICAL LOGS

LANL: natural gamma ray, induction, video
Schlumberger: natural gamma ray, elemental capture (ECS), compensated neutron (CNTG), litho-density (TLD)

DRILLING INFORMATION

Drilling Company
Boart Longyear

Drill Rig
Foremost DR-24HD

Drilling Methods
Dual Rotary
Fluid-assisted air rotary, Foam-assisted air rotary

Drilling Fluids
Air, potable water, AQF-2 Foam

MILESTONE DATES

Drilling

Start:	11/10/2008
Finished:	12/08/2008

Well Completion

Start:	12/13/2008
Finished:	01/15/2009

Well Development

Start:	01/15/2009
Finished:	01/20/2009

WELL DEVELOPMENT

Development Methods
Performed swabbing, bailing, and pumping
Total Volume Purged: 16005 gallons (both screens)

Parameter Measurments (Final, upper screen/lower screen)

pH:	8.22/8.19
Temperature:	18.48/18.78˚C
Specific Conductance:	142/193 µS/cm
Turbidity:	0.0/0.0 NTU

AQUIFER TESTING

Step-Tests and Constant Rate Pumping Tests

Upper Screen

Water Produced:	38223 gallons
Average Flow Rate:	24.1 gpm
Performed on:	02/14–17/2009

Lower Screen

Water Produced:	38701 gallons
Average Flow Rate:	23.9 gpm
Performed on:	02/19–22/2009

DEDICATED SAMPLING SYSTEM

Pump
Type: TBD
Model: TBD
TBD U.S. gpm, intake at TBD ft bgs
Environmental Retrofit

Motor
Type: TBD
Model: TBD

Pump Column
TBD

Transducer Tubes
TBD

Transducers
Type: TBD
Model: TBD
S/N: TBD

NOTES:
1) Additional information available in "Final Completion Report, Characterization Well R44 and R45, Los Alamos National Laboratory, Los Alamos, New Mexico, TBD 2009".
2) Coordinates based on New Mexico State Plane Grid Coordinates, Central Zone (NAD83); Elevation expressed in feet above mean sea level using the National Geodetic Vertical Datum of 1929.

TerranearPMC		**R-44 TECHNICAL NOTES** Mortandad Canyon Los Alamos National Laboratory Los Alamos, New Mexico	Figure 8.3-1b NOT TO SCALE
Drafted By: TPMC Project Number: 86000	Date: March 23, 2009 Filename: R44_TechnicalNotes_Fig8-3-1b_r1		

Figure 8.3-1b As-built technical notes for R-44

Table 3.1-1
Fluid Quantities Used during Drilling and Well Construction

Date	Water (gal.)	Cumulative Water (gal.)	AQF-2 Foam (gal.)	Cumulative AQF-2 Foam (gal.)
Drilling				
11/10/08	1700	1700	3	3
11/11/08	1400	3100	5	8
11/14/08	4500	7600	45	53
11/15/08	6500	14,100	40	93
11/16/08	4000	18,100	0	93
12/02/08	1100	19,200	8	101
12/05/08	200	19,400	0	101
12/06/08	1300	20,700	0	101
12/07/08	900	21,600	0	101
Well Construction				
12/18/08	200	21,800	n/a*	n/a
12/19/08	7000	28,800	n/a	n/a
12/20/08	5700	34,500	n/a	n/a
12/21/08	1000	35,500	n/a	n/a
12/22/08	1000	36,500	n/a	n/a
01/05/09	1500	38,000	n/a	n/a
01/06/09	9800	47,800	n/a	n/a
01/07/09	5000	52,800	n/a	n/a
01/08/09	8700	61,500	n/a	n/a
01/09/09	3500	65,000	n/a	n/a
01/10/09	5500	70,500	n/a	n/a
01/11/09	2500	73,000	n/a	n/a
01/12/09	1600	74,600	n/a	n/a
01/13/09	2150	76,750	n/a	n/a
01/15/09	70	76,820	n/a	n/a
Total Volume (gal.)				
R-44		**76,820**		

Note. Cumulative returns in the pit following drilling and well development are estimated to be approximately 30,000 gal.

*n/a = Not applicable. Foam use and pit use discontinued after drilling activities; therefore, no additional fluids were produced.

Table 4.2-1
Summary of Groundwater-Screening Samples Collected during Drilling, Well Development, and Aquifer Testing of Well R-44

Location ID	Sample ID	Date Collected	Collection Depth (ft bgs)	Sample Type	Analysis
Drilling					
R-44	GW44-09-1292	11/17/08	739.0–739.5	Possible intermediate groundwater	Anions, metals
R-44	GW44-09-1315	11/17/08	739.0–739.5	Possible intermediate groundwater	Tritium
R-44	GW44-09-1293	12/07/08	920	Regional groundwater	Anions, metals
R-44	GW44-09-1294	12/07/08	957	Regional groundwater	Anions, metals
R-44	GW44-09-1295	12/07/08	977	Regional groundwater	Anions, metals
R-44	GW44-09-1296	12/07/08	997	Regional groundwater	Anions, metals
R-44	GW44-09-1297	12/07/08	1017	Regional groundwater	Anions, metals
R-44	GW44-09-1298	12/08/08	1037	Regional groundwater	Anions, metals
R-44	GW44-09-1299	12/08/08	1056	Regional groundwater	Anions, metals
R-44	GW44-09-1301	12/08/08	1076	Regional groundwater	Anions, metals
R-44	GW44-09-1300	12/08/08	1094	Regional groundwater	Anions, metals
Well Development					
R-44	GW44-09-1272	01/18/09	895–905	Regional groundwater, upper screen	Anions, metals, TOC
R-44	GW44-09-1273	01/18/09	895–905	Regional groundwater, upper screen	Anions, metals, TOC
R-44	GW44-09-1274	01/20/09	985.3–995.2	Regional groundwater, lower screen	Anions, metals, TOC
R-44	GW44-09-1275	01/20/09	985.3–995.2	Regional groundwater, lower screen	Anions, metals, TOC
Aquifer Pump Test					
R-44	GW44-09-1276	02/16/09	895–905	Regional groundwater, upper screen	Anions, metals, TOC
R-44	GW44-09-1277	02/16/09	895–905	Regional groundwater, upper screen	Anions, metals, TOC
R-44	GW44-09-1278	02/16/09	895–905	Regional groundwater, upper screen	Anions, metals, TOC
R-44	GW44-09-1279	02/17/09	895–905	Regional groundwater, upper screen	Anions, metals, TOC
R-44	GW44-09-1280	02/17/09	895–905	Regional groundwater, upper screen	Anions, metals, TOC
R-44	GW44-09-1281	02/17/09	895–905	Regional groundwater, upper screen	Anions, metals, TOC
R-44	GW44-09-1282	02/21/09	985.3–995.2	Regional groundwater, lower screen	Anions, metals, TOC
R-44	GW44-09-1283	02/21/09	985.3–995.2	Regional groundwater, lower screen	Anions, metals, TOC
R-44	GW44-09-1284	02/21/09	985.3–995.2	Regional groundwater, lower screen	Anions, metals, TOC
R-44	GW44-09-1285	02/21/09	985.3–995.2	Regional groundwater, lower screen	Anions, metals, TOC
R-44	GW44-09-1286	02/22/09	985.3–995.2	Regional groundwater, lower screen	Anions, metals, TOC
R-44	GW44-09-1287	02/21/09	985.3–995.2	Regional groundwater, lower screen	Anions, metals, TOC

Note: Tritium was submitted for off-site analysis.

Table 6.0-1
R-44 Video and Geophysical Logging Runs

Date	Depth (ft bgs)	Description
11/17/08	0–<762.0	Run LANL natural gamma-ray, induction, and video tools. Video shows water in borehole at 739 ft bgs. Depths suspect because of “knots” in logging wire line.
12/09/08	0–1094.0	Run Schlumberger suite: cased-hole logs consist of a natural gamma ray, ECS, CNL, and TLD after reaching TD.

Table 7.2-1
R-44 Annular Fill Materials

Material	Volume
Surface seal: cement slurry	701.4 ft^3
Upper seal: bentonite chips	548.7 ft^3
Upper fine sand collar: 20/40 silica sand	3.5 ft^3
Upper filter pack: 10/20 silica sand	28.0 ft^3
Middle seal: bentonite pellets/chips	58.6 (13.4/45.2) ft^3
Lower fine sand collar: 20/40 silica sand	1.5 ft^3
Lower filter pack:	22.0 ft^3
Lower seal: bentonite pellets/chips	2.0 (1.3/0.7) ft^3
Backfill material: 10/20 silica sand	46.5 ft^3
Backfill material: formation slough	8.9 ft^3
Potable water used in the regional aquifer (drilling and well construction)	76,820 gal.

Table 8.5-1
R-44 Survey Coordinates

North	East	Elevation	Identification
1767109.85	1640061.34	6714.91	R-44 brass pin embedded in pad
1767105.66	1640062.81	6715.10	R-44 ground surface near pad
1767104.88	1640063.73	6718.40	R-44 top of 10-in. protective casing
1767104.36	1640063.49	6717.56	R-44 top of stainless-steel well casing

Notes: All coordinates are expressed as New Mexico State Plane Coordinate System Central Zone (NAD 83). Elevation is expressed in feet above mean sea level using the National Geodetic Vertical Datum of 1929.

Table 8.6-1
Summary of Waste Samples Collected during Drilling and Development of R-44

Location ID	Sample ID	Date Collected	Description	Sample Type
R-44	RC05-09-1519	1/26/09	Decontamination water	Liquid
R-44	RC05-09-1520	1/26/09	Decontamination water	Liquid
R-44	RC05-09-1521	1/26/09	Decontamination water	Liquid
R-44	RC05-09-1522	1/26/09	Trip blank	Liquid
R-44	RC05-09-1527	1/26/09	Drilling fluid	Liquid
R-44	RC05-09-1528	1/26/09	Drilling fluid	Liquid
R-44	RC05-09-1529	1/26/09	Drilling fluid	Liquid
R-44	RC05-09-1530	1/26/09	Trip blank	Liquid
R-44	RC05-09-1535	1/26/09	Purge water	Liquid
R-44	RC05-09-1536	1/26/09	Purge water	Liquid
R-44	RC05-09-1537	1/26/09	Purge water	Liquid
R-44	RC05-09-1538	1/26/09	Trip blank	Liquid
R-44	RC05-09-1543	1/26/09	Drill cuttings	Solid
R-44	RC05-09-1544	1/26/09	QC sample of -1543	Solid

Appendix A

Well R-44 Lithologic Log

Los Alamos National Laboratory
Regional Hydrogeologic Characterization Project
Borehole Lithologic Log

COREHOLE IDENTIFICATION (ID): R-44	**TECHNICAL AREA (TA):** 5	**PAGE:** 1 of 16
DRILLING COMPANY: Boart Longyear Company	**START DATE/TIME:** 11/10/2008:0145	**END DATE/TIME:** 12/8/2008: 1735
DRILLING METHOD: Dual Rotary	**MACHINE**: Foremost DR24 HD	**SAMPLING METHOD:** Grab
GROUND ELEVATION:		**TOTAL DEPTH:** 1094 ft below ground surface (bgs)
DRILLERS: J. Staloch, C. Johnson	**SITE GEOLOGISTS:** A. Miller, C. Pigman, J. R. Lawrence	

Depth (ft bgs)	Lithology	Lithologic Symbol	Notes
0–47	ALLUVIUM: Unconsolidated tuffaceous sediments—light grayish tan (7.5YR 7/1) to pale pinkish tan (7.5YR 8/4) silty fine to medium sand with minor pebble gravel; detrital grains/clasts of indurated tuff, quartz and sanidine crystals, pumice and volcanic lithics. 0–5 ft surficial construction fill. 5–20 ft +10F: quartz and sanidine crystal grains, mixed angular volcanic clasts and fragments of siltstone/very fine-grained sandstones. 20–47 ft +10F/+35F: siltstone fragments, quartz and sanidine grains, granules of weathered pumice. 95–108 ft +10F: mixed weathered pumice fragments, subangular granules of various volcanic rocks, fragments of silty very fine-grained sandstone.	Qal	Note: Drill cuttings for microscopic and descriptive analysis were collected at 5-ft intervals from 0 ft bgs to borehole total depth (TD) at 1094 ft bgs. Quaternary alluvial sediments, from 0 to 47 ft bgs, are estimated to be 47 ft thick. The Qal–Qbt 1g contact is estimated to be at 47 ft bgs.
47–70	**UNIT 1g OF THE TSHIREGE MEMBER OF THE BANDELIER TUFF:** Tuff—light grayish tan (7.5YR 7/1), very poorly welded, locally abundant ash matrix. 47—55 ft WR: silty ash matrix. +10F/+35F: 30%–40% fragments tuffaceous fragments with abundant quartz and sanidine grains; 30%–40% subangular lithics (up to 10 mm in diameter) of diverse intermediate volcanic rocks; 10%–20% weathered pumices. 55–60 ft +10F: 60%–70% white and gray subangular dacitic lithics; 20%–30% weathered pumices fragments; 10% fragments of silty sandstone. 60–70 ft +10F: 90-95% subrounded granule-size lithics of various volcanic lithologies (dacites, obsidian, rhyodacite(?); 10% weathered pumices fragments.	Qbt 1g	Unit 1g of the Tshirege Member of the Bandelier Tuff, from 47 to 70 ft bgs, is estimated to be 23 ft thick. The Qbt 1g–Qct contact is estimated to be at 70 ft bgs, based on natural gamma log interpretation.

Borehole Lithologic Log (continued)

Borehole ID: R-44	**TA:** 5	**Page:** 2 of 16	
Depth (ft bgs)	Lithology	Lithologic Symbol	Notes
70–94	**CERRO TOLEDO INTERVAL OF THE BANDELIER TUFF:** Tuffaceous sediments—light grayish tan (7.5YR 7/1) to pale pinkish tan (7.5YR 8/4) poorly consolidated to unconsolidated silty fine- to medium-grained sandstone with local pebble gravel, locally abundant ash matrix. 70–80 ft +10F/+35F: 30%–40% fragments of tuffaceous silty sandstone with abundant quartz and sanidine grains; 30%–40% subangular lithics (up to 10 mm in diameter) of diverse intermediate volcanic lithologies; 10%–20% weathered pumices. 80–94 ft+10F: very little material retained of this size fraction; minor dacite granules. +35F: abundant quartz and sanidine crystal grains, pumices and volcanic lithic fragments.	Qbo	The Cerro Toledo interval, from 70 to 94 ft bgs, is estimated to be 24 ft thick. The Qct–Qbo contact is estimated to be at 94 ft bgs, based on natural gamma log interpretation.
94–110	**OTOWI MEMBER OF THE BANDELIER TUFF:** Tuff—pale orange tan (7.5YR 8/6) to pinkish white (7.5YR 8/2), poorly welded, lithic-bearing, locally abundant ash and silt matrix; this interval likely represents the weathered upper part of Qbo. 94–105 ft +10F: mixed weathered pumice fragments, various subangular volcanic lithics. 105–110 ftWR: abundant silt and ash matrix. +10F: 75% weathered to glassy pumices (up to 20 mm in diameter); 15%–25% dacite fragments.	Qbo	Otowi Member ash-flow tuff, encountered from 94 to 296 ft bgs, is estimated to be 202 ft thick.
110–120	Tuff—white (7.5YR 8/2), poorly welded, crystal-rich, lithic-bearing, abundant ash matrix. 110—120 ft +10F: 100% pumice fragments (up to 22 mm in diameter), mostly glassy to locally devitrified, quartz- and sanidine-phyric. +35F: 30%–35% quartz and sanidine crystals, 40%–45% pumice fragments (mostly glassy).	Qbo	
120–135	Tuff—white (10YR 8/1), poorly welded, pumice-rich, crystal-rich, lithic-bearing, abundant ash matrix. 120–135 ft +10F: 80%–85% vitric pumice fragments (up to 14 mm in diameter), quartz- and sanidine-phyric. +35F: 15%–20% broken volcanic lithic fragments (up to 15 mm) composed of light gray and pinkish biotite-dacites. 35F: 30%–40% quartz and sanidine crystals, 40%–50% glassy pumice fragments; 15%–20% lithic fragments.	Qbo	125—135 ft +10F contains large dacite fragments up to 25 mm in diameter.
135–145	Tuff—white (10YR 8/1), poorly welded, pumice-rich, crystal-rich, lithic-poor, abundant fine volcanic ash matrix. 135—145 ft +10F: 100% vitric pumice fragments (up to 20 mm in diameter), quartz- and sanidine-phyric; trace volcanic lithics. +35F: 40%–50% quartz and sanidine crystals, 30%–40% 10%–15% volcanic lithic grains.	Qbo	

Borehole Lithologic Log (continued)

Borehole ID: R-44	**TA:** 5	**Page:** 3 of 16	
Depth (ft bgs)	Lithology	Lithologic Symbol	Notes
145–155	Tuff—white (10YR 8/1), poorly welded, pumiceous, crystal-rich, lithic-bearing to lithic-rich, moderate volcanic ash matrix. 145—155 ft +10F: 40%–50% white vitric quartz-sanidine-phyric pumice fragments; 40%–50% broken, angular and subangular gray and pinkish dacites. +35F: 50%–60% quartz and sanidine crystals, 30%–40% glassy pumice fragments, 10%–15% volcanic lithic fragments. 125–135 ft 10%–20% light gray dacite fragments (i.e., xenoliths) up to 25 mm in diameter.	Qbo	
155–170	Tuff—pale yellowish tan (10YR 7/4), poorly welded, pumiceous, lithic-rich, crystal-rich, abundant ash matrix. 155—160 ft +10F: 40%–50% angular lithics (up to 9 mm) of intermediate volcanic compositions (porphyritic dacites are common); 40%–50% white to pink glassy pumices, quartz-sanidine-phyric. 160–170 ft contains 65%–70% angular, porphyritic biotite-phyric dacite lithic fragments (up to 18 mm in diameter).	Qbo	
170–175	Tuff—white (10YR 8/1), poorly welded, pumiceous, lithic-bearing, crystal-rich, abundant volcanic ash matrix. 170—175 ft +10F: 100% white glassy pumices, quartz- and sanidine-phyric. +35F: 20%–30% glassy pumice fragments, 30%–40% quartz and sanidine crystals, 30%–40% dacitic grains.	Unit 1g, Qbt	
175-185	Tuffaceous/volcaniclastic sediments (?? Tuff ?? It would be unusual to find tuffaceous sediments in the middle of the Qbo ash-flow tuffs.) —pale pinkish tan (2.5YR 8/4) to white (10YR 8/1) poorly consolidated, silty fine to medium sand and pebble gravels. 175–180 ft+10F: pale pinkish tan (2.5YR 8/4), 40%–50% broken/angular volcanic lithic fragments/clasts (up to 12 mm in diameter) composed of dacite and flow-banded rhyolite; 40%–50% vitric pumices grains, quartz- and sanidine-phyric. 180-185 ft +10F: white (10YR 8/1), 90%–95% broken/angular volcanic lithic fragments/clasts (up to 11 mm in diameter) of diverse composition: pink and gray dacites, flow-banded rhyolites, dark brown andesite(?), minor vesicular basalt; 5%–10% vitric white and pinkish pumices, quartz- and sanidine-phyric.	Qbo	

Borehole Lithologic Log (continued)

Borehole ID: R-44	**TA:** 5	**Page:** 4 of 16	
Depth (ft bgs)	Lithology	Lithologic Symbol	Notes
185-220	Tuff—pale orange tan (5YR 7/4), poorly welded, pumiceous, lithic-poor, crystal-rich. 185—195 ft WR/+10F: 97%–99% white to pale orange (i.e., limonite-stained) vitric quartz-sanidine-phyric pumice fragments (up to 18 mm in diameter), commonly with black specks of secondary Fe-oxide; 1%–3% dacite lithic fragments. +35F: 20%–30% glassy pumice fragments, 50%–60% quartz and sanidine crystals, 20%–30% volcanic lithic grains. 195'–200 ft WR: more abundant pale orange volcanic ash matrix. +10F: contains 25%–35% biotite-phyric dacite lithics. 200–215 ft+10F: similar to 185—190 ft. 215–220 ft +10F: 85-90% white to pale orange vitric quartz-sanidine-phyric pumice fragments (up to 13 mm in diameter); 10%–15% volcanic lithic fragments.	Qbo	
220–240	Tuff—pale orange tan (7.5YR 7/6), poorly welded, pumiceous, lithic-rich, crystal-rich, locally abundant ash matrix. 220–230 ft WR: abundant pale orange volcanic ash matrix. +10F: 75%–80% white to pale orange vitric quartz-sanidine-phyric pumice fragments (up to 14 mm in diameter), frequently exhibiting black specks of secondary Fe-oxide; 20%–25% pinkish to light gray biotite-dacite lithic fragments. +35F: 40%–50% glassy pumice fragments, 30%–40% quartz and sanidine crystals, 5%–10% volcanic lithic grains. 230—235 ft +10F: 60%–70% white and pale orange glassy pumice, quartz- and sanidine phyric, commonly with abundant dark Fe-oxide specks; 30%–40% subangular volcanic lithics (up to 8 mm in diameter) composed of various volcanic lithologies: pink and gray dacites, banded dacites, dark porphyritic vitrophyre. 235—240 ft +10F: similar to 230—235 ft.	Qbo	
240–250	Tuff—very pale orange tan (7.5YR 8/4), poorly welded, pumiceous, lithic-poor, crystal-rich. 240–250 ftWR: locally with abundant pale orange volcanic ash matrix. +10F: 99%–100% white to pale orange-pink vitric quartz-sanidine-phyric pumice fragments (up to 25 mm in diameter) with locally abundant specks of dark secondary Fe-oxide; <1% dacite lithics. +35F: 50%–60% quartz and sanidine crystals; 20%–30% dacite grains; 20%–30% pumice fragments.	Qbo	

Borehole Lithologic Log (continued)

Borehole ID: R-44	**TA:** 5	**Page:** 5 of 16	
Depth (ft bgs)	Lithology	Lithologic Symbol	Notes
250–265	Tuff—pinkish white (7.5YR 8/2), poorly welded, pumiceous, lithic-bearing to lithic rich, crystal-rich. 250—265 ft +10F: 65%–75% white to pale pink glassy quartz-sanidine-phyric pumice fragments (up to 14 mm in diameter) with locally abundant specks of dark secondary Fe-oxide; 35%–25% angular fragments (up to 10 mm in diameter) composed of dark and light gray dacites. +35F: 30%–40% quartz and sanidine crystals; 25%–35% dacite lithic grains; 30%–40% pumice fragments.	Qbo	
265–285	Tuff—pale pinkish white (7.5YR 8/2), poorly welded, pumice-rich, lithic-bearing, crystal-rich. 265—270 ft +10F: 95%–98% white to pale pinkish white, fibrous, vitric, quartz-sanidine-phyric pumice fragments (up to 23 mm in diameter); 2%–5% gray and light pink dacite lithics (up to 6 mm in diameter). +35F: 50%–60% quartz and sanidine crystals; 15%–25% dacitic lithic fragments with minor basalt, black vitrophyre; 15%–25% pumice grains. 270–275 ft+10F: note increased abundances and varieties of lithics–80% vitric pumices; 20% mixed volcanic (dacite, basalt, rhyolite) fragments (up to 7 mm in diameter). 275–285 ft no cuttings available for description.	Qbo	
285–296	Tuff—pale pinkish white (7.5YR 8/2), poorly welded, pumice-rich, lithic-poor, crystal-poor. 285–296 ft WR: silty matrix. +10F: 95%–98% white fibrous, vitric, quartz-sanidine-phyric pumice fragments (up to 22 mm in diameter); 2%–5% dacite lithics. +35F: Note poor representation of this sample size fraction, 50%–60% pumice fragments; 10%–15% quartz and sanidine crystals; 20%–25% volcanic lithic fragments (dacite, black vitrophyre).	Qbo	The Qbo-Qbog contact is placed at 296 ft bgs, based on interpretation of natural gamma geophysical log data.
296–313	**GUAJE PUMICE BED:** Tuff— white (5YR 8/1) to very pale orange (7.5YR 7/6), pumice-rich, lithic-poor, crystal-poor, no apparent volcanic ash matrix. 296—305 ft WR/+10F: 97%–98% white to locally yellowish (i.e., weak limonite-staining) vitric pumices (up to 22 mm in diameter); 2%–3% dacitic lithic fragments (up to 20 mm in diameter). 305—315 ft WR/+10F: 100% white and locally pinkish vitric pumices (up to 22 mm in diameter); phenocryst-poor, having pristine, very fresh appearance. 310—315 ft +35F: no returns of this sample size fraction.	Qbog	The Guaje Pumice Bed, from 296 to 313 ft bgs, is estimated to be 17 ft thick. The contact between Qbog and underlying basalt-rich sediments is placed at 313 ft bgs, based on interpretation of natural gamma geophysical log.

Borehole Lithologic Log (continued)

Borehole ID: R-44	**TA:** 5	**Page:** 6 of 16	
Depth (ft bgs)	Lithology	Lithologic Symbol	Notes
313–340	**BASALT-RICH SEDIMENTS:** Pale orange tan (7.5YR 7/6) siltstone to silty fine- to medium-grained sandstone with pebble gravel. 313–325' ft +10F: 60% orange-tan fragments of indurated siltstone with fine basalt grains; 20% fragments of vitric pumice; 20% broken to subangular clasts of hornblende-dacite and minor black basalt scoria. 325—330 ft +10F: 100% large pebbles (up to 20 mm in diameter) subrounded clasts of black basalt scoria with adhered rinds of orange-tan siltstone. +35F: 80% siltstone fragments, 10% pumice fragments plus quartz and sanidine crystals, 10% basalt and dacitic grains. 330–340 ft +10F: No sample recovery.	N/S	Unassigned basalt-rich volcaniclastic sediments, encountered from 313 to 344 ft bgs, are estimated to be 31 ft thick.
340–344	Pale pinkish tan (7.5YR 8/4) siltstone and fine-grained sandstone with subordinate chips of basalt-bearing siltstone similar to 340–345 ft. Coarse- to medium-grained sand with pebble gravel. 340–345 ft WR: 100% siltstone fragments with basalt pebbles. +10F: 40% silt-coated basalt pebbles (up to 15mm), 60% siltstone and fine-grained sandstone fragments with basalt, dacite, and quartzite granules.	N/S	Estimated contact between basalt-rich sediments and underlying Tb4 is placed at 344 ft bgs, based on natural gamma log interpretation.
344–375	**CERROS DEL RIO BASALT:** Basalt lava–medium gray (GLEY1 6/0) strongly vesicular, porphyritic with aphanitic groundmass, clinopyroxene (cpx), plagioclase and minor olivine present as phenocrysts. 344–355 ft +10F/+35F: 100% basalt chips, phenocrysts 2%–4% by volume, anhedral (up to 3 mm in diameter) dark brown to opaque cpx and minor small (up to 1 mm in diameter) green olivine; olivine commonly intergrown with cpx. 355–375 ft +10F/+35F: 100% basalt chips, compositionally similar to 344–355 ft; degree of vesicularity diminishing rapidly downward.	Tb4	The Cerros del Rio basalt section, encountered from 344 to 707 ft bgs, is estimated to be 363 ft thick. 344–355 ft represents the strongly vesicular top of cpx-basalt flow.
375–392	Basaltic cinder deposits–dark reddish brown (2.5YR 4/4) to orange brown (2.5YR 5/6) scoriaceous basalt. 375–395 ft WR/+10F: 95%–97% scoriaceous basalt chips and orange-brown ferruginous cinders (up to 20 mm in diameter); 3%–5% vesicular crystal-poor cpx-basalt chips, trace locally abundant white amygdaloidal zeolite (?) and zeolite-encrusted scoria.	Tb4	

Borehole Lithologic Log (continued)

Borehole ID: R-44	**TA:** 5	**Page:** 7 of 16	
Depth (ft bgs)	Lithology	Lithologic Symbol	Notes
392–435	Basalt lava–light gray (GLEY1 7/0), weakly vesicular to massive, phenocryst-poor, aphanitic groundmass, clinopyroxene-bearing basalt, moderately altered groundmass. 392–435 ft+10F/+35F: 99% basalt chips of altered cpx-phyric basalt, minor basalt scoria; phenocrysts (2%–4% by volume) of anhedral clinopyroxene (up to 2 mm in diameter) and minor small (up to 1 mm in diameter) green olivine; olivine and cpx commonly intergrown.	Tb4	392–435 ft characteristic of this lava is the strong recrystallization of groundmass feldspars yielding bleached coloration and webs/tiny veinlets of clay; dusty appearance and rounding (i.e., apparent milling because of the drilling process) of chips.
435–468	Basalt lava–light gray (GLEY1 7/1) massive to weakly vesicular, weakly porphyritic with aphanitic GM, groundmass feldspar strongly altered. 435–455 ft +10F: 100% basalt chips that are commonly rounded or milled by drilling process, sparse phenocrysts 2%–3% by volume of anhedral dark brown clinopyroxene (up to 1 mm in diameter) and lesser small green translucent olivine (<1 mm in diameter); cpx and olivine are commonly intergrown. Groundmass is distinctive in that the felty feldspars are bleached and recrystallized. 455–460 ft WR/+10F: 100% basalt chips, edges milled during drilling process. Olivine becoming more abundant and large (up to 2 mm in diameter) as euhedral phenocrysts downward in section. 460–468 ft: Similar to 435–455 ft.	Tb4	
468–471	Basaltic lava and cinder deposits–varicolored light gray (GLEY1 7/1) and reddish brown (10YR 5/6) mixed basalts with altered GM and scoriaceous basalt. WR: finely milled basalt chips with abundant white powder produced from altered feldspars. 468–471 ft: +10F: 70% angular to rounded (milled) basalt chips, massive to weakly vesicular, phenocrysts 3%–5% by volume anhedral olivine (up to 3 mm in diameter) and lesser small (1 mm in diameter) cpx; black cpx commonly occurs as rinds/overgrowths of olivine. GM strongly bleached; 30% angular chips of brick-red scoriaceous basalt.	Tb4	

Borehole Lithologic Log (continued)

Borehole ID: R-44	**TA:** 5	**Page:** 8 of 16	
Depth (ft bgs)	Lithology	Lithologic Symbol	Notes
471–490	Basalt lava–light gray (GLEY1 6/1) basalt chips, massive, altered groundmass; minor reddish (10YR 5/6) basalt scoria. 471–475 ft WR/+10F: 75%–80% abraded/milled chips olivine+cpx-basalt, groundmass strongly altered. 20%–25% broken chips of ferruginous basalt scoria. 475–485 ft WR: abundant finely ground white powder; basalt chips abraded/milled. +10F/+35F: 95%–97% chips of olivine-cpx porphyritic basalt, phenocrysts of anhedral pale green olivine (up to 2 mm in diameter) and small (up to 1 mm in diameter) black cpx, groundmass feldspars are bleached/recrystallized. 3%–5% chips of hematite-stained basalt scoria. 485–490 ft+10F: Locally more abundant (15%–20% by volume) basalt scoria chips.	Tb4	
490–505	Basalt lava–light gray (GLEY1 6/1) moderately altered massive to weakly vesicular olivine-cpx basalt, with moderately to slightly altered groundmass. 490–505 ft WR/+10F: 99%–100%% massive basalt chips, phenocrysts (2%–4% by volume) of small (1 mm in diameter) olivine and cpx; groundmass feldspar altered/recrystallized/bleached; up to 1% reddish brown scoria chips.	Tb4	
505–530	Basaltic cinders and volcaniclastic sediments–varicolored light gray (GLEY 6/1) and brick-red (2.5 YR 5/8), mixed massive basaltic lava and scoria/cinders. 505–515 ft WR/+10F: 50% light gray chips of cpx- and minor olivine-phyric basalt; groundmass feldspar recrystallized/bleached. 50% hematitic vesicular basalt and glassy scoriaceous cinders (up to 15 mm in diameter). +35F: moderately abundant fragments of volcaniclastic sediments. 515–530 ft +10F/+35F: Mixed basalt fragments of brick-red glassy scoria, minor dacitic detritus and fragments of fine-grained volcaniclastic sediments.	Tb4	505–530 interval possibly of hydromagmatic origin.
530–535	Pumiceous volcaniclastic sediments–varicolored light gray (GLEY1 6/1), reddish brown (10YR 4/8) and white (10YR 8/1) fragments of basalt, pumice and brown scoria. 530–535 ft WR +35F/+10F: 55%–65% chips and partly subrounded detrital grains of weakly vesicular cpx-bearing basalt. 20%–25% fragments of weathered quartz- and sanidine-phyric pumice, detrital grains of dacite.	Tb4	530–535 ft some evidence of reworked volcanic materials indicated by local subrounding of basalt, pumice, and dacite fragments.

Borehole Lithologic Log (continued)

Borehole ID: R-44	**TA:** 5	**Page:** 9 of 16	
Depth (ft bgs)	Lithology	Lithologic Symbol	Notes
535–560	Basalt lava–reddish gray (10YR 5/1) massive to weakly vesicular cpx-basalt, porphyritic with aphanitc groundmass, groundmass feldspars weakly altered and bleached. 535–540 ft WR/+10F: 100% angular basalt chips, phenocrysts (3%–5% by volume) of anhedral opaque black cpx (up to 3 mm in diameter); groundmass weakly bleached; minor local white calcite on fractured surfaces.	Tb4	
560–575	Basalt lava–light gray (GLEY1 7/1) massive to weakly vesicular cpx-basalt, porphyritic with aphanitc groundmass that is moderately altered. 560–565 ft +10F/+35F: 95-97% angular chips of cpx-phyric basalt, cpx-phenocrysts (2%–4% by volume); groundmass moderately recrystallized/bleached. 3%–5% subangular detrital granules/grains of pumice and quartzite. 565–575 ft+10F/+35F: minor to trace fragments of fine-grained volcaniclastic sandstone.	Tb4	
575–590	Basalt lava–light gray (GLEY1 7/1) massive cpx-basalt, porphyritic with strongly altered aphanitic groundmass. 575–580 ft +10F/+35F: 80%–85% subrounded (i.e., milled because of drilling) chips of cpx-basalt; 15%–20% detrital grains of pumice and quartz crystal, also fragments of pale tan clay and fine-grained sandstone. 580–590 ft+10F/+35F: trace abundances of pale orange clay.	Tb4	
590–650	Basalt lava–light gray (GLEY1 7/1) massive to weakly vesicular cpx- and ol-phyric basalt, porphyritic with moderately strongly altered aphanitic groundmass. 590'–610 ft +10F/+35F: 100% subrounded (i.e., milled because of drilling) chips of basalt, phenocrysts (3%–5% by volume) of subhedral cpx (up to 1 mm in diameter) and lesser green olivine (up to 4 mm in diameter) that are commonly rimmed by black cpx; groundmass altered and bleached; trace pale tan clay fragments. 610–620 ft +10F/+35F: 99%–100% cpx-basalt chips with strongly altered groundmass; <1% detrital grains of ferruginous scoria, quartzite, and tan clay fragments. 620–630 ft +10F: olivine phenocrysts frequently exhibit cpx overgrowths. 630–650 ft +10F/35F: 98%–99% milled cpx-olivine basalt chips exhibiting strongly altered groundmass; olivine phenocrysts frequently have cpx overgrowths 1%–2% detrital grains of pumice, quartz crystal and fragments of very fine-grained silty sandstone.	Tb4	647–648 ft possible thin sedimentary interlayer containing pumice fragments and basalt granules.

Borehole Lithologic Log (continued)

Borehole ID: R-44	**TA:** 5	**Page:** 10 of 16	
Depth (ft bgs)	Lithology	Lithologic Symbol	Notes
650–665	Basalt lava–light gray (GLEY1 7/1) massive olivine-phyric basalt, weakly porphyritic with altered aphanitic groundmass. 650–665 ft WR/+10F: 100% subrounded (i.e., milled because of drilling) chips of ol-basalt, phenocrysts (1%–3% by volume) of small anhedral green olivine and trace cpx; groundmass moderately to strongly altered and bleached; minor white clay on fracture surfaces; trace fragments of light pink claystone.	Tb4	
665–685	Basaltic volcaniclastic sediments–varicolored white (2.5YR 8/1), medium gray (GLEY16/1) and reddish brown (2.5YR 4/6), mixed detrital clasts/grains of pumice and basalt 665–670 ft +10F: 100% subangular to subrounded detrital pebbles/clasts (up to 17 mm in diameter) composed mostly of glassy quartz- and sanidine-phyric pumices with subordinate amounts of gray massive and reddish scoriaceous basalt. 670%–685 ft +10F: 40%–50% gray basaltic detrital clasts (locally rounded) and chips; 40%–50% pale pinkish porphyritic, vitric pumices and fragments of welded tuff (crystal-rich, lithic-bearing, pumiceous).	Tb4	665–685 ft apparent sedimentary interlayer between Tb4 basalt flows.
685–698	Basalt lava—medium gray (GLEY1 6/1) massive basalt, olivine-phyric, phenocryst-poor, moderate very fine-grained alteration of groundmass feldspars. 685–698 ft WR/+10F: 99%–100% angular basalt chips, phenocrysts (1%–2% by volume) of pale green anhedral olivine (up to 1mm in diameter); groundmass feldspars moderately recrystallized and bleached; minor fragments of white clay or claystone.	Tb4	
698–707	Basalt lava and volcaniclastic sediments—varicolored medium gray (GLEY1 6/1) to light pinkish tan (2.5YR 8/3), mostly chips/detritus of olivine-basalt and lesser volcaniclastic detritus. 698–707 ftWR/+10F: 80%–90% angular chips and subrounded detrital granules of olivine-phyric basalt; 10%–20% subangular to subrounded detrital volcanic clasts (up to 7 mm in diameter) including gray dacite, white pumices, red scoriaceous cinders; note trace white clay adhered to detrital basaltic grains.	Tb4	698–707 ft apparent rubbly base of basaltic flow with intercalated thins volcaniclastic sedimentary layer. Estimated Tb4-Tpf contact placed at 707 ft bgs.
707–715	**PUYE FORMATION:** Volcaniclastic sediments—varicolored light gray (GLEY1 7/0) and pale tan (5YR 8/3) coarse to medium gravels with fine-grained sand to silty sand matrix, subangular to rounded clasts of diverse volcanic compositions 707–715 ft WR/+10F: 40% subrounded light and dark gray olivine-basalt granules (up to 10 mm in diameter); 60% subangular to subrounded pebbles and broken clasts (up to 22 mm in diameter) composed of dacites, minor pinkish pumice and fragments of indurated dacitic silty sandstone.	Tpf	Puye volcaniclastic sediments, encountered from 707 to 1005 ft bgs, are estimated to be 298 ft thick.

Borehole Lithologic Log (continued)

Borehole ID: R-44	**TA:** 5	**Page:** 11 of 16	
Depth (ft bgs)	Lithology	Lithologic Symbol	Notes
715–735	Volcaniclastic sediments—varicolored pale pinkish gray (5YR 7/2) to light gray (GLEY1 7/1) coarse to medium gravels with fine-grained sandy to silty matrix, subangular to rounded clasts of dacite and minor basalt. 715–735 ft WR/+10F: 90%–95% broken and subrounded to rounded clasts (up to 25 mm in diameter) light gray bt- and hbn-phyric dacites; 5%–10% fragments to indurated fine-grained sandstone. +35F: subangular to subrounded grains: 75%–80% dacites; 20%–25% basalt; 3%–5% quartz and sanidine crystals; trace red scoria.	Tpf	
735–750	Volcaniclastic sediments—light gray (GLEY1 7/1) coarse gravels with fine- to medium-grained sandstone, subangular to subrounded clasts dominantly of dacites. 10F: broken and subrounded clasts (up to 19 mm in diameter) mostly porphyritic dacites; 10%–15% reddish vesicular basalt, minor weathered pumices.	Tpf	
750–760	Volcaniclastic sediments—light gray (GLEY1 7/1) to pinkish gray (5YR 7/2) medium- to coarse-grained sandstone with minor pebble gravel, detritus composed dominantly of porphyritic hbn- and bt-dacites. 750—760 ft WR/+10F: broken and subrounded clasts (up to 13 mm in diameter), 70% white and grayish bt-phyric dacites 30% fragments of silty fine-grained volcanic sandstone.	Tpf	
760–785	Volcaniclastic sediments—varicolored light gray (GLEY1 7/1) to pinkish gray (5YR 7/2) coarse gravels and medium- to coarse-grained sandstones, detrital clasts composed of various volcanic lithologies, predominantly dacites. 760–770 ft WR/+10F: subangular to subrounded clasts (up to 17 mm in diameter) light gray to pinkish porphyritic dacites, minor dark brown andesite. 770–785 ft +10F: very coarse gravels indicated by abundantly large (up to 20 mm in diameter) broken chips of porphyritic dacites, minor dark gray vitrophyre, and minor fragments of indurated sandstone.	Tpf	
785–795	Volcaniclastic sediments—light pinkish gray (7.5YR 7/1) very coarse- to medium-grained sandstones with small pebbles, predominantly dacitic detritus. 785—795 ft WR/+10F: subangular to subrounded granules (up to 4 mm in diameter) almost exclusively of gray porphyritic dacites.	Tpf	

Borehole Lithologic Log (continued)

Borehole ID: R-44	**TA:** 5	**Page:** 12 of 16	
Depth (ft bgs)	Lithology	Lithologic Symbol	Notes
795–815	Volcaniclastic sediments—light pinkish gray (7.5YR 7/1) very coarse- to medium-grained sandstones with silt, composition of grains predominantly dacitic. 795—815 ft WR/+10F: subangular to subrounded grains and granules mostly of gray to pinkish gray dacites, lesser abundances other volcanics.	Tpf	795–815 ft silt percentage of silt increasing downward in this interval.
815–840	Volcaniclastic sediments—varicolored light pinkish gray (GLEY1 7/0) to light pinkish gray (7.5YR 7/1) coarse gravels and medium- to coarse-grained sandstones; clast composition predominantly dacitic. 815–820 ft WR/+10F: subangular to subrounded clasts (up to 18 mm) mostly gray porphyritic dacites, minor orange and dark gray porphyritic vitrophyre, trace cpx-phyric basalt. 820–830' ftWR/+10F: clast composition more diverse: gray dacites, white bt-phyric dacite, gray and white dacitic(?) vitrophyre. 830–840 ft WR/+10F: subangular to subrounded clasts (up to 13 mm) almost exclusively light gray dacites, trace white bt-dacite.	Tpf	
840-860	Volcaniclastic sediments—pale pinkish tan (7.5YR 7/3) fine to coarse gravels and fine- to medium-grained sandstone with silt; clast composition predominantly dacitic. 840–850 ft WR: silt-rich matrix. +10F: broken and subangular to subrounded granules and small pebbles (up to 12 mm) mostly of light gray porphyritic dacites, minor white bt-phyric dacite. 850–860 ft texturally similar to 840–850 ft; contains also 2%–3% fragments of medium- to coarse-grained silty sandstone, also minor porphyritic vitrophyre.	Tpf	
860–870	Volcaniclastic sediments—pale pinkish gray (7.5YR 7/2) fine to medium gravel and medium- to coarse-grained sandstone, predominantly dacitic detritus. 860–870 ft WR/+10F: broken and subangular to subrounded clasts (up to 11 mm in diameter) composed almost exclusively of light gray porphyritic dacites, minor white bt -phyric dacite matrix. +10F	Tpf	
870–875	Volcaniclastic sediments—pale pinkish gray (7.5YR 7/2) fine-grained to very coarse-grained sandstone to silty sandstone with gravel, clasts predominantly dacitic. 870–875 ft WR: moderately silty matrix. +10F: broken and subangular to subrounded clasts (up to 16 mm in diameter) of gray porphyritic dacite, white bt-bearing dacite, and minor chips of indurated sandstone.	Tpf	

Borehole Lithologic Log (continued)

Borehole ID: R-44	**TA:** 5	**Page:** 13 of 16	
Depth (ft bgs)	Lithology	Lithologic Symbol	Notes
875–890	Volcaniclastic sediments—pale pinkish gray (7.5YR 7/2) fine to coarse gravel and medium- to coarse-grained sandstone, clasts predominantly dacitic. 875–885 ft WR/+10F: broken and subangular clasts (up to 10 mm in diameter) of gray porphyritic dacites, pink dacites, white bt-phyric dacite(?); minor fragments of indurated medium-grained sandstone. 885–890 ftWR/+10F: broken to subrounded detrital clasts (up to 18 mm in diameter) of light gray dacites and reddish brown hornblende (hbn)-biotite (bt)-bearing dacites.	Tpf	
890–900	Volcaniclastic sediments—very pale pinkish gray (7.5YR 7/1) fine- to coarse-grained sandstones with gravel to silty sand with gravel, clasts predominantly dacitic. 890–900 ftWR: silty matrix. +10F: broken and subangular clasts (up to 15 mm in diameter) composed of porphyritic hbn-dacite and minor bt-bearing dacite.	Tpf	
900–905	Volcaniclastic sediments—pale pinkish gray (7.5YR 7/1) to very light gray (GLEY1 7/0) fine- to coarse- grained sandstones, dacitic detritus. 900–905 ft +10F: broken and subrounded granules (up to 5 mm in diameter) of light gray hbn-dacite and minor white bt-phyric dacite(?).	Tpf	
905–920	Volcaniclastic sediments—light gray (GLEY1 7/0) to pale pinkish gray (7.5YR 7/1) coarse gravels with medium- to coarse-grained, clasts, predominantly dacitic. 905–920 ft WR/+10F: broken and subangular to subrounded clasts (up to 17 mm in diameter) composed mainly of light gray porphyritic hbn-dacites, minor bt-bearing dacite.	Tpf	
920–940	Volcaniclastic sediments—very pale pinkish gray (7.5YR 7/1) medium to coarse gravels and silty medium- to coarse-grained sandstones, dacite-rich detritus. . 920–935 ft WR: moderately silty matrix. +10F: broken and subangular clasts (up to 10 mm in diameter) composed predominantly of light gray hbn-dacites and minor white bt-bearing dacite. 935–940 ft WR: silty fine sand with gravel. +10F: compositionally similar to 920—935 ft. +35F: abundant fragments very fine-grained silty sandstone.	Tpf	

Borehole Lithologic Log (continued)

Borehole ID: R-44	**TA:** 5	**Page:** 14 of 16	
Depth (ft bgs)	Lithology	Lithologic Symbol	Notes
940–960	Volcaniclastic sediments—pale pinkish gray (7.5YR 7/1) medium to coarse gravels and coarse-grained sandstones, dacite-rich detritus. 940–950 ft +10F: broken and subangular clasts (up to 12 mm in diameter) composed predominantly of light gray porphyritic hbn-dacites and minor bt-bearing dacite. 950–960 ft +10F: broken and subrounded clasts (up to 13 mm in diameter) of hbn- and bt-phyric dacites, minor orange pink rhyodacite(?).	Tpf	
960–985	Volcaniclastic sediments—pale pinkish gray (7.5YR 7/1) fine gravels and fine- to medium-grained sandstone with silt, predominantly dacitic detritus. 960–970 ft WR: moderately silty matrix. +10F: broken and subangular to subrounded clasts (up to 6 mm in diameter) composed predominantly of hbn-dacites and minor bt-bearing dacite, trace vesicular rhyodacite(?), and indurated sandstone fragments. 970–975 ft WR: fine to coarse sand with pebble gravel, silty matrix. +10F: broken and subangular clasts (up to 8 mm in diameter) hbn- and tt-bearing dacites. 975–980 ft WR: fine gravel and fine- to medium-grained sandstone. +10F: subangular to subrounded clasts (up to 10 mm in diameter) composed of light gray, pinkish and white hbn- and bt-bearing dacites.	Tpf	
985–990	Volcaniclastic sediments—pale pinkish gray (7.5YR 7/1) coarse gravels and medium to very coarse-grained sandstone, dacitic detritus. 985–990 ft +10F: subangular to subrounded clasts (up to 18 mm in diameter) composed of light gray hbn-dacites and minor white bt-bearing dacite.	Tpf	
990–1005	Volcaniclastic sediments—pale pinkish gray (7.5YR 7/1) fine- to very coarse grained sandstone with some pebble gravel, dacitic detritus. 990–1005 ft +10F: broken and subangular clasts (up to 15 mm in diameter) composed predominantly of coarsely porphyritic light gray hbn-dacites and lesssr bt-bearing dacite.	Tpf	Estimated contact between Puye volcaniclastic sediments and underlying Miocene pumiceous sediments is placed at 1005 ft bgs.

Borehole Lithologic Log (continued)

Borehole ID: R-44	**TA:** 5	**Page:** 15 of 16	
Depth (ft bgs)	Lithology	Lithologic Symbol	Notes
1005–1010	**MIOCENE PUMICEOUS SEDIMENTS:** Pumiceous volcaniclastic sediments—varicolored light gray (GLEY1 7/0) to white (5YR 8/1) fine to very coarse sand with granules, detritus of mixed pumice, and dacite. 1005–110 ft WR/ +10F: broken and subangular granule-size clasts (up to 7 mm in diameter)composed of 60% pumice fragments (glassy, phenocryst-poor), 40% light gray dacite with minor aphyric rhyolite.	Tjfp	Miocene pumice-rich volcaniclastic sediments, encountered from 1005 to 1088 ft bgs, are estimated to be 83 ft thick.
1010–1020	Pumiceous volcaniclastic sediments—pinkish white (5YR 8/2) fine to coarse sand with pebble gravel and silt, mixed pumice, and dacitic detritus. 1010–1015 ft WR: moderately silty matrix. +10F: 100% pumice fragments that are vitric and phenocryst-poor. +35F: 80%–85% pumices; 15%–20% gray dacite grains. 1015–1020 ft +10F: broken and subangular clasts, 70%–75% white glassy phenocryst-poor pumices (up to 10 mm in diameter); 25%–30% light gray dacite and white rhyolites.	Tifp	
1020–1045	Pumiceous volcaniclastic sediments—varicolored pinkish white (5YR 8/2) to very light gray (GLEY1 7/0) fine (i.e., pebble-size clasts) gravel and very coarse sand, mixed detritus of pumice, and dacite. 1020–1025 ft WR/+10F: 60%–70% white glassy, phenocryst-poor pumice fragments; 10%–20% subangular to subrounded dacite and lesser rhyodacite clasts (up to 13 mm in diameter); 7%–10% fragments of fine- to medium-grained pumiceous sandstone. 1025–1030 ft WR/+10F: 65%–70% white glassy pumice fragments; 15%–20% pink tan pumiceous sandstone fragments; 10%–15% dacite clasts. 1030–1035 ft WR/+10F: 85-95% white glassy phenocryst-poor (rare quartz, biotite) pumice fragments; 5%–10% light pinkish tan pumiceous sandstone fragments; 3%–5% dacitic detritus. 1035–1045 ft WR/+10f: 60%–70% white glassy pumices; 15%–20% pale pink tan pumiceous sandstone fragments, 1%–20% subangular clasts (up to 12 mm in diameter) mixed volcanic detritus (dacite, andesite, basalt).	Tifp	

Borehole Lithologic Log (continued)

Borehole ID: R-44	**TA:** 5	**Page:** 16 of 16	
Depth (ft bgs)	Lithology	Lithologic Symbol	Notes
1045–1075	Pumiceous volcaniclastic sediments—varicolored pinkish white (5YR 8/2) to medium gray (GLEY1 5/0) fine to coarse sand with pebble gravel mixed detritus composed of pumice and a variety of volcanic lithologies. 1045–1055 ft WR/+10F: 50%–60% white vitric pumices (both phenocryst-poor and biotite-bearing varieties present); 30%–40% subangular clasts (up to 10 mm in diameter) mixed andesite and dacite; 3%–5% pink tan fragments pumiceous sandstone. 1055–1065 ft WR/+10F: 40%–50% white vitric pumices; 40%–50% mixed volcanic detritus (dacite, andesite, basalt). 1065–1070 ft WR/+10F: 50-60% white pumices; 30%–40% pinkish tan fine-grained sandstone with abundant pumice grains; 10–15% mixed volcanic detritus. 1070–1075 ft WR: silty matrix. +10F: 50%–60% white pumices; 25%–35% mixed volcanic detritus; 10%–15% pumiceous sandstone fragments.	Tifp	
1075–1088	Pumiceous volcaniclastic sediments—varicolored, white (%YR 8/2), pale pinkish tan (5YR 7/3) and medium gray (GLEY1 5/0) fine to medium gravels with fine to coarse sand, detritus predominantly of dacite and lesser pumices. 1075–1088 ft WR/+10F: 50%–60% broken and subangular clasts (up to 15 mm in diameter) of dacite and minor andesite; 25%–30% white vitric pumice fragments; 10%–20% indurated pumiceous sandstone fragments.	Tifp	Estimated contact between Miocene pumiceous sediments and underlying Miocene riverine sediments is placed at 1088 ft bgs.
1088–1094	**MIOCENE RIVERINE SEDIMENTS:** Axial-river gravel deposits—varicolored medium gray (GLEY1 5/0) to pink tan (5YR 7/4) fine to coarse gravels with fine to coarse sand, commonly rounded detrital clasts composed of diverse volcanic and Precambrian quartzo-feldspathic lithologies. +10F: 20%–30% well-rounded quartzite and granitic pebbles (up to 22 mm in diameter); 70%–80% broken and well rounded volcanic clasts (up to 13 mm in diameter) composed of dark gray fine-grained andesite and varieties of dacite.	Tcar	Miocene riverine gravel deposits were encountered at the bottom of the R-44 borehole through the 6-ft interval, from 1088 to 1094 ft bgs (TD). Note: R-44 borehole drilling was concluded at a TD of 1094 ft bgs.

Borehole Lithologic Log (continued)

ABBREVIATIONS

5YR 8/4 = Munsell rock color notation where hue (e.g., 5YR), value (e.g., 8), and chroma (e.g. 4) are expressed. Hue indicates soil color's relation to red, yellow, green, blue, and purple. Value indicates soil color's lightness. Chroma indicates soil color's strength.

% = estimated per cent by volume of a given sample constituent

bgs = below ground surface

bt = biotite

cpx = clinopyroxene

ft = feet

GM = groundmass

hbn = hornblende

N/S = no assigned symbol for geologic unit

ol = olivine

Qal = Quaternary Alluvium

Qbt 1g = vitric unit 1g of the Tshirege member of Bandelier Tuff

Qct = Cerro Toledo Interval

Qbo = Otowi Member of Bandelier Tuff

Qbog = Guaje Pumice Bed

Tb4 = Cerros del Rio Basalt

Tpf = Puye Formation

Y = Yellow

YR = Yellow red

+10F = plus No. 10 sieve sample fraction

+35F = plus No. 35 sieve sample fraction

Appendix B

Groundwater Analytical Results

B-1.0 SAMPLING AND ANALYSIS OF GROUNDWATER AT R-44

A total of 15 groundwater samples were collected at the regional aquifer well R-44; 11 samples during drilling and 4 samples during well development. Two groundwater samples potentially were collected from the vadose zone and 9 from the regional aquifer during drilling. The two vadose zone samples most likely consist of municipal water used during drilling, based on very small volumes of water produced from the borehole. In addition, low concentrations of key contaminants, including chloride, chromium, nitrate, and sulfate measured in the borehole samples, were not consistent with those measured at wells MCOI-4, MCOI-5, MCOI-6, SCI-1, SCI-2, R-28, and R-42. Perched intermediate-depth groundwater was not encountered during drilling at R-42 and R-28. The two vadose zone water samples were not analyzed for tritium, another key contaminant found in groundwater in Mortandad Canyon. The lack of tritium analysis on the two water samples places some small uncertainty on the occurrence of perched intermediate groundwater within the deep vadose zone at well R-44. During aquifer performance (pumping) testing, six groundwater samples were collected from screen 1 between a depth interval ranging from 895 to 905 ft below ground surface (bgs), and six groundwater samples were collected from screen 2 between a depth interval of 985 and 995 ft bgs. All of the groundwater samples were collected within the Puye Formation. The filtered samples were analyzed for cations, anions, perchlorate, and metals. A total of 16,005 gal. of groundwater was pumped from well R-44 during development before the aquifer tests. During the pumping tests conducted at well R-44, a total of 76,924 gal. of groundwater was pumped from screens 1 and 2.

B-1.1 Field Preparation and Analytical Techniques

Chemical analyses of groundwater-screening samples collected from well R-44 were performed at Los Alamos National Laboratory's (LANL's, or the Laboratory's) Earth and Environmental Sciences Group 14 (EES-14). Groundwater samples were filtered (0.45-µm membranes) before preservation and chemical analyses. Samples were acidified at the EES-14 wet chemistry laboratory with analytical grade nitric acid to a pH of 2.0 or less for metal and major cation analyses.

Groundwater samples were analyzed using techniques specified in the U.S. Environmental Protection Agency SW-846 manual. Ion chromatography (IC) was the analytical method for bromide, chloride, fluoride, nitrate, nitrite, oxalate, perchlorate, phosphate, and sulfate. The instrument detection limits for perchlorate were 0.002 and 0.005 ppm, depending on the sample type (borehole water versus developed well water) and analyte interferences due to the presence of drilling fluid (AQF-2) used during drilling. Inductively coupled (argon) plasma optical emission spectroscopy (ICPOES) was used for analyses of dissolved aluminum, barium, boron, calcium, total chromium, iron, lithium, magnesium, manganese, potassium, silica, sodium, strontium, titanium, and zinc. Dissolved aluminum, antimony, arsenic, barium, beryllium, boron, cadmium, cesium, chromium, cobalt, copper, iron, lead, lithium, manganese, mercury, molybdenum, nickel, rubidium, selenium, silver, thallium, thorium, tin, vanadium, uranium, and zinc were analyzed by inductively coupled (argon) plasma mass spectrometry (ICPMS). The precision limits (analytical error) for major ions and trace elements were generally less than ±7% using ICPOES and ICPMS. Concentrations of total organic carbon (TOC) in nonfiltered groundwater samples collected during well development and aquifer performance testing were determined by using an organic carbon analyzer. Charge balance errors for total cations and anions were generally less than ±10% for complete analyses of the above inorganic chemicals. The negative cation-anion charge balance values indicate excess anions for the filtered samples. Total carbonate alkalinity was measured using standard titration techniques.

B-1.2 Field Parameters

B-1.2.1 Well Development

Water samples were drawn from the pump flow line into sealed containers, and field parameters were measured using a YSI multimeter. Results of field parameters, consisting of pH, temperature, dissolved oxygen (DO), oxidation-reduction potential (ORP), specific conductance, and turbidity measured during well development at R-44, are provided in Table B-1.2.1-1. Seven measurements of pH and temperature varied from 8.22 to 8.30 and from 18.30°C to 18.56°C, respectively, in groundwater pumped from well R-44 screen 1 during development. Concentrations of DO ranged from 9.70 to 10.66 mg/L, and these anomalously high DO measurements suggest that the groundwater was aerated during field parameter measurements. Uncorrected ORP values varied from –135.1 to –129.7 millivolts (mV) during well development of R-44 screen 1 (Table B-1.2.1-1). These ORP measurements taken during well development are not considered to be reliable and representative of the known relatively oxidizing conditions characteristic of the regional aquifer beneath the Pajarito Plateau, based on analytical results for redox-sensitive solutes, including detectable chromium, nitrate, sulfate, and uranium provided in Table B-1.3.1-1. Measurable concentrations of these solutes are consistent with overall oxidizing conditions encountered at the well. Specific conductance ranged from 142 to 148 microsiemens per centimeter (μS/cm), and turbidity ranged from 0 to 0.1 nephelometric turbidity unit (NTU) during well development of R-44 screen 1 (Table B-1.2.1-1).

Thirteen measurements of pH and temperature varied slightly from 8.19 to 8.30 and from 17.47°C to 18.78°C, respectively, in groundwater pumped from well R-44 screen 2 during development (Table B-1.2.1-1). Concentrations of DO varied from 11.57 to 13.72 mg/L, and these anomalously high DO measurements suggest that the groundwater was aerated during field parameter measurements. Uncorrected ORP values varied from –130.8 to –118.9 mV (Table B-1.2.1-1) during well development of R-44 screen 2, which also are not consistent with analytical results for several of the redox-sensitive solutes listed above. The regional aquifer is relatively oxidizing beneath the Pajarito Plateau and positive, uncorrected ORP measurements are typically recorded at adjacent regional aquifer wells, including R-1, R-13, R-15, and R-28. Specific conductance ranged from 193 to 204 μS/cm in groundwater pumped from R-44 screen 2 during well development, and turbidity decreased from 55.8 to 0 NTUs. Eight of the 13 measurements had turbidity greater than 5 NTUs during well development of R-44 screen 2.

B-1.2.2 Aquifer Performance Testing

During aquifer performance testing, 29 measurements of pH and temperature varied from 7.80 to 8.04 and from 14.99°C to 19.08°C, respectively, at well R-44 screen 1 (Table B-1.2.1-1). Concentrations of DO varied from 7.95 to 9.30 mg/L and positive, uncorrected ORP values varied from 117.3 to 204.4 mV during aquifer performance testing of R-44 screen 1. The uncorrected ORP values are generally consistent with both the DO measurements and analytical results for redox-sensitive solutes listed above and are provided in Table B-1.3-1. Specific conductance ranged from 60 to 140 μS/cm, and turbidity varied from 0 to 2.8 NTUs for groundwater pumped from R-44 screen 1 during aquifer performance testing.

Twenty-three measurements of pH and temperature varied from 8.31 to 8.67 and from 15.14°C to 20.31°C, respectively, during aquifer performance testing conducted at well R-44 screen 2. Concentrations of DO ranged from 8.60 to 11.14 mg/L. The anomalously high DO concentrations (greater than 9 mg/L) suggest that the water samples were aerated during parameter measurement. Positive, uncorrected ORP values varied from 144.9 to 212.1 mV during aquifer performance testing of R-44 screen 2. Specific conductance decreased from 173 to 154 μS/cm for the R-44 screen 2 samples measured during aquifer performance testing. Turbidity varied from 1.6 to 5.9 NTUs with one turbidity value greater than 5 NTUs.

B-1.3 Analytical Results for R-44 Groundwater-Screening Samples

B-1.3.1 Well Development

Analytical results for groundwater-screening samples collected at well R-44 during drilling, well development, and aquifer performance testing are provided in Table B-1.3.1-1. Four groundwater samples were collected from R-44 screens 1 and 2 during well development, and selected analytical results for these samples are combined in the following discussion. Calcium and sodium are the dominant cations in regional aquifer groundwater pumped from well R-44. During well development, dissolved concentrations of calcium and sodium ranged from 12.29 to 13.01 ppm (12.29 to 13.01 mg/L) and from 11.61 to 30.05 ppm, respectively. Dissolved concentrations of chloride and fluoride varied from 4.84 to 8.13 ppm and from 0.39 to 0.42 ppm, respectively, during development conducted at well R-44 (Table B-1.3.1-1). Dissolved concentrations of nitrate(N) and sulfate ranged from 0.57 to 1.01 ppm and from 5.83 to 13.8 ppm, respectively, during development at well R-44. Dissolved concentrations of chloride, nitrate(N), and sulfate exceeded Laboratory median background for regional aquifer groundwater (LANL 2007, 095817). Median background concentrations for dissolved chloride, nitrate plus nitrite(N), and sulfate in the regional aquifer are 2.17 mg/L, 0.31 mg/L, and 2.83 mg/L, respectively (LANL 2007, 095817). Concentrations of TOC ranged from 0.55 to 0.71 mgC/L in groundwater-screening samples collected during development conducted at well R-44 (Table B-1.3.1-1). The median background concentration of TOC is 0.34 mgC/L for regional aquifer groundwater (LANL 2007, 095817). Concentrations of perchlorate were less than analytical detection (<0.002 ppm, IC method) in groundwater-screening samples collected from well R-44 during development (Table B-1.3.1-1).

During well development conducted at R-44, dissolved concentrations of iron ranged from 0.180 to 0.430 ppm (180 to 430 μg/L or 180 to 430 ppb) using ICPOES (Table B-1.3.1-1), which exceeded the maximum background value of 147 μg/L for regional aquifer groundwater (LANL 2007, 095817). Dissolved concentrations of manganese ranged from 0.011 to 0.019 ppm (Table B-1.3.1-1), which exceeded the median background value of 1.0 μg/L for regional aquifer groundwater (LANL 2007, 095817). A carbon-steel discharge pipe was used during well development at R-44, which contributed iron and manganese in the form of colloidal rust to the filtered groundwater samples. Dissolved concentrations of boron ranged from 0.006 to 0.023 ppm (Table B-1.3.1-1) at well R-44, which is below the maximum background value of 51.6 μg/L for the regional aquifer (LANL 2007, 095817). Dissolved concentrations of nickel were less than analytical detection (0.001 ppm, ICPMS method) (Table B-1.3.1-1) in four groundwater-screening samples collected during well development conducted at R-44. Dissolved concentrations of zinc ranged from 0.003 to 0.007 ppm in groundwater-screening samples collected at well R-44 during development (Table B-1.3.1-1). The background median concentration of zinc in filtered samples is 1.45 μg/L for the regional aquifer (LANL 2007, 095817). Total dissolved concentrations of chromium ranged from 0.004 to 0.008 ppm (4 to 8 μg/L) at well R-44 during well development, with the higher concentrations of this metal measured in groundwater samples collected from screen 1 (Table B-1.3.1-1). Background mean, median, and maximum concentrations of total dissolved chromium are 3.07 μg/L, 3.05 μg/L, and 7.20 μg/L, respectively, for the regional aquifer (LANL 2007, 095817).

B-1.3-2 Aquifer Performance Testing

Dissolved concentrations of calcium and sodium ranged from 11.54 to 12.0 ppm and from 8.65 to 9.74 ppm, respectively, during aquifer performance testing conducted at R-44 screen 1 (Table B-1.3.1-1). Dissolved concentrations of chloride and fluoride varied from 3.29 to 3.44 ppm and from 0.36 to 0.37 ppm, respectively, during this phase of testing conducted at well R-44 screen 1 (Table B-1.3.1-1). Dissolved concentrations of nitrate(N) and sulfate varied slightly from 1.12 to 1.14 ppm and from 4.20 to 4.44 ppm, respectively, during aquifer performance testing performed at well R-44 screen 1. Dissolved

concentrations of chloride, nitrate(N), and sulfate in groundwater-screening samples collected from R-44 screen 1 exceeded Laboratory median background within regional aquifer groundwater (LANL 2007, 095817). Median background concentrations for dissolved chloride, nitrate plus nitrite(N), and sulfate in the regional aquifer are 2.17 mg/L, 0.31 mg/L, and 2.83 mg/L, respectively (LANL 2007, 095817). Elevated above-background concentrations of chloride, nitrate(N), and sulfate at well R-44 screen 1 suggest the presence of a contaminant plume(s) consisting, in part, of treated sewage effluent most likely released from Technical Area 03 (TA-03) discharges and possibly from other sewage/industrial waste streams released within Mortandad Canyon. Concentrations of TOC measured in groundwater-screening samples were 0.50 mgC/L during aquifer performance testing conducted at well R-44 screen 1 (Table B-1.3.1-1). Concentrations of perchlorate were less than detection (<0.002 ppm, IC method) in groundwater-screening samples collected from well R-44 screen 1 during aquifer performance testing (Table B-1.3.1-1).

During aquifer performance testing at R-44 screen 1, dissolved concentrations of iron were generally less than analytical detection (0.010 ppm) using ICPOES (Table B.1-3-1). A stainless-steel discharge pipe was used during aquifer performance testing conducted at R-44 screens 1 and 2, which is much less corrodible than the carbon steel used during development. Dissolved concentrations of manganese varied slightly from 0.002 to 0.003 ppm (Table B-1.3.1-1 at well R-44 screen 1 during this phase of testing. Dissolved concentrations of boron ranged from 0.013 to 0.018 ppm (Table B-1.3.1-1) in groundwater-screening samples collected from well R-44 screen 1, which is below the maximum background value of 51.6 μg/L for the regional aquifer (LANL 2007, 095817). Dissolved concentrations of nickel were less than analytical detection (0.001 ppm, ICPMS method) (Table B-1.3.1-1) in six groundwater-screening samples collected from R-44 screen 1 during aquifer performance testing. Dissolved concentrations of zinc ranged from 0.005 to 0.0013 ppm in groundwater-screening samples collected from R-44 screen 1 during this phase of testing (Table B-1.3.1-1). The background median concentration of zinc in filtered samples is 1.45 μg/L for the regional aquifer (LANL 2007, 095817). Total dissolved concentrations of chromium were 0.014 ppm (14 μg/L) in six groundwater-screening samples collected from R-44 screen 1 during aquifer performance testing (Table B-1.3.1-1). Background mean, median, and maximum concentrations of total dissolved chromium are 3.07 μg/L, 3.05 μg/L, and 7.20 μg/L, respectively, for the regional aquifer (LANL 2007, 095817). The most likely source of dissolved chromium measured in groundwater samples collected from well R-44 screen 1 is from past releases associated with the TA-03 cooling towers, in which potassium dichromate was used as a corrosion inhibitor from 1956 to 1972. Chromate (CrO_4^{2-}) is mobile in groundwater under oxidizing and basic pH conditions characteristic of most perched intermediate saturated zones and the regional aquifer at Los Alamos.

During aquifer performance testing of R-44 screen 2, dissolved concentrations of calcium and sodium ranged from 12.82 to 13.49 ppm and from 11.46 to 15.27 ppm, respectively, which are slightly higher than those measured in groundwater-screening samples collected from R-44 screen 1. Dissolved concentrations of chloride and fluoride varied slightly from 3.62 to 4.31 ppm and from 0.40 to 0.42 ppm, respectively, during aquifer performance testing conducted at well R-44 screen 2 (Table B-1.3.1-1). Dissolved concentrations of nitrate(N) varied slightly from 0.60 to 0.62 ppm, which are less than dissolved concentrations of nitrate(N) measured in groundwater-screening samples collected from R-44 screen 1. Dissolved concentrations of sulfate decreased from 7.38 to 4.71 ppm during aquifer performance testing conducted at well R-44 screen 2, which are higher than those measured in groundwater-screening samples collected from R-44 screen 1. Dissolved concentrations of chloride, nitrate(N), and sulfate at well R-44 exceeded Laboratory median background within regional aquifer groundwater (LANL 2007, 095817). Concentrations of TOC were 0.50 mgC/L during aquifer performance testing conducted at well R-44 screen 2 (Table B-1.3.1-1). Concentrations of perchlorate were less than detection (<0.002 ppm, IC method) in groundwater-screening samples collected from well R-44 screen 2 during aquifer performance testing (Table B-1.3.1-1).

During aquifer performance testing conducted at R-44 screen 2, dissolved concentrations of iron were generally less than analytical detection (0.010 ppm) using ICPOES (Table B-1.3.1-1). Dissolved concentrations of manganese varied slightly from 0.007 to 0.008 ppm (Table B-1.3.1-1) at well R-44 screen 2. Dissolved concentrations of boron ranged from 0.014 to 0.020 ppm (Table B-1.3.1-1) at well R-44 screen 2, which is below the maximum background value of 51.6 μg/L for the regional aquifer (LANL 2007, 095817). Dissolved concentrations of boron are similar in groundwater-screening samples collected from both screens at R-44 (Table B-1.3.1-1). Detectable dissolved concentrations of nickel were 0.002 ppm in groundwater-screening samples collected from R-44 screen 2 during aquifer performance testing (Table B-1.3.1-1). Dissolved concentrations of zinc varied slightly from 0.005 to 0.006 ppm in groundwater-screening samples collected from R-44 screen 2 during aquifer performance testing (Table B-1.3.1-1). Total dissolved concentrations of chromium ranged from 0.004 to 0.006 ppm (4 to 6 μg/L) at well R-44 screen 2 (Table B-1.3.1-1). Background mean, median, and maximum concentrations of total dissolved chromium are 3.07 μg/L, 3.05 μg/L, and 7.20 μg/L, respectively, for the regional aquifer (LANL 2007, 095817). Total dissolved concentrations of chromium are lower in groundwater-screening samples collected from screen 2 compared with those pumped from screen 1 at well R-44.

B-2.0 REFERENCES

The following list includes all documents cited in this appendix. Parenthetical information following each reference provides the author(s), publication date, and ER ID number. This information is also included in text citations. ER ID numbers are assigned by the Environmental Programs Directorate's Records Processing Facility (RPF) and are used to locate the document at the RPF and, where applicable, in the master reference set.

Copies of the master reference set are maintained at the NMED Hazardous Waste Bureau and the Directorate. The set was developed to ensure that the administrative authority has all material needed to review this document, and it is updated with every document submitted to the administrative authority. Documents previously submitted to the administrative authority are not included.

LANL (Los Alamos National Laboratory), May 2007. "Groundwater Background Investigation Report, Revision 3," Los Alamos National Laboratory document LA-UR-07-2853, Los Alamos, New Mexico. (LANL 2007, 095817)

Table B-1.2.1-1
Well Development Volumes, Aquifer Pump Test Volumes, and Associated Field Water-Quality Parameters for R-44

Date	pH	Temp (°C)	DO (mg/L)	ORP (mV)	Specific Conductivity (µS/cm)	Turbidity (NTU)	Purge Volume between Samples (gal.)	Cumulative Purge Volume (gal.)
Well Development								
01/15/09	n/r*, bailing						500	500
01/16/09	n/r, bailing						300	800
01/17/09	n/r, pumping						3000	3800
01/18/09	n/r, pumping						1785	5585
01/18/09 (upper screen)	8.30	18.30	10.66	–133.6	148	0.1	1150	6735
	8.27	18.33	9.88	–133.7	145	0.0	235	6970
	8.26	18.35	10.12	–133.0	144	0.0	235	7205
	8.26	18.42	11.02	–132.9	144	0.0	235	7440
	8.25	18.56	9.77	–135.1	144	0.0	235	7675
	8.23	18.47	9.70	–133.3	144	0.0	235	7910
	8.22	18.48	10.30	–129.7	142	0.0	235	8145
01/19/09	n/r, pumping						2340	10,485
01/20/09	n/r, pumping						2610	13,095
01/20/09 (lower screen)	8.29	17.47	13.65	–125.2	204	55.8	664	13,759
	8.29	17.49	13.72	–118.9	204	43.2	246	14,005
	8.26	17.55	12.96	–121.4	201	35.9	248	14,253
	8.26	17.63	12.84	–120.8	199	15.4	248	14,501
	8.25	17.67	12.91	–120.2	198	22.2	248	14,749
	8.22	17.75	12.50	–122.5	195	14.8	248	14,997
	8.20	18.03	11.94	–129.9	195	7.2	144	15,141
	8.20	18.45	12.07	–130.6	196	7.1	144	15,285
	8.22	18.58	12.00	–130.5	195	4.7	144	15,429
	8.23	18.65	11.64	–130.8	195	1.2	144	15,573
	8.22	18.68	12.03	–130.4	194	0.0	144	15,717
	8.20	18.75	11.57	–130.2	193	0.0	144	15,861
	8.19	18.78	12.48	–129.9	193	0.0	144	16,005

Table B-1.2.1-1 (Continued)

Date	pH	Temp (°C)	DO (mg/L)	ORP (mV)	Specific Conductivity (µS/cm)	Turbidity (NTU)	Purge Volume between Samples (gal.)	Cumulative Purge Volume (gal.)
Aquifer Pumping Test Volumes								
02/14/09	n/r, pumping, step-test upper screen						3312	3312
02/15/09	n/r, pumping, step-test upper screen						145	3457
02/16–17/09 (upper screen)	7.80	17.94	8.59	121.0	140	0.7	724	4181
	8.04	16.50	8.78	117.3	130	0.2	724	4905
	7.97	16.67	9.00	158.9	130	0.0	724	5629
	7.96	17.27	8.81	156.7	130	0.1	725	6354
	7.89	18.55	8.96	162.6	70	0.3	1448	7802
	7.98	18.72	8.67	170.8	130	0.5	1449	9251
	7.97	17.18	8.71	168.7	130	0.4	1448	10,699
	8.00	17.65	8.90	171.5	130	0.4	1449	12,148
	8.01	16.42	9.18	189.7	130	0.5	1448	13,596
	7.94	15.65	8.81	178.9	130	0.1	1449	15,045
	7.96	14.99	9.07	183.6	130	0.2	1448	16,493
	8.00	17.25	8.59	189.0	130	0.1	1449	17,942
	7.98	17.18	9.30	184.1	130	1.1	1448	19,390
	7.97	17.01	8.35	204.4	130	0.1	5794	25,184
	7.98	17.12	9.29	199.6	130	0.2	1448	26,632
	7.99	16.85	8.25	194.4	60	0.2	724	27,356
	8.03	17.69	8.17	195.2	120	2.8	724	28,080
	7.99	16.15	8.56	192.9	60	0.3	1448	29,528
	7.98	17.21	8.32	193.7	110	0.2	1449	30,977
	8.01	17.16	8.26	192.6	130	0.1	1448	32,425
	7.98	18.37	8.16	151.3	120	0.4	1449	33,874
	8.02	18.86	8.03	161.9	130	0.5	1448	35,322
	8.01	18.41	8.01	169.7	120	0.4	1449	36,771
	8.02	18.79	8.18	179.4	67	0.1	242	37013
	8.02	18.68	8.14	184.9	130	0.2	242	37,255
	8.01	18.65	7.98	188.4	130	0.2	242	37,497
	8.03	18.70	7.95	188.9	130	0.1	242	37,739
	8.03	18.55	8.04	189.9	130	0.1	242	37,981
	8.01	19.08	8.16	189.4	130	0.2	242	38,223
02/19/09	n/r, pumping, step-tests lower screen						4275	42,498
02/21–22/09 (lower screen)	8.31	17.47	8.72	145.7	173	5.0	956	43,454
	8.35	15.14	10.64	157.6	167	4.3	478	43,932
	8.67	18.72	8.90	144.9	173	3.1	1434	45,366
	8.66	19.50	10.38	148.7	171	4.0	1434	46,800
	8.65	19.41	8.79	149.0	168	5.9	1434	48,234

Table B-1.2.1-1 (Continued)

Date	pH	Temp (°C)	DO (mg/L)	ORP (mV)	Specific Conductivity (µS/cm)	Turbidity (NTU)	Purge Volume between Samples (gal.)	Cumulative Purge Volume (gal.)
	8.62	19.60	9.05	180.7	167	4.7	1434	49,668
	8.62	19.84	9.06	165.6	166	3.0	1434	51,102
	8.63	20.31	8.60	166.8	164	3.1	1434	52,536
	8.61	19.96	9.70	167.1	163	3.5	1434	53,970
	8.60	19.06	9.34	163.2	161	4.7	1434	55,404
	8.67	16.59	9.26	176.2	156	2.4	1434	56,838
	8.63	17.12	9.12	179.9	157	1.8	1434	58,272
	8.64	17.81	11.14	182.4	152	4.0	4302	62,574
	8.62	17.82	9.55	187.4	158	4.0	1434	64,008
	8.60	17.66	10.45	192.4	157	3.8	1434	65,442
	8.57	18.96	10.47	161.2	156	2.5	1434	66,876
	8.58	18.56	10.77	189.3	157	3.5	1434	68,310
	8.56	n/r	9.18	191.2	156	2.2	1434	69,744
	8.60	n/r	10.11	192.9	155	2.1	1434	71,178
	8.62	n/r	10.32	192.9	157	3.0	1434	72,612
	8.63	n/r	8.73	194.8	154	1.7	1434	74,046
	8.61	19.39	8.47	212.1	155	1.6	1434	75,480
	8.62	19.27	8.62	197.8	155	1.6	1195	76,675
	n/r						249	76,924

Note: Cumulative purge volumes for pump test calculated using average pump discharge rate of 24.1gal./min in the upper screen and 23.9 1 gal./min in the lower screen.

* n/r = Not recorded.

Table B-1.3.1-1
Analytical Results for Groundwater-Screening Samples Collected from Well R-44, Mortandad Canyon

Sample ID	Date Received	Time	Sample Type	ER/RRES-WQH	Screen	Depth (ft)	Ag rslt (ppm)	stdev (Ag)	Al rslt (ppm)	stdev (Al)	As rslt (ppm)	stdev (As)	B rslt (ppm)	stdev (B)	Ba rslt (ppm)
GW44-09-1292	11/17/2008	Not applicable	Borehole	09-329	Not applicable	739	0.001	U	0.21	0.00	0.0011	0.0000	0.038	0.001	0.015
GW44-09-1293	12/8/2008	Not applicable	Borehole	09-453	Not applicable	920	0.001	U	0.43	0.00	0.0005	0.0000	0.079	0.001	0.456
GW44-09-1294	12/8/2008	Not applicable	Borehole	09-453	Not applicable	937	0.001	U	0.42	0.00	0.0012	0.0000	0.088	0.001	0.453
GW44-09-1295	12/8/2008	Not applicable	Borehole	09-453	Not applicable	977	0.001	U	0.30	0.00	0.0003	0.0000	0.093	0.001	0.383
GW44-09-1296	12/8/2008	Not applicable	Borehole	09-453	Not applicable	997	0.001	U	1.39	0.01	0.0018	0.0002	0.076	0.001	0.418
GW44-09-1297	12/8/2008	Not applicable	Borehole	09-453	Not applicable	1017	0.001	U	1.54	0.06	0.0011	0.0002	0.118	0.004	0.509
GW44-09-1298	12/8/2008	Not applicable	Borehole	09-453	Not applicable	1037	0.001	U	0.98	0.02	0.0007	0.0000	0.076	0.002	0.386
GW44-09-1299	12/8/2008	Not applicable	Borehole	09-453	Not applicable	1056	0.001	U	0.93	0.00	0.0009	0.0000	0.073	0.001	0.271
GW44-09-1300	12/9/2008	Not applicable	Borehole	09-473	Not applicable	1094	0.001	U	0.02	0.00	0.0011	0.0000	0.070	0.001	0.434
GW44-09-1301	12/9/2008	Not applicable	Borehole	09-473	Not applicable	1076	0.001	U	0.29	0.01	0.0004	0.0000	0.147	0.001	0.536
GW44-09-1272	1/20/2009	Not applicable	Well, development	09-658	1	895-905	0.001	U	0.004	0.000	0.0008	0.0000	0.009	0.000	0.031
GW44-09-1273	1/20/2009	Not applicable	Well, development	09-658	1	895-905	0.001	U	0.004	0.000	0.0007	0.0000	0.006	0.001	0.027
GW44-09-1274	1/20/2009	Not applicable	Well, development	09-679	2	985-995	0.001	U	0.022	0.000	0.0016	0.0000	0.023	0.001	0.056
GW44-09-1275	1/20/2009	Not applicable	Well, development	09-679	2	985-995	0.001	U	0.006	0.000	0.0013	0.0000	0.017	0.000	0.048
GW44-09-1276	2/16/2009	12:00:00 PM	Well, pumping test	Not provided	1	895-905	0.001	U	0.005	0.000	0.0008	0.0000	0.014	0.000	0.025
GW44-09-1277	2/16/2009	2:00:00 PM	Well, pumping test	Not provided	1	895-905	0.001	U	0.004	0.000	0.0007	0.0000	0.018	0.001	0.024
GW44-09-1278	2/16/2009	8:00:00 PM	Well, pumping test	Not provided	1	895-905	0.001	U	0.007	0.000	0.0007	0.0000	0.016	0.001	0.025
GW44-09-1279	2/17/2009	12:00:00 AM	Well, pumping test	Not provided	1	895-905	0.001	U	0.005	0.000	0.0008	0.0000	0.014	0.000	0.024
GW44-09-1280	2/17/2009	4:00:00 AM	Well, pumping test	Not provided	1	895-905	0.001	U	0.006	0.000	0.0008	0.0000	0.014	0.000	0.023
GW44-09-1281	2/17/2009	8:00:00 AM	Well, pumping test	Not provided	1	895-905	0.001	U	0.005	0.000	0.0007	0.0000	0.013	0.001	0.022
GW44-09-1282	2/21/2009	12:00:00 PM	Well, pumping test	09-972	2	985-995	0.001	U	0.005	0.000	0.0010	0.0000	0.020	0.001	0.031
GW44-09-1283	2/21/2009	4:00:00 PM	Well, pumping test	09-972	2	985-995	0.001	U	0.011	0.000	0.0009	0.0000	0.018	0.000	0.029
GW44-09-1284	2/21/2009	8:00:00 PM	Well, pumping test	09-972	2	985-995	0.001	U	0.005	0.000	0.0009	0.0000	0.016	0.000	0.028
GW44-09-1285	2/22/2009	12:00:00 AM	Well, pumping test	09-972	2	985-995	0.001	U	0.005	0.000	0.0009	0.0000	0.015	0.001	0.028
GW44-09-1286	2/22/2009	4:00:00 AM	Well, pumping test	09-972	2	985-995	0.001	U	0.006	0.000	0.0009	0.0000	0.014	0.000	0.027
GW44-09-1287	2/22/2009	8:00:00 AM	Well, pumping test	09-972	2	985-995	0.001	U	0.005	0.000	0.0009	0.0000	0.014	0.000	0.027

Notes: U = Not detected. Total organic carbon not analyzed in borehole samples collected in high-density polyethylene containers.

Table B-1.3.1-1
Analytical Results for Groundwater-Screening Samples Collected from Well R-44, Mortandad Canyon

Sample ID	Date Received	Time	Sample Type	stdev (Ba)	Be rslt (ppm)	stdev (Be)	Br(-) ppm	TOC rslt (ppm)	TOC (U)	Ca rslt (ppm)	stdev (Ca)	Cd rslt (ppm)	stdev (Cd)	Cl(-) ppm	ClO4(-) ppm	ClO4(-) (U)	Co rslt (ppm)
GW44-09-1292	11/17/2008	Not applicable	Borehole	0.000	0.001	U	0.15	Not analyzed		13.77	0.08	0.001	U	7.07	0.005	U	0.001
GW44-09-1293	12/8/2008	Not applicable	Borehole	0.002	0.001	U	0.05	Not analyzed		14.46	0.10	0.001	U	7.89	0.005	U	0.001
GW44-09-1294	12/8/2008	Not applicable	Borehole	0.006	0.001	U	0.04	Not analyzed		14.79	0.17	0.001	U	7.24	0.005	U	0.001
GW44-09-1295	12/8/2008	Not applicable	Borehole	0.003	0.001	U	0.05	Not analyzed		10.59	0.05	0.001	U	5.30	0.005	U	0.001
GW44-09-1296	12/8/2008	Not applicable	Borehole	0.002	0.001	U	0.05	Not analyzed		11.64	0.01	0.001	U	7.87	0.005	U	0.001
GW44-09-1297	12/8/2008	Not applicable	Borehole	0.001	0.001	U	0.03	Not analyzed		11.83	0.04	0.001	U	4.62	0.002	U	0.001
GW44-09-1298	12/8/2008	Not applicable	Borehole	0.002	0.001	U	0.04	Not analyzed		11.62	0.09	0.001	U	3.65	0.002	U	0.001
GW44-09-1299	12/8/2008	Not applicable	Borehole	0.001	0.001	U	0.04	Not analyzed		11.57	0.05	0.001	U	3.76	0.002	U	0.001
GW44-09-1300	12/9/2008	Not applicable	Borehole	0.002	0.001	U	0.04	Not analyzed		21.75	0.07	0.001	U	3.94	0.005	U	0.001
GW44-09-1301	12/9/2008	Not applicable	Borehole	0.002	0.001	U	0.04	Not analyzed		9.13	0.04	0.001	U	4.62	0.005	U	0.001
GW44-09-1272	1/20/2009	Not applicable	Well, development	0.000	0.001	U	0.07	0.55		13.01	0.04	0.001	U	5.05	0.002	U	0.001
GW44-09-1273	1/20/2009	Not applicable	Well, development	0.000	0.001	U	0.07	0.66		12.95	0.02	0.001	U	4.84	0.002	U	0.001
GW44-09-1274	1/20/2009	Not applicable	Well, development	0.000	0.001	U	0.07	0.70		12.29	0.04	0.001	U	8.13	0.002	U	0.001
GW44-09-1275	1/20/2009	Not applicable	Well, development	0.001	0.001	U	0.06	0.71		12.84	0.14	0.001	U	7.39	0.002	U	0.001
GW44-09-1276	2/16/2009	12:00:00 PM	Well, pumping test	0.000	0.001	U	0.03	0.50	U	11.78	0.04	0.001	U	3.44	0.002	U	0.001
GW44-09-1277	2/16/2009	2:00:00 PM	Well, pumping test	0.000	0.001	U	0.04	0.50	U	11.54	0.03	0.001	U	3.35	0.002	U	0.001
GW44-09-1278	2/16/2009	8:00:00 PM	Well, pumping test	0.000	0.001	U	0.03	0.50	U	11.82	0.06	0.001	U	3.34	0.002	U	0.001
GW44-09-1279	2/17/2009	12:00:00 AM	Well, pumping test	0.000	0.001	U	0.03	0.50	U	12.00	0.13	0.001	U	3.33	0.002	U	0.001
GW44-09-1280	2/17/2009	4:00:00 AM	Well, pumping test	0.001	0.001	U	0.03	0.50	U	11.71	0.10	0.001	U	3.29	0.002	U	0.001
GW44-09-1281	2/17/2009	8:00:00 AM	Well, pumping test	0.000	0.001	U	0.02	0.50	U	11.69	0.05	0.001	U	3.30	0.002	U	0.001
GW44-09-1282	2/21/2009	12:00:00 PM	Well, pumping test	0.000	0.001	U	0.03	0.50	U	12.82	0.11	0.001	U	4.31	0.002	U	0.001
GW44-09-1283	2/21/2009	4:00:00 PM	Well, pumping test	0.000	0.001	U	0.03	0.50	U	13.11	0.08	0.001	U	4.09	0.002	U	0.001
GW44-09-1284	2/21/2009	8:00:00 PM	Well, pumping test	0.000	0.001	U	0.03	0.50	U	13.24	0.02	0.001	U	3.91	0.002	U	0.001
GW44-09-1285	2/22/2009	12:00:00 AM	Well, pumping test	0.000	0.001	U	0.03	0.50	U	13.33	0.10	0.001	U	3.83	0.002	U	0.001
GW44-09-1286	2/22/2009	4:00:00 AM	Well, pumping test	0.000	0.001	U	0.03	0.50	U	13.40	0.05	0.001	U	3.62	0.002	U	0.001
GW44-09-1287	2/22/2009	8:00:00 AM	Well, pumping test	0.000	0.001	U	0.03	0.50	U	13.49	0.09	0.001	U	3.65	0.002	U	0.001

Notes: U = Not detected. Total organic carbon not analyzed in borehole samples collected in high-dens

Table B-1.3.1-1
Analytical Results for Groundwater-Screening Samples Collected from Well R-44, Mortandad Canyon

Sample ID	Date Received	Time	Sample Type	stdev (Co)	Alk-CO3 rslt (ppm)	ALK-CO3 (U)	Cr rslt (ppm)	stdev (Cr)	Cs rslt (ppm)	stdev (Cs)	Cu rslt (ppm)	stdev (Cu)	F(-) ppm	Fe rslt (ppm)	stdev (Fe)
GW44-09-1292	11/17/2008	Not applicable	Borehole	U	0.8	U	0.005	0.000	0.001	U	0.003	0.000	0.3	0.54	0.01
GW44-09-1293	12/8/2008	Not applicable	Borehole	U	0.8	U	0.001	0.000	0.001	U	0.002	0.000	0.79	0.51	0.00
GW44-09-1294	12/8/2008	Not applicable	Borehole	U	0.8	U	0.001	0.000	0.001	U	0.001	0.000	1.08	0.23	0.00
GW44-09-1295	12/8/2008	Not applicable	Borehole	U	0.8	U	0.001	0.000	0.001	U	0.001	U	0.66	0.18	0.00
GW44-09-1296	12/8/2008	Not applicable	Borehole	U	0.8	U	0.003	0.001	0.001	U	0.003	0.001	0.81	0.83	0.03
GW44-09-1297	12/8/2008	Not applicable	Borehole	U	0.8	U	0.002	0.000	0.001	U	0.002	0.000	0.81	0.68	0.23
GW44-09-1298	12/8/2008	Not applicable	Borehole	U	0.8	U	0.005	0.001	0.001	U	0.002	0.000	0.44	2.59	0.03
GW44-09-1299	12/8/2008	Not applicable	Borehole	U	0.8	U	0.002	0.000	0.001	U	0.002	0.000	0.63	1.13	0.02
GW44-09-1300	12/9/2008	Not applicable	Borehole	U	6.89		0.009	0.001	0.001	U	0.001	U	0.67	0.02	0.00
GW44-09-1301	12/9/2008	Not applicable	Borehole	U	0.8	U	0.006	0.000	0.001	U	0.001	U	0.69	0.20	0.00
GW44-09-1272	1/20/2009	Not applicable	Well, development	U	0.8	U	0.008	0.000	0.001	U	0.001	U	0.39	0.24	0.00
GW44-09-1273	1/20/2009	Not applicable	Well, development	U	0.8	U	0.008	0.000	0.001	U	0.001	U	0.39	0.23	0.00
GW44-09-1274	1/20/2009	Not applicable	Well, development	U	0.8	U	0.004	0.001	0.001	U	0.001	U	0.42	0.18	0.00
GW44-09-1275	1/20/2009	Not applicable	Well, development	U	0.8	U	0.004	0.001	0.001	U	0.001	U	0.41	0.43	0.01
GW44-09-1276	2/16/2009	12:00:00 PM	Well, pumping test	U	0.8	U	0.014	0.000	0.001	U	0.001	U	0.36	0.01	U
GW44-09-1277	2/16/2009	2:00:00 PM	Well, pumping test	U	0.8	U	0.014	0.000	0.001	U	0.001	U	0.36	0.01	U
GW44-09-1278	2/16/2009	8:00:00 PM	Well, pumping test	U	0.8	U	0.014	0.000	0.001	U	0.001	U	0.36	0.01	0.00
GW44-09-1279	2/17/2009	12:00:00 AM	Well, pumping test	U	0.8	U	0.014	0.000	0.001	U	0.001	U	0.37	0.01	U
GW44-09-1280	2/17/2009	4:00:00 AM	Well, pumping test	U	0.8	U	0.014	0.000	0.001	U	0.001	U	0.36	0.01	U
GW44-09-1281	2/17/2009	8:00:00 AM	Well, pumping test	U	0.8	U	0.014	0.001	0.001	U	0.001	U	0.37	0.01	U
GW44-09-1282	2/21/2009	12:00:00 PM	Well, pumping test	U	0.8	U	0.005	0.000	0.001	U	0.001	U	0.40	0.01	U
GW44-09-1283	2/21/2009	4:00:00 PM	Well, pumping test	U	0.8	U	0.005	0.000	0.001	U	0.001	U	0.41	0.03	0.00
GW44-09-1284	2/21/2009	8:00:00 PM	Well, pumping test	U	0.8	U	0.004	0.000	0.001	U	0.001	U	0.42	0.01	U
GW44-09-1285	2/22/2009	12:00:00 AM	Well, pumping test	U	0.8	U	0.005	0.001	0.001	U	0.001	U	0.41	0.01	U
GW44-09-1286	2/22/2009	4:00:00 AM	Well, pumping test	U	0.8	U	0.006	0.000	0.001	U	0.001	U	0.40	0.01	U
GW44-09-1287	2/22/2009	8:00:00 AM	Well, pumping test	U	0.8	U	0.005	0.000	0.001	U	0.001	U	0.41	0.01	0.00

Notes: U = Not detected. Total organic carbon not analyzed in borehole samples collected in high-dens

Table B-1.3.1-1
Analytical Results for Groundwater-Screening Samples Collected from Well R-44, Mortandad Canyon

Sample ID	Date Received	Time	Sample Type	Alk-CO3+HCO3 rslt (ppm)	Hg rslt (ppm)	stdev (Hg)	K rslt (ppm)	stdev (K)	Li rslt (ppm)	stdev (Li)	Mg rslt (ppm)	stdev (Mg)	Mn rslt (ppm)	stdev (Mn)
GW44-09-1292	11/17/2008	Not applicable	Borehole	128	0.00005	U	2.12	0.03	0.030	0.001	4.38	0.06	0.059	0.000
GW44-09-1293	12/8/2008	Not applicable	Borehole	85	0.00108	0.00004	2.71	0.01	0.037	0.000	4.58	0.01	0.198	0.001
GW44-09-1294	12/8/2008	Not applicable	Borehole	99	0.00210	0.00004	3.05	0.06	0.036	0.001	4.51	0.06	0.080	0.006
GW44-09-1295	12/8/2008	Not applicable	Borehole	68	0.00017	0.00000	2.06	0.02	0.035	0.000	3.31	0.03	0.075	0.002
GW44-09-1296	12/8/2008	Not applicable	Borehole	85	0.00062	0.00003	2.35	0.02	0.032	0.000	4.72	0.04	0.044	0.007
GW44-09-1297	12/8/2008	Not applicable	Borehole	88	0.00299	0.00012	2.31	0.01	0.048	0.000	4.28	0.03	0.033	0.004
GW44-09-1298	12/8/2008	Not applicable	Borehole	81	0.00012	0.00001	1.66	0.01	0.028	0.000	4.04	0.03	0.090	0.001
GW44-09-1299	12/8/2008	Not applicable	Borehole	91	0.00078	0.00002	3.51	0.02	0.051	0.000	4.53	0.02	0.067	0.002
GW44-09-1300	12/9/2008	Not applicable	Borehole	138	0.00148	0.00002	2.11	0.01	0.048	0.003	6.32	0.05	0.008	0.001
GW44-09-1301	12/9/2008	Not applicable	Borehole	83	0.00173	0.00003	1.59	0.00	0.039	0.002	3.27	0.01	0.028	0.001
GW44-09-1272	1/20/2009	Not applicable	Well, development	84	0.00005	U	1.20	0.02	0.023	0.000	3.62	0.08	0.013	0.000
GW44-09-1273	1/20/2009	Not applicable	Well, development	83	0.00005	U	1.08	0.02	0.021	0.000	3.36	0.04	0.011	0.000
GW44-09-1274	1/20/2009	Not applicable	Well, development	113	0.00005	U	1.68	0.01	0.030	0.000	4.23	0.02	0.018	0.000
GW44-09-1275	1/20/2009	Not applicable	Well, development	107	0.00005	U	1.56	0.03	0.028	0.001	4.25	0.08	0.019	0.000
GW44-09-1276	2/16/2009	12:00:00 PM	Well, pumping test	82	0.00005	U	1.07	0.01	0.021	0.000	3.37	0.02	0.003	0.000
GW44-09-1277	2/16/2009	2:00:00 PM	Well, pumping test	78	0.00005	U	1.07	0.01	0.021	0.000	3.31	0.03	0.002	0.000
GW44-09-1278	2/16/2009	8:00:00 PM	Well, pumping test	77	0.00005	U	1.07	0.01	0.021	0.000	3.38	0.02	0.002	0.000
GW44-09-1279	2/17/2009	12:00:00 AM	Well, pumping test	78	0.00005	U	1.09	0.01	0.022	0.000	3.45	0.02	0.002	0.000
GW44-09-1280	2/17/2009	4:00:00 AM	Well, pumping test	81	0.00005	U	1.05	0.01	0.021	0.000	3.32	0.01	0.001	0.000
GW44-09-1281	2/17/2009	8:00:00 AM	Well, pumping test	79	0.00005	U	1.02	0.00	0.020	0.000	3.23	0.02	0.001	0.000
GW44-09-1282	2/21/2009	12:00:00 PM	Well, pumping test	91	0.00005	U	1.35	0.00	0.022	0.000	3.66	0.02	0.008	0.000
GW44-09-1283	2/21/2009	4:00:00 PM	Well, pumping test	88	0.00005	U	1.35	0.01	0.022	0.000	3.80	0.03	0.008	0.000
GW44-09-1284	2/21/2009	8:00:00 PM	Well, pumping test	87	0.00005	U	1.33	0.01	0.022	0.000	3.85	0.02	0.007	0.000
GW44-09-1285	2/22/2009	12:00:00 AM	Well, pumping test	87	0.00005	U	1.33	0.01	0.022	0.000	3.89	0.02	0.007	0.000
GW44-09-1286	2/22/2009	4:00:00 AM	Well, pumping test	86	0.00005	U	1.29	0.01	0.022	0.000	3.87	0.02	0.007	0.000
GW44-09-1287	2/22/2009	8:00:00 AM	Well, pumping test	85	0.00005	U	1.30	0.01	0.022	0.000	3.91	0.00	0.007	0.000

Notes: U = Not detected. Total organic carbon not analyzed in borehole samples collected in high-dens

Table B-1.3.1-1
Analytical Results for Groundwater-Screening Samples Collected from Well R-44, Mortandad Canyon

Sample ID	Date Received	Time	Sample Type	Mo rslt (ppm)	stdev (Mo)	Na rslt (ppm)	stdev (Na)	Ni rslt (ppm)	stdev (Ni)	NO2(ppm)	NO2-N rslt	NO2-N (U)	NO3 ppm	NO3-N rslt	C2O4 rslt (ppm)
GW44-09-1292	11/17/2008	Not applicable	Borehole	0.069	0.000	26.96	0.27	0.003	0.000	0.04	0.01	0.001	0.46	0.10	0.08
GW44-09-1293	12/8/2008	Not applicable	Borehole	0.238	0.002	16.53	0.07	0.002	0.000	0.01	0.00	U	6.36	1.44	0.58
GW44-09-1294	12/8/2008	Not applicable	Borehole	0.243	0.002	17.32	0.20	0.001	0.000	0.01	0.00	U	3.64	0.82	0.52
GW44-09-1295	12/8/2008	Not applicable	Borehole	0.145	0.001	13.78	0.06	0.001	0.000	0.01	0.00	U	7.22	1.63	0.44
GW44-09-1296	12/8/2008	Not applicable	Borehole	0.052	0.002	13.33	0.06	0.002	0.000	0.01	0.00	U	6.38	1.44	0.61
GW44-09-1297	12/8/2008	Not applicable	Borehole	0.049	0.001	14.85	0.07	0.001	0.000	0.01	0.00	U	2.73	0.62	0.26
GW44-09-1298	12/8/2008	Not applicable	Borehole	0.050	0.001	12.27	0.03	0.003	0.000	0.01	0.00	U	2.04	0.46	0.14
GW44-09-1299	12/8/2008	Not applicable	Borehole	0.065	0.000	14.70	0.03	0.002	0.000	0.01	0.00	U	2.18	0.49	0.02
GW44-09-1300	12/9/2008	Not applicable	Borehole	0.069	0.000	14.85	0.09	0.001	U	0.01	0.00	U	1.93	0.44	0.27
GW44-09-1301	12/9/2008	Not applicable	Borehole	0.097	0.000	15.48	0.07	0.001	U	0.01	0.00	U	2.00	0.45	0.31
GW44-09-1272	1/20/2009	Not applicable	Well, development	0.001	U	13.04	0.22	0.001	U	0.01	0.00	U	4.38	0.99	0.01
GW44-09-1273	1/20/2009	Not applicable	Well, development	0.001	U	11.61	0.15	0.001	U	0.01	0.00	U	4.48	1.01	0.01
GW44-09-1274	1/20/2009	Not applicable	Well, development	0.001	U	30.05	0.09	0.001	U	0.01	0.00	U	2.51	0.57	0.01
GW44-09-1275	1/20/2009	Not applicable	Well, development	0.001	U	23.86	0.29	0.001	U	0.01	0.00	U	2.54	0.57	0.01
GW44-09-1276	2/16/2009	12:00:00 PM	Well, pumping test	0.001	U	9.74	0.05	0.001	U	0.01	0.00	U	4.99	1.13	0.01
GW44-09-1277	2/16/2009	2:00:00 PM	Well, pumping test	0.001	U	9.43	0.07	0.001	U	0.01	0.00	U	4.97	1.12	0.01
GW44-09-1278	2/16/2009	8:00:00 PM	Well, pumping test	0.001	U	9.39	0.08	0.001	U	0.01	0.00	U	5.04	1.14	0.01
GW44-09-1279	2/17/2009	12:00:00 AM	Well, pumping test	0.001	U	9.45	0.11	0.001	U	0.01	0.00	U	5.04	1.14	0.01
GW44-09-1280	2/17/2009	4:00:00 AM	Well, pumping test	0.001	U	9.04	0.02	0.001	U	0.01	0.00	U	5.00	1.13	0.01
GW44-09-1281	2/17/2009	8:00:00 AM	Well, pumping test	0.001	U	8.65	0.05	0.001	U	0.01	0.00	U	5.08	1.15	0.01
GW44-09-1282	2/21/2009	12:00:00 PM	Well, pumping test	0.001	0.000	15.27	0.02	0.002	0.000	0.01	0.00	U	2.67	0.60	0.01
GW44-09-1283	2/21/2009	4:00:00 PM	Well, pumping test	0.001	0.000	13.99	0.18	0.002	0.000	0.01	0.00	U	2.69	0.61	0.01
GW44-09-1284	2/21/2009	8:00:00 PM	Well, pumping test	0.001	U	12.63	0.05	0.001	U	0.01	0.00	U	2.69	0.61	0.01
GW44-09-1285	2/22/2009	12:00:00 AM	Well, pumping test	0.001	U	12.42	0.14	0.001	U	0.01	0.00	U	2.70	0.61	0.01
GW44-09-1286	2/22/2009	4:00:00 AM	Well, pumping test	0.001	U	11.62	0.12	0.001	U	0.01	0.00	U	2.66	0.60	0.01
GW44-09-1287	2/22/2009	8:00:00 AM	Well, pumping test	0.001	U	11.46	0.04	0.002	0.000	0.01	0.00	U	2.73	0.62	0.01

Notes: U = Not detected. Total organic carbon not analyzed in borehole samples collected in high-dens

Table B-1.3.1-1
Analytical Results for Groundwater-Screening Samples Collected from Well R-44, Mortandad Canyon

Sample ID	Date Received	Time	Sample Type	C2O4 (U)	Pb rslt (ppm)	stdev (Pb)	Lab pH	PO4(-3) rslt (ppm)	Rb rslt (ppm)	stdev (Rb)	Sb rslt (ppm)	stdev (Sb)	Se rslt (ppm)	stdev (Se)	Si rslt (ppm)
GW44-09-1292	11/17/2008	Not applicable	Borehole		0.0002	U	7.08	0.01, U	0.003	0.000	0.001	U	0.001	U	38.0
GW44-09-1293	12/8/2008	Not applicable	Borehole		0.0002	0.0000	7.90	0.03	0.002	0.000	0.001	U	0.001	U	22.9
GW44-09-1294	12/8/2008	Not applicable	Borehole		0.0002	U	8.03	0.03	0.002	0.000	0.001	U	0.001	U	21.7
GW44-09-1295	12/8/2008	Not applicable	Borehole		0.0002	U	7.66	0.07	0.001	U	0.001	U	0.001	U	12.0
GW44-09-1296	12/8/2008	Not applicable	Borehole		0.0009	0.0001	7.92	0.03	0.004	0.001	0.001	U	0.001	U	35.4
GW44-09-1297	12/8/2008	Not applicable	Borehole		0.0012	0.0002	7.93	0.07	0.003	0.000	0.001	U	0.001	U	32.4
GW44-09-1298	12/8/2008	Not applicable	Borehole		0.0007	0.0002	7.70	0.08	0.002	0.000	0.001	U	0.001	U	28.3
GW44-09-1299	12/8/2008	Not applicable	Borehole		0.0016	0.0000	7.70	0.05	0.006	0.000	0.001	U	0.001	U	30.1
GW44-09-1300	12/9/2008	Not applicable	Borehole		0.0002	U	8.25	0.03	0.001	U	0.001	U	0.001	U	19.8
GW44-09-1301	12/9/2008	Not applicable	Borehole		0.0002	U	7.95	0.17	0.001	U	0.001	U	0.001	U	20.4
GW44-09-1272	1/20/2009	Not applicable	Well, development	U	0.0002	U	7.57	0.01, U	0.002	0.000	0.001	U	0.001	U	32.5
GW44-09-1273	1/20/2009	Not applicable	Well, development	U	0.0002	U	7.56	0.01, U	0.002	0.000	0.001	U	0.001	U	30.2
GW44-09-1274	1/20/2009	Not applicable	Well, development	U	0.0002	U	7.83	0.08	0.002	0.000	0.001	U	0.001	U	37.1
GW44-09-1275	1/20/2009	Not applicable	Well, development	U	0.0002	U	7.82	0.01, U	0.002	0.000	0.001	U	0.001	U	35.9
GW44-09-1276	2/16/2009	12:00:00 PM	Well, pumping test	U	0.0002	U	7.78	0.07	0.002	0.000	0.001	U	0.001	U	33.1
GW44-09-1277	2/16/2009	2:00:00 PM	Well, pumping test	U	0.0002	U	7.62	0.08	0.002	0.000	0.001	U	0.001	U	32.8
GW44-09-1278	2/16/2009	8:00:00 PM	Well, pumping test	U	0.0002	U	7.66	0.06	0.002	0.000	0.001	U	0.001	U	33.3
GW44-09-1279	2/17/2009	12:00:00 AM	Well, pumping test	U	0.0002	U	7.75	0.08	0.002	0.000	0.001	U	0.001	U	33.9
GW44-09-1280	2/17/2009	4:00:00 AM	Well, pumping test	U	0.0002	U	7.76	0.08	0.002	0.000	0.001	U	0.001	U	32.8
GW44-09-1281	2/17/2009	8:00:00 AM	Well, pumping test	U	0.0002	U	7.78	0.09	0.002	0.000	0.001	U	0.001	U	32.0
GW44-09-1282	2/21/2009	12:00:00 PM	Well, pumping test	U	0.0002	U	7.75	0.04	0.002	0.000	0.001	U	0.001	U	33.8
GW44-09-1283	2/21/2009	4:00:00 PM	Well, pumping test	U	0.0002	U	7.75	0.06	0.002	0.000	0.001	U	0.001	U	34.9
GW44-09-1284	2/21/2009	8:00:00 PM	Well, pumping test	U	0.0002	U	7.79	0.07	0.002	0.000	0.001	U	0.001	U	34.6
GW44-09-1285	2/22/2009	12:00:00 AM	Well, pumping test	U	0.0002	U	7.80	0.06	0.002	0.000	0.001	U	0.001	U	35.0
GW44-09-1286	2/22/2009	4:00:00 AM	Well, pumping test	U	0.0002	U	7.79	0.07	0.002	0.000	0.001	U	0.001	U	34.4
GW44-09-1287	2/22/2009	8:00:00 AM	Well, pumping test	U	0.0002	U	7.81	0.06	0.002	0.000	0.001	U	0.001	U	34.8

Notes: U = Not detected. Total organic carbon not analyzed in borehole samples collected in high-dens

Table B-1.3.1-1
Analytical Results for Groundwater-Screening Samples Collected from Well R-44, Mortandad Canyon

Sample ID	Date Received	Time	Sample Type	stdev (Si)	SiO2 rslt (ppm)	stdev (SiO2)	Sn rslt (ppm)	stdev (Sn)	SO4(-2) rslt (ppm)	Sr rslt (ppm)	stdev (Sr)	Th rslt (ppm)	stdev (Th)	Ti rslt (ppm)	stdev (Ti)
GW44-09-1292	11/17/2008	Not applicable	Borehole	0.4	81.3	0.9	0.001	U	4.93	0.062	0.001	0.001	U	0.016	0.000
GW44-09-1293	12/8/2008	Not applicable	Borehole	0.1	49.0	0.3	0.001	U	6.63	0.067	0.001	0.001	U	0.032	0.000
GW44-09-1294	12/8/2008	Not applicable	Borehole	0.4	46.5	0.8	0.001	U	7.66	0.061	0.001	0.001	U	0.014	0.001
GW44-09-1295	12/8/2008	Not applicable	Borehole	0.1	25.6	0.2	0.001	U	4.46	0.042	0.000	0.001	U	0.009	0.000
GW44-09-1296	12/8/2008	Not applicable	Borehole	0.0	75.7	0.1	0.001	U	6.65	0.052	0.000	0.001	U	0.038	0.000
GW44-09-1297	12/8/2008	Not applicable	Borehole	0.1	69.3	0.3	0.001	U	3.60	0.048	0.000	0.001	U	0.052	0.000
GW44-09-1298	12/8/2008	Not applicable	Borehole	0.2	60.6	0.4	0.001	U	2.88	0.044	0.000	0.001	U	0.031	0.001
GW44-09-1299	12/8/2008	Not applicable	Borehole	0.6	64.4	1.2	0.001	U	3.70	0.053	0.000	0.001	U	0.056	0.000
GW44-09-1300	12/9/2008	Not applicable	Borehole	0.1	42.4	0.3	0.001	U	4.90	0.081	0.001	0.001	U	0.002	U
GW44-09-1301	12/9/2008	Not applicable	Borehole	0.2	43.7	0.4	0.001	U	3.28	0.036	0.000	0.001	U	0.007	0.000
GW44-09-1272	1/20/2009	Not applicable	Well, development	0.4	69.6	0.9	0.001	U	6.07	0.058	0.001	0.001	U	0.002	U
GW44-09-1273	1/20/2009	Not applicable	Well, development	0.5	64.6	1.1	0.001	U	5.83	0.053	0.001	0.001	U	0.002	U
GW44-09-1274	1/20/2009	Not applicable	Well, development	0.4	79.4	0.8	0.001	U	13.8	0.089	0.000	0.001	U	0.003	0.000
GW44-09-1275	1/20/2009	Not applicable	Well, development	0.6	76.7	1.2	0.001	U	11.5	0.083	0.001	0.001	U	0.002	U
GW44-09-1276	2/16/2009	12:00:00 PM	Well, pumping test	0.4	70.8	0.8	0.001	U	4.44	0.052	0.000	0.001	U	0.002	U
GW44-09-1277	2/16/2009	2:00:00 PM	Well, pumping test	0.2	70.3	0.3	0.001	U	4.31	0.050	0.000	0.001	U	0.002	U
GW44-09-1278	2/16/2009	8:00:00 PM	Well, pumping test	0.2	71.2	0.5	0.001	U	4.33	0.051	0.001	0.001	U	0.002	U
GW44-09-1279	2/17/2009	12:00:00 AM	Well, pumping test	0.3	72.6	0.7	0.001	U	4.45	0.052	0.001	0.001	U	0.002	U
GW44-09-1280	2/17/2009	4:00:00 AM	Well, pumping test	0.1	70.2	0.2	0.001	U	4.20	0.050	0.000	0.001	U	0.002	U
GW44-09-1281	2/17/2009	8:00:00 AM	Well, pumping test	0.2	68.4	0.4	0.001	U	4.25	0.048	0.000	0.001	U	0.002	U
GW44-09-1282	2/21/2009	12:00:00 PM	Well, pumping test	0.1	72.4	0.3	0.001	U	7.38	0.065	0.001	0.001	U	0.002	U
GW44-09-1283	2/21/2009	4:00:00 PM	Well, pumping test	0.2	74.8	0.5	0.001	U	6.32	0.063	0.000	0.001	U	0.002	U
GW44-09-1284	2/21/2009	8:00:00 PM	Well, pumping test	0.2	74.0	0.4	0.001	U	5.74	0.062	0.000	0.001	U	0.002	U
GW44-09-1285	2/22/2009	12:00:00 AM	Well, pumping test	0.4	74.9	0.8	0.001	U	5.25	0.061	0.000	0.001	U	0.002	U
GW44-09-1286	2/22/2009	4:00:00 AM	Well, pumping test	0.3	73.5	0.7	0.001	U	4.79	0.059	0.001	0.001	U	0.002	U
GW44-09-1287	2/22/2009	8:00:00 AM	Well, pumping test	0.1	74.6	0.3	0.001	U	4.71	0.058	0.000	0.001	U	0.002	U

Notes: U = Not detected. Total organic carbon not analyzed in borehole samples collected in high-dens

Table B-1.3.1-1
Analytical Results for Groundwater-Screening Samples Collected from Well R-44, Mortandad Canyon

Sample ID	Date Received	Time	Sample Type	Tl rslt (ppm)	stdev (Tl)	U rslt (ppm)	stdev (U)	V rslt (ppm)	stdev (V)	Zn rslt (ppm)	stdev (Zn)	TDS (ppm)	Cations	Anions	Balance
GW44-09-1292	11/17/2008	Not applicable	Borehole	0.001	U	0.0003	0.0000	0.004	0.000	0.003	0.000	272.0	2.28	2.50	-0.05
GW44-09-1293	12/8/2008	Not applicable	Borehole	0.001	U	0.0011	0.0001	0.002	0.000	0.046	0.000	196.7	1.91	1.93	-0.01
GW44-09-1294	12/8/2008	Not applicable	Borehole	0.001	U	0.0013	0.0000	0.002	0.000	0.026	0.000	207.8	1.96	2.15	-0.05
GW44-09-1295	12/8/2008	Not applicable	Borehole	0.001	U	0.0003	0.0000	0.002	0.000	0.037	0.000	143.1	1.47	1.54	-0.03
GW44-09-1296	12/8/2008	Not applicable	Borehole	0.001	U	0.0024	0.0003	0.006	0.001	0.041	0.002	218.0	1.62	1.95	-0.09
GW44-09-1297	12/8/2008	Not applicable	Borehole	0.001	U	0.0014	0.0002	0.005	0.001	0.047	0.002	206.7	1.67	1.80	-0.04
GW44-09-1298	12/8/2008	Not applicable	Borehole	0.001	U	0.0005	0.0001	0.004	0.001	0.052	0.001	185.1	1.50	1.59	-0.03
GW44-09-1299	12/8/2008	Not applicable	Borehole	0.001	U	0.0010	0.0000	0.003	0.000	0.017	0.002	203.3	1.69	1.79	-0.03
GW44-09-1300	12/9/2008	Not applicable	Borehole	0.001	U	0.0034	0.0001	0.006	0.000	0.020	0.000	244.7	2.32	2.78	-0.09
GW44-09-1301	12/9/2008	Not applicable	Borehole	0.001	U	0.0007	0.0000	0.002	0.000	0.009	0.000	168.6	1.45	1.66	-0.07
GW44-09-1272	1/20/2009	Not applicable	Well, development	0.001	U	0.0008	0.0000	0.005	0.000	0.004	0.001	202.0	1.55	1.77	-0.07
GW44-09-1273	1/20/2009	Not applicable	Well, development	0.001	U	0.0008	0.0000	0.004	0.000	0.003	0.001	193.0	1.46	1.74	-0.09
GW44-09-1274	1/20/2009	Not applicable	Well, development	0.001	U	0.0019	0.0000	0.007	0.000	0.006	0.001	267.0	2.32	2.46	-0.03
GW44-09-1275	1/20/2009	Not applicable	Well, development	0.001	U	0.0016	0.0000	0.007	0.000	0.007	0.002	250.0	2.08	2.29	-0.05
GW44-09-1276	2/16/2009	12:00:00 PM	Well, pumping test	0.001	U	0.0005	0.0000	0.005	0.000	0.013	0.001	193.0	1.32	1.66	-0.11
GW44-09-1277	2/16/2009	2:00:00 PM	Well, pumping test	0.001	U	0.0005	0.0000	0.005	0.000	0.010	0.001	188.0	1.29	1.59	-0.10
GW44-09-1278	2/16/2009	8:00:00 PM	Well, pumping test	0.001	U	0.0005	0.0000	0.005	0.000	0.009	0.001	188.0	1.31	1.58	-0.10
GW44-09-1279	2/17/2009	12:00:00 AM	Well, pumping test	0.001	U	0.0005	0.0000	0.006	0.000	0.008	0.002	190.0	1.33	1.59	-0.09
GW44-09-1280	2/17/2009	4:00:00 AM	Well, pumping test	0.001	U	0.0005	0.0000	0.005	0.000	0.007	0.002	190.0	1.28	1.63	-0.12
GW44-09-1281	2/17/2009	8:00:00 AM	Well, pumping test	0.001	U	0.0005	0.0000	0.005	0.000	0.005	0.000	186.0	1.26	1.60	-0.12
GW44-09-1282	2/21/2009	12:00:00 PM	Well, pumping test	0.001	U	0.0009	0.0000	0.007	0.000	0.006	0.001	212.0	1.65	1.85	-0.06
GW44-09-1283	2/21/2009	4:00:00 PM	Well, pumping test	0.001	U	0.0008	0.0000	0.006	0.000	0.006	0.000	210.0	1.62	1.79	-0.05
GW44-09-1284	2/21/2009	8:00:00 PM	Well, pumping test	0.001	U	0.0008	0.0000	0.006	0.000	0.005	0.001	205.0	1.57	1.74	-0.05
GW44-09-1285	2/22/2009	12:00:00 AM	Well, pumping test	0.001	U	0.0008	0.0000	0.007	0.000	0.006	0.001	206.0	1.57	1.73	-0.05
GW44-09-1286	2/22/2009	4:00:00 AM	Well, pumping test	0.001	U	0.0007	0.0000	0.007	0.000	0.005	0.002	202.0	1.53	1.70	-0.05
GW44-09-1287	2/22/2009	8:00:00 AM	Well, pumping test	0.001	U	0.0007	0.0000	0.006	0.000	0.006	0.001	203.0	1.53	1.69	-0.05

Notes: U = Not detected. Total organic carbon not analyzed in borehole samples collected in high-dens

Appendix C

Aquifer Testing Report

C-1.0 INTRODUCTION

This appendix describes the hydraulic analysis of pumping tests at well R-44 screens 1 and 2 located in Mortandad Canyon near the edge of the existing chromium plume beneath the canyon. The tests were conducted in conjunction with testing of nearby well R-45 screens 1 and 2. The primary objective of the analysis was to determine the hydraulic properties of the zones screened in R-44, as well as the intervening sediments between the two screen zones. A secondary objective was to look for cross-connection between R-44 and surrounding wells R-45, R-11, R-13, and R-28.

Testing consisted primarily of constant-rate pumping tests conducted on R-44 screens 1 and 2. During the tests on each screen, water levels were monitored in the nonpumped screen zone in R-44 to examine the properties of the intervening sediments, and in R-45 screens 1 and 2 to monitor cross-connection between the wells. In addition, water levels were monitored in adjacent wells R-11, R-13, and R-28.

Consistent with most of the R-well pumping tests conducted on the plateau, an inflatable packer system was used in R-44 to isolate the screens and eliminate the effects of casing storage on the test data.

Conceptual Hydrogeology

R-44 is a dual-screen well completed in the Puye Formation just above the Miocene pumiceous deposits, with 10 ft of screen from 895.0 to 905.0 ft below ground surface (bgs) (screen 1)] and 9.9 ft of screen from 985.3 to 995.2 ft bgs (screen 2); the screens are separated by 80.3 ft of intervening sediments. The composite static water level measured on February 13 at the onset of testing was 878.86 ft bgs. When the zones were isolated with inflatable packers, the water level in screen 1 rose 0.06 ft to 878.80 ft bgs, while the level in screen 2 dropped 0.14 ft to 879.00 ft bgs. Thus, the initial water level in screen 1 was 0.2 ft higher than that in screen 2, implying a downward gradient. The head difference between the two screen zones in R-44 was modest (0.0022 ft downward gradient from the center of screen 1 to the center of screen 2) compared with differences measured at other multiscreen wells on the plateau, which show head differences of feet or tens of feet in most cases. The brass cap elevation at R-44 is 6714.91 ft above mean sea level (amsl), making the approximate static water-level elevations in screens 1 and 2 5836 ft.

Well R-45, also a dual-screen well, is located about 1000 ft north of R-44 and is completed at the top of the regional aquifer with the upper screen in the Puye Formation and the lower screen in the Miocene pumiceous sediments. Screen 1 is 10 ft long, set between 880 and 890 ft bgs. Screen 2 is 20 ft long, extending from 974.9 to 994.9 ft bgs. The composite water level in R-45 measured at the outset of testing R-44 and R-45 was 868.27 ft bgs. When the zones were isolated with inflatable packers, the water level in screen 1 rose from 0.04 to 868.23 ft bgs, while the level in screen 2 dropped 0.07 to 868.34 ft bgs. Thus, the initial water level in screen 1 was just 0.11 ft above that in screen 2. The brass cap elevation at R-44 is 6704.02 ft amsl, making the approximate static water-level elevations 5836 ft in screens 1 and 2.

R-44 Screen 1 Testing

R-44 screen 1 was tested from February 14 to February 18, 2009. Testing consisted of brief trial pumping on February 14, background data collection, and a 24-h constant-rate pumping test that was begun on February 16.

Two trial tests were conducted on February 14. Trial 1 was conducted at an average discharge rate of 19.2 gpm for 60 min from 8:00 to 9:00 a.m. (all times Mountain Standard Time) and was followed by 60 min of recovery until 10:00 a.m. Trial 2 was conducted for 120 min from 10:00 a.m. to 12:00 p.m. at 20.0 gpm. Following shutdown, recovery/background was monitored for 44 h until 8:00 a.m. on February 16.

During the trial tests, the generator supplying power to the submersible pump operated erratically with fluctuating voltage and alternating current frequency as well as substandard current frequency. This caused undesirable fluctuations in the discharge rate and limited the maximum rate that could be obtained. On February 15, a replacement generator was installed and run for about 10 mi from 11:34 to 11:44 a.m. to verify operation and rotation direction on the pump.

At 8:00 a.m. on February 16, the 24-h pumping test was begun at a rate of 24.2 gpm. Pumping continued until 8:00 a.m. on February 17. Following shutdown, recovery measurements were recorded for 24 h until 8:00 a.m. on February 18.

R-44 Screen 2 Testing

R-44 screen 2 was tested from February 19 to February 23, 2009. Testing consisted of brief trial pumping on February 19, background data collection, and a 24-h constant-rate pumping test that was begun on February 21.

Two trial tests were conducted on February 19. Trial 1 was conducted at a discharge rate of 23.9 gpm for 60 min from 8:00 to 9:00 a.m. and was followed by 60 min of recovery until 10:00 a.m. Trial 2 was conducted for 120 min from 10:00 a.m. to 12:00 p.m. at 24.0 gpm. Following shutdown, recovery/ background was monitored for 44 h until 8:00 a.m. on February 21.

At 8:00 a.m. on February 21, the 24-h pumping test was begun at a rate of 23.9 gpm. Pumping continued until 8:00 a.m. on February 22. Following shutdown, recovery measurements were recorded for 24 h until 8:00 a.m. on February 23.

Leaky Drop Pipe Joints

During the R-44 testing, there was leakage through the threaded joints on the 1 ½-in. stainless-steel drop pipe (1.90-in. outside diameter [O.D.] × 1.61-in. inside diameter [I.D.]), creating downhole voids inside the drop pipe beneath the check valves. This allowed initial pump operation against reduced head until the voids were refilled. The result was an elevated pumping rate for a brief period at the beginning of most of the tests. This effect corrupted the early startup data and added uncertainty to the analyses of the early drawdown data. The leaks were caused by either worn or improperly manufactured threads, as well as the need to avoid wrenching the pipe extremely as a precaution against galling the stainless-steel threads.

C-2.0 BACKGROUND DATA

The background water-level data collected in conjunction with running the pumping tests allow the analyst to see what water-level fluctuations occur naturally in the aquifer and help distinguish between water-level changes caused by conducting the pumping test and changes associated with other causes.

Background water-level fluctuations have several causes, among them barometric pressure changes, operation of other wells in the aquifer, Earth tides, and long-term trends related to weather patterns. The background data hydrographs from the monitored wells were compared with barometric pressure data from the area to determine if a correlation existed.

Previous pumping tests on the plateau have demonstrated a barometric efficiency for most wells of between 90% and 100%. Barometric efficiency is defined as the ratio of water-level change divided by barometric pressure change, expressed as a percentage. In the initial pumping tests conducted on the early R-wells, downhole pressure was monitored using a vented pressure transducer. This equipment measures the difference between the total pressure applied to the transducer and the barometric pressure, this difference being the true height of water above the transducer.

Subsequent pumping tests, including R-44, have utilized nonvented transducers. These devices simply record the total pressure on the transducer, that is, the sum of the water height plus the barometric pressure. This results in an attenuated “apparent” hydrograph in a barometrically efficient well. Take as an example a 90% barometrically efficient well. When monitored using a vented transducer, an increase in barometric pressure of 1 unit causes a decrease in recorded downhole pressure of 0.9 unit because the water level is forced downward 0.9 unit by the barometric pressure change. However, using a nonvented transducer, the total measured pressure increases by 0.1 unit (the combination of the barometric pressure increase and the water-level decrease). Thus, the resulting apparent hydrograph changes by a factor of 100 minus the barometric efficiency, and in the same direction as the barometric pressure change, rather than in the opposite direction.

Barometric pressure data were obtained from Technical Area 54 (TA-54) tower site from the Waste and Environmental Services Division-Environmental Data and Analysis (WES-EDA). The TA-54 measurement location is at an elevation of 6548 ft amsl, whereas the wellhead elevation is approximately 6715 ft amsl. The static water levels of the two zones were about 879 ft below land surface, making the water-table elevation roughly 5836 ft amsl. Therefore, the measured barometric pressure data from TA-54 had to be adjusted to reflect the pressure at the elevation of the water table within R-44.

The following formula was used to adjust the measured barometric pressure data:

$$P_{WT} = P_{TA54} \exp\left[-\frac{g}{3.281R} \left(\frac{E_{R44} - E_{TA54}}{T_{TA54}} + \frac{E_{WT} - E_{R44}}{T_{WELL}} \right) \right]$$

Equation C-1

Where, P_{WT} = barometric pressure at the water table inside R-44

P_{TA54} = barometric pressure measured at TA-54

g = acceleration of gravity, in m/sec^2 (9.80665 m/sec^2)

R = gas constant, in J/Kg/degree Kelvin (287.04 J/Kg/degree Kelvin)

E_{R44} = land surface elevation at R-44 site, in feet (6715 ft)

E_{TA54} = elevation of barometric pressure measuring point at TA-54, in feet (6548 ft)

E_{WT} = elevation of the water level in R-44, in feet (approximately 5836 ft)

T_{TA54} = air temperature near TA-54, in degrees Kelvin (assigned a value of 34.2 degrees Fahrenheit, or 284.4 degrees Kelvin)

T_{WELL} = air temperature inside R-44, in degrees Kelvin (assigned a value of 62.1 degrees Fahrenheit, or 289.9 degrees Kelvin)

This formula is an adaptation of an equation WES-EDA provided. It can be derived from the ideal gas law and standard physics principles. An inherent assumption in the derivation of the equation is that the air temperature between TA-54 and the well is temporally and spatially constant, and that the temperature of the air column in the well is similarly constant.

The corrected barometric pressure data reflecting pressure conditions at the water table were compared with the water-level hydrographs to discern the correlation between the two.

C-3.0 IMPORTANCE OF EARLY DATA

When pumping or recovery first begins, the vertical extent of the cone of depression is limited to approximately the well screen length, the filter pack length or, the aquifer thickness in relatively thin permeable strata. For many pumping tests on the plateau, the early pumping period is the only time that the effective height of the cone of depression is known with certainty. Thus, the early data often offer the best opportunity to obtain hydraulic conductivity information because conductivity would equal the earliest-time transmissivity divided by the well screen length.

Unfortunately, in many pumping tests, casing-storage effects dominate the early-time data, hindering the effort to determine the transmissivity of the screened interval. The duration of casing-storage effects can be estimated using the following equation (Schafer 1978, 098240).

$$t_c = \frac{0.6\left(D^2 - d^2\right)}{\frac{Q}{s}}$$

Equation C-2

Where, t_c = duration of casing storage effect, in minutes

D = inside diameter of well casing, in inches

d = outside diameter of column pipe, in inches

Q = discharge rate, in gallons per minute

s = drawdown observed in pumped well at time t_c, in feet

In some instances, it is possible to eliminate casing storage effects by setting an inflatable packer above the tested screen interval before conducting the test. Therefore, this option has been implemented for the R-well testing program, including the R-44 pumping tests.

C-4.0 TIME-DRAWDOWN METHODS

Time-drawdown data can be analyzed using a variety of methods. Among them is the Theis method (1934-1935, 098241). The Theis equation describes drawdown around a well as follows:

$$s = \frac{114.6Q}{T} W(u)$$

Equation C-3

Where,

$$W(u) = \int_u^\infty \frac{e^{-x}}{x} dx$$

Equation C-4

and

$$u = \frac{1.87 r^2 S}{Tt}$$

Equation C-5

and where, s = drawdown, in feet

Q = discharge rate, in gallons per minute

T = transmissivity, in gallons per day per foot

S = storage coefficient (dimensionless)

t = pumping time, in days

r = distance from center of pumpage, in feet

To use the Theis method of analysis, the time-drawdown data are plotted on log-log graph paper. Then, Theis curve matching is performed using the Theis type curve—a plot of the Theis well function W(u) versus 1/u. Curve matching is accomplished by overlaying the type curve on the data plot and, while keeping the coordinate axes of the two plots parallel, shifting the data plot to align with the type curve, effecting a match position. An arbitrary point, referred to as the match point, is selected from the overlapping parts of the plots. Match-point coordinates are recorded from the two graphs, yielding four values:W(u): 1/u, s, and t. Using these match-point values, transmissivity and storage coefficient are computed as follows:

$$T = \frac{114.6Q}{s} W(u)$$

Equation C-6

$$S = \frac{Tut}{2693r^2}$$

Equation C-7

Where, *T* = transmissivity, in gallons per day per foot

S = storage coefficient

Q = discharge rate, in gallons per minute

W(u) = match-point value

s = match-point value, in feet

u = match-point value

t = match-point value, in minutes

An alternative solution method applicable to time-drawdown data is the Cooper–Jacob method (1946, 098236), a simplification of the Theis equation that is mathematically equivalent to the Theis equation for most pumped well data. The Cooper–Jacob equation describes drawdown around a pumping well as follows:

$$s = \frac{264Q}{T} \log \frac{0.3Tt}{r^2 S}$$

Equation C-8

The Cooper–Jacob equation is a simplified approximation of the Theis equation and is valid whenever the u value is less than about 0.05. For small radius values (e.g., corresponding to borehole radii), u is less than 0.05 at very early pumping times and therefore is less than 0.05 for most or all measured drawdown values. Thus, for the pumped well, the Cooper–Jacob equation usually can be considered a valid approximation of the Theis equation.

According to the Cooper–Jacob method, the time-drawdown data are plotted on a semilog graph, with time plotted on the logarithmic scale. Then a straight line of best fit is constructed through the data points and transmissivity is calculated using:

$$T = \frac{264Q}{\Delta s}$$

Equation C-9

Where, T = transmissivity, in gallons per day per foot

Q = discharge rate, in gallons per minute

Δs = change in head over one log cycle of the graph, in feet

Because the R-wells are severely partially penetrating, an alternate solution considered for assessing aquifer conditions is the Hantush equation for partially penetrating wells (Hantush 1961, 098237; Hantush 1961, 106003). The Hantush equation is as follows:

Equation C-10

$$s = \frac{Q}{4\pi T}\left[W(u) + \frac{2b^2}{\pi^2 (l-d)(l'-d')}\sum_{n=1}^{\infty}\frac{1}{n^2}\left(\sin\frac{n\pi l}{b} - \sin\frac{n\pi d}{b}\right)\left(\sin\frac{n\pi l'}{b} - \sin\frac{n\pi d'}{b}\right)W\left(u, \sqrt{\frac{K_z}{K_r}}\frac{n\pi r}{b}\right)\right]$$

Where, in consistent units, s, Q, T, t, r, S, and u are as previously defined and

b = aquifer thickness

d = distance from top of aquifer to top of well screen in pumped well

l = distance from top of aquifer to bottom of well screen in pumped well

d' = distance from top of aquifer to top of well screen in observation well

l' = distance from top of aquifer to bottom of well screen in observation well

K_z = vertical hydraulic conductivity

K_r = horizontal hydraulic conductivity

In this equation, $W(u)$ is the Theis well function and $W(u,\beta)$ is the Hantush well function for leaky aquifers where:

$$\beta = \sqrt{\frac{K_z}{K_r}}\frac{n\pi r}{b}$$

Equation C-11

Note that for single-well tests, $d = d'$ and $l = l'$.

C-5.0 RECOVERY METHODS

Recovery data were analyzed using the Theis recovery method. This is a semilog analysis method similar to the Cooper–Jacob procedure.

In this method, residual drawdown is plotted on a semilog graph versus the ratio *t/t'*, where *t* is the time since pumping began and *t'* is the time since pumping stopped. A straight line of best fit is constructed through the data points and *T* is calculated from the slope of the line as follows:

$$T = \frac{264Q}{\Delta s}$$ **Equation C-12**

The recovery data are particularly useful compared with time-drawdown data. Because the pump is not running, spurious data responses associated with dynamic discharge rate fluctuations are eliminated. The result is that the data set is generally "smoother" and easier to analyze. This was of paramount importance in the R-44 pumping tests because of the entrained air induced discharge rate fluctuations.

C-6.0 SPECIFIC CAPACITY METHOD

The specific capacity of the pumped well can be used to obtain a lower-bound value of hydraulic conductivity. The hydraulic conductivity is computed using formulas that are based on the assumption that the pumped well is 100% efficient. The resulting hydraulic conductivity is the value required to sustain the observed specific capacity. If the actual well is less than 100% efficient, it follows that the actual hydraulic conductivity would have to be greater than calculated to compensate for well inefficiency. Thus, because the efficiency is unknown, the computed hydraulic conductivity value represents a lower bound. The actual conductivity is known to be greater than or equal to the computed value.

For fully penetrating wells, the Cooper–Jacob equation can be iterated to solve for the lower-bound hydraulic conductivity. However, the Cooper–Jacob equation (assuming full penetration) ignores the contribution to well yield from permeable sediments above and below the screened interval. To account for this contribution, it is necessary to use a computation algorithm that includes the effects of partial penetration. One such approach was introduced by Brons and Marting (1961, 098235) and augmented by Bradbury and Rothchild (1985, 098234).

Brons and Marting introduced a dimensionless drawdown correction factor, s_P, approximated by Bradbury and Rothschild as follows:

$$s_P = \frac{1-\frac{L}{b}}{\frac{L}{b}}\left[\ln\frac{b}{r_w} - 2.948 + 7.363\frac{L}{b} - 11.447\left(\frac{L}{b}\right)^2 + 4.675\left(\frac{L}{b}\right)^3\right]$$ **Equation C-13**

In this equation, L is the well screen length, in ft. Incorporating the dimensionless drawdown parameter, the conductivity is obtained by iterating the following formula:

$$K = \frac{264Q}{sb}\left(\log\frac{0.3Tt}{r_w^2 S} + \frac{2s_P}{\ln 10}\right)$$ **Equation C-14**

To apply this procedure, a storage coefficient value must be assigned. Unconfined conditions were assumed for screen 1, while confined to leaky-confined conditions were applied to screen 2. Storage coefficient values for confined conditions can be expected to range from about 10^{-5} to 10^{-3}, depending on aquifer thickness, while those for unconfined conditions can be expected to range from about 0.01 to 0.25 (Driscoll 1986, 104226). The calculation result is not particularly sensitive to the choice of storage coefficient value, so a rough estimate of the storage coefficient is generally adequate to support the calculations. An assumed value of 0.1 was used in the calculations for screen 1, while values of 10^{-3} and $10–^{2}$ were used for screen 2. For screen 2, a storage coefficient value of 10^{-3} was deemed appropriate for the assumption of confined conditions (with perhaps very minor leakage from above), while 10^{-2} was used to simulate leaky-confined conditions.

The analysis also requires assigning a value for the saturated aquifer thickness, b. For calculation purposes, the screen 1 zone was assumed to extend from the water table, at 879 ft bgs, to the midpoint of the blank pipe section between the two screens, at approximately 945 ft bgs. This resulted in an assigned aquifer thickness of 67 ft for screen 1. This was equivalent to assuming that the resistive zone between screens 1 and 2 was at the midpoint of the intervening blank section, even though the actual location of the aquitard was not known. However, the computed result is not particularly sensitive to the exact aquifer thickness, because sediments far above or below the screen have little effect on yield and drawdown response. Therefore, the calculation based on the assumed aquifer thickness value was deemed to be adequate. For screen 2, an arbitrary thickness of 200 ft was assigned in the calculations.

Computing the lower-bound estimate of hydraulic conductivity can provide a useful frame of reference for evaluating the other pumping test calculations.

C-7.0 BACKGROUND DATA ANALYSIS

Background aquifer pressure data collected during the R-44 tests were plotted along with barometric pressure to determine the barometric effect on water levels and to look for pumping response in the surrounding observation wells. The four screen zones in R-44 and R-45 were monitored using nonvented pressure transducers, while the remaining wells—R-11, R-13, and R-28—were monitored using vented transducers.

Figure C-7.0-1 shows aquifer pressure data from R-44 screen 1 along with barometric pressure data from TA-54 that have been corrected to equivalent barometric pressure in feet of water at the water table. The R-44 data are referred to in the figure as the “apparent hydrograph” because the measurements reflect the sum of water pressure and barometric pressure, having been recorded using a nonvented pressure transducer. The times of the pumping periods for the screen 1 and screen 2 pumping tests are included on the figure for reference.

The transducers used in screens 1 and 2 were switched between tests, accounting for the different appearance in the data output from the screen 1 tests to the screen 2 tests. The transducer used initially (during the screen 1 test) showed substantial scatter, giving the thick-appearing plot of data points. The second transducer (right side of graph) showed less scatter, except during the pumping periods when significant scatter was observed. This resulted from the transducer having to be located adjacent to the pump power cable (inevitable when pumping screen 2 and monitoring screen 1), which interfered with transducer operation when the pump was running. The second transducer showed some sort of a dry problem (oil-canning) as indicated by the “striped” or “layered” effect seen in the data trace on February 19, 22 and 23. This effect had been seen previously during the testing of R-16r in 2005 and is believed to indicate a transducer malfunction of some sort.

To minimize the data scatter on Figure C-7.0-1, a rolling average of the data was plotted in Figure C-7.0-2. The average included data over a 1-h interval.

It appeared in Figures C-7.0-1 and C-7.0-2 that changes in barometric pressure had no discernible effect on water levels. An example illustrating this was the abrupt drop and subsequent rise in barometric pressure on February 20 that appeared to have no corresponding effect on the total aquifer pressure.

As a check on this, a plot was made of background data collected subsequently from R-44 screen 1 during the R-45 pumping tests conducted in late February and early March. Figure C-7.0-3 shows the observed apparent hydrograph and the corresponding barometric pressure. Figure C-7.0-3 confirmed that changes in barometric pressure had no effect on the aquifer pressure. The clincher was the tremendous change in barometric pressure that occurred from February 27 to 28 with no corresponding perturbation in the apparent hydrograph. This implied a high barometric efficiency for screen 1, essentially 100%.

Aside from the lack of response to barometric pressure changes, there were two other key observations made from the data shown in Figures C-7.0-1 and C-7.0-2. First, during the background data collection before the screen 1 pumping test, there was a distinct, steady decline in aquifer pressure totaling about 0.03 ft over 2.5 d. It was believed that this was a response to operation of Los Alamos County well PM-4, which began pumping on February 11 and ran continuously until March 4. The other supply wells cycled randomly throughout this period (illustrated below) and would not have caused the observed effect.

Second, there was a distinct response in screen 1 to pumping screen 2—both during the trial tests on February 19 and the 24-h test on February 21. During the 24-h screen 2 pumping period, the observed drawdown in screen 1 was about 0.05 ft. Following pump shutoff, there was a slow recovery effect, typical of the response of distant observation wells or wells separated from the pumped zone by an aquitard.

Figure C-7.0-4 shows the apparent hydrograph for R-44 screen 2 recorded during the screen 1 and 2 test periods. The times of the screen 1 and 2 pumping tests are included in the figure for reference. Again, the transducers were switched between tests, accounting for the difference in the appearance of the data plots from one test to the other. Note that the transducer used during the screen 2 test (right side of Figure C-7.0-4) was the same one that was used to monitor screen 1 during the screen 1 pumping test (left side of Figure C-7.0-1). The broad data scatter was consistent in both plots and apparently unique to that particular transducer.

To remove some of the scatter in the plot, a rolling average of the data was prepared as shown in Figure C-7.0-5.

Finally, an additional plot was prepared in Figure C-7.0-6 comparing the aquifer pressure response with the times of operation of Los Alamos County production wells PM-3, PM-5, and O-4. PM-4 was not included in the plot, as it operated continuously throughout the time period shown on the graph.

The data from Figures C-7.0-4, C-7.0-5, and C-7.0-6 were examined to discern the relationships between aquifer pressure and both barometric pressure fluctuations and municipal pumping. There were some hints of a possible correlation of aquifer pressure and changes in barometric pressure. For example, a decline in barometric pressure on February 16 seemed to coincide with a drop in aquifer pressure, while rises in barometric pressure late on February 18 and 20 matched increases in aquifer pressure. The decline in aquifer pressure on February 16 occurred during the 24-h pumping test, so it may have been a response to pumping. However, there was no such analogous explanation for the aquifer pressure increases.

To provide further insight into the relationship between screen 2 water levels and barometric pressure, a plot was made of background data collected subsequently from R-44 screen 2 during the R-45 pumping tests conducted in late February and early March. Figure C-7.0-7 shows the observed apparent

hydrograph and the corresponding barometric pressure. Because of the scatter in the data set, a rolling average plot was prepared as shown in Figure C-7.0-8.

The data shown in Figures C-7.0-7 and C-7.0-8 showed that barometric pressure changes, in fact, caused no change in aquifer pressure. This was best illustrated by the observations made from February 27 to 28. The tremendous rise in barometric pressure during this period had no effect on aquifer pressure. This implied essentially a 100% barometric efficiency for screen 2, similar to what was observed for screen 1. This meant that the aquifer pressure increases seen on February 18 and 20, as well as the decline observed on February 16, were not attributable to barometric pressure fluctuations. (The diurnal fluctuations having a magnitude of about 0.03 ft in Figures C-7.0-7 and C-7.0-8 were responses to Earth tides.)

The data in Figures C-7.0-4 and C-7.0-5 were reexamined in light of knowing that barometric pressure fluctuations did not affect the apparent hydrograph. The background data leading up to the screen 1 24-h pumping test (February 13 to 16) showed a steady pressure decline of about 0.06 ft in 2.5 d. This was likely attributable to operation of PM-4, which was started on February 11 and run continuously. The response to pumping PM-4 in screen 2 was twice as great as that in screen 1 (0.06 ft versus 0.03 ft). This implied the possibility of a zone of limited permeability separating screens 1 and 2, effectively providing greater hydraulic isolation of screen 1 from the effects of PM-4 operation. This was also consistent with the minimal drawdown observed in each screen (0.05 ft) due to pumping the other screen.

During the 24-h pumping test on screen 1, the rate of water-level decline in screen 2 increased, indicating a response to the pumping test. Following pump shutoff, there was a slow recovery, typical of the response of distant observation wells or wells separated from the pumped zone by an aquitard. A rough estimate of the drawdown induced in screen 2 by pumping screen 1 was 0.05 ft.

An examination of the production well operation schedule in Figure C-7.0-6 showed no correlation between screen 2 aquifer pressure and cycling of production wells PM-3, PM-5, and O-4. There was no obvious explanation for the aquifer pressure increases observed on February 18 and 20 and no such response was observed in R-44 screen 1. It is possible that these fluctuations may have been attributable to Earth tides.

Figure C-7.0-9 shows the apparent hydrograph for R-45 screen 1. The transducer output showed the same bizarre striped/layered effect that was observed from one of the transducers used to monitor R-44. There appeared to be no aquifer pressure response to changes in barometric pressure, implying a barometric efficiency of essentially 100%.

The gradual decline in pressure from February 13 to February 19 likely was caused by the startup and continuous operation of production well PM-4 beginning on February 11. The aquifer pressure declined approximately 0.11 ft over a 6-d period.

There was no discernible response in R-45 screen 1 to test pumping R-44 screen 1, although the unusual transducer output may have masked subtle changes in water level. There appeared to be a response, however, to pumping R-44 screen 2. The water level in R-45 screen 1 dropped roughly 0.02 ft during the 24-h pumping test in R-44 screen 2.

The data in Figure C-7.0-9 were replotted in Figure C-7.0-10 along with operating times for production wells PM-3, PM-5 and O-4. Examination of the data showed that there was no discernible response in R-45 screen 1 to cycling these three production wells.

Figure C-7.0-11 shows the apparent hydrograph for R-45 screen 2. To eliminate some of the data scatter, a rolling average plot was prepared also as shown in Figure C-7.0-12. Several observations can be made from these graphs.

The aquifer pressure declined for a few days before the R-44 screen 1 pumping test and continued to show declines during the test as well. During the 3-d period leading up to the test, the water-level decline was approximately 0.04 ft. This change in water level probably was caused by the startup and continuous operation of PM-4.

Water-level perturbations (diurnal in places) having a magnitude of a few hundredths of a foot appeared throughout the monitoring period. It was believed that these were Earth tide effects.

Pumping R-44 screen 1 appeared to induce slight drawdown in R-45 screen 2. The magnitude of the effect was estimated to be about 0.02 ft. Figure 13 shows an expanded-scale plot of the apparent R-45 screen 2 hydrograph along with a straight line of fit for visual reference. The effect caused by pumping R-44 screen 1 was slight, but distinct.

Pumping R-44 screen 2 caused a greater effect in R-45 screen 2 than did pumping R-44 screen 1. The drawdown in R-45 screen 2 was approximately 0.06 ft during the 24-h constant-rate pumping test conducted in R-44 screen 2.

There was a prominent water-level rise in R-45 screen 2 from late February 20 to the start of the 24-h test on R-44 screen 2 on February 21. This was similar to the water-level rise seen in R-44 screen 2 during the same period. This response was absent from the R-45 screen 1 data. Thus, the distinct water-level increase from this period was observed in both R-44 screen 2 and R-45 screen 2 but was absent from screen 1 in both wells. It was suspected that Earth tides may have caused these perturbations in the water level because no other cause could be identified. The other such rise seen in R-44 screen 2 from February 18 to 19 (Figures C-7.0-4 and C-7.0-5) was not evident in R-45 screen 2.

Figure C-7.0-14 shows a plot of the R-45 screen 2 apparent hydrograph along with operating times for production wells PM-3, PM-5, and O-4. There was no discernible correlation between production well cycling and water-level fluctuations in R-45 screen 2. It appeared that continuous operation of PM-4 beginning on February 11 caused the only identifiable water-level changes in R-45 screen 2.

Figure C-7.0-15 shows the hydrograph obtained from well R-11 located in Sandia Canyon less than half a mile north of R-44. The data were recorded using the permanently installed vented transducer, so the hydrograph fluctuated with barometric pressure rather than showing the more flat-line response typical of nonvented transducers. The times of the pumping tests on R-44 screens 1 and 2 are included on the graph for reference.

Visual examination of the hydrograph and barometric pressure curve showed that they nearly coincided. There was, however, a clear downward water-level trend from the start of monitoring on February 13 to about February 19. This was evidenced by the hydrograph lying above the barometric pressure curve initially and gradually approaching it from above. Beginning February 19, the hydrograph and barometric pressure curve pretty much coincided. It was likely that the decline in water level from February 13 to February 19 was caused by startup and operation of PM-4, which began on February 11.

Because the barometric pressure fluctuations in the hydrograph were large, it was necessary to correct the water-level data by removing the barometric effect. This was done in two ways. One procedure involved correcting the data using BETCO (barometric and Earth tide correction) software, a mathematically complex correction algorithm that uses regression deconvolution (Toll and Rasmussen 2007, 104799) to modify the data. The BETCO correction not only removes barometric pressure effects, but Earth tides as well. The BETCO corrected data are shown in Figure 15.

A visual examination of the corrected hydrograph showed minor perturbations on the order of a few hundredths of a foot, but no identifiable response to pumping either screen 1 or screen 2 in R-44.

A second correction approach was applied to the hydrograph data by correcting directly for the change in barometric pressure assuming 100% barometric efficiency and immediate response. Figure C-7.0-16 shows the hydrograph corrected in this manner. The BETCO correction was retained on the graph for comparison.

The direct correction method seemed to produce better results for R-11. The corrected hydrograph reflected the small, steady drop in level from February 13 to 19 caused by operation of PM-4. The water-level decline attributable to pumping PM-4 was about 0.06 ft over a 6-d period. Then, beginning February 19, the corrected hydrograph was nearly flat. Visual examination of the hydrograph showed no correlation between water-level fluctuations and the pumping of either screen in R-44.

Figure C-7.0-17 shows the hydrograph obtained from R-13 located roughly 980 ft east of R-44. Again the times of the R-44 pumping tests and the BETCO hydrograph correction are included on the graph.

Visual examination of the hydrograph and barometric pressure curve showed that they nearly coincided. Similar to the R-11 response, there was a clear downward water-level trend from the start of monitoring on February 13 to about February 20. This was evidenced by the hydrograph lying above the barometric pressure curve initially and gradually approaching it from above. The initial gap between the curves was wider than in R-11, indicating a more rapid water-level decline in R-13 caused by the operation of PM-4.

Beginning February 20, the hydrograph and barometric pressure curve coincided, except for a departure that occurred during the R-44 screen 2 pumping test. This indicated a possible response to pumping screen 2. Indeed, the BETCO correction showed a clear pumping response to the screen 2 test of approximately 0.06 ft. The BETCO plot suggested the lack of a response, however, to the pumping test conducted on R-44 screen 1. Finally, the BETCO plot indicated roughly 0.15 ft of water-level decline due to PM-4 pumping over roughly a 7-d period.

A second correction was performed, this time using the direct approach of correcting for barometric pressure only, assuming 100% barometric efficiency and immediate response. Figure C-7.0-18 shows the resulting corrected hydrograph. The BETCO hydrograph was retained on the figure for comparison purposes.

Similar to the BETCO plot, the corrected hydrograph in Figure C-7.0-18 showed a clear response to pumping R-44 screen 2. Unlike the BETCO plot, however, the corrected hydrograph suggested a possible subtle response to pumping screen 1. This was evidenced by the increase in the slope of the hydrograph during the pumping period followed by a flattening (cessation of the downward background trend) during recovery. To clarify this, an expanded-scale plot of the corrected hydrograph was prepared. Figure C-7.0-19 shows the expanded-scale plot of the R-13 corrected hydrograph along with a straight line of fit for visual reference. The resulting data indicated a possible pumping effect from R-44 screen 1 of about 0.03 ft. Because of the small magnitude of the effect and the fact that the BETCO correction removed it altogether, it is possible that it was an Earth tide or delayed barometric effect rather than a response to pumping R-44 screen 1.

A final observation from the corrected hydrograph in Figures C-7.0-18 and C-7.0-19 was the abrupt rise in water level from late February 20 to early February 21. This was similar to that seen in R-44 screen 2 (Figures C-7.0-4 and C-7.0-5) and R-45 screen 2 (Figures C-7.0-11 through C-7.0-14). This effect was absent, however, on the BETCO hydrograph correction (Figures C-7.0-17 and C-7.0-18). Because the BETCO algorithm removes Earth tide effects, this may be evidence that this prominent feature in all three wells was indeed caused by Earth tides.

Figure C-7.0-20 shows the hydrograph obtained from R-28 located roughly 1620 ft northwest of R-44. Again, the times of the R-44 pumping tests and the BETCO hydrograph correction are included on the graph.

Visual examination of the hydrograph and barometric pressure curve showed that they were nearly identical. Similar to the R-11 and R-13 responses, there was a clear downward water-level trend from the start of monitoring on February 13 to about February 20. This was evidenced by the hydrograph lying above the barometric pressure curve initially and gradually approaching it from above. As in the other wells, this background trend was likely caused by startup and continuous operation of PM-4.

Beginning February 20, the hydrograph and barometric pressure curve coincided, except for a departure that occurred during the R-44 screen 2 pumping test. This indicated a possible response to pumping screen 2. Indeed, the BETCO correction showed a clear pumping response to the screen 2 test of approximately 0.03 ft. The BETCO plot suggested the lack of a response, however, to the pumping test conducted on R-44 screen 1. Finally, the BETCO plot indicated roughly 0.14 ft of water-level decline due to PM-4 pumping over roughly a 7-d period.

A second correction was performed, this time using the direct approach of correcting for barometric pressure only, assuming 100% barometric efficiency and immediate response. Figure C-7.0-21 shows the resulting corrected hydrograph. The BETCO hydrograph was retained in the figure for comparison purposes.

Similar to the BETCO plot, the corrected hydrograph in Figure C-7.0-21 showed a clear response to pumping R-44 screen 2. Unlike the BETCO plot, however, there was a hint of a possible response to pumping R-44 screen 1. This was evidenced by a slight increase in the slope of the hydrograph during the pumping period followed by a reduction in slope during recovery. To clarify these subtle effects, an expanded-scale plot of the corrected hydrograph was prepared. Figure C-7.0-22 shows the expanded-scale plot of the R-28 hydrograph along with a straight line of fit for visual reference. The data indicated a possible tiny response to pumping R-44 screen 1 of no more than about 0.01 ft. (Perhaps a logarithmic-shaped reference curve of some sort would have been more appropriate than the straight line shown on Figure C-7.0-22, but the conclusion of a deflection in the hydrograph would have been the same.) Because the effect was so small and the BETCO correction removed it altogether, it is possible that it was caused by something other than the R-44 screen 1 pumping test such as Earth tides or delayed barometric response. However, the striking coincidence of occurring during the screen 1 pumping test coupled with similar, though larger, responses observed in the other monitored wells, made it possible that the screen 1 pumping effects reached R-28.

A final observation from the corrected hydrograph in Figure C-7.0-22 was the data segment from late February 20 to early February 21. Contrary to the antecedent decline in water levels, there was a small rise in level during this period—a subdued version of the pronounced water-level rise seen in R-13, R-44 screen 2, and R-45 screen 2 probably caused by Earth tides.

C-8.0 R-44 SCREEN 1 DATA ANALYSIS

This section presents the data obtained from the R-44 screen 1 pumping tests and the results of the analytical interpretations. Data are presented for drawdown and recovery for trials 1 and 2 and the 24-h constant-rate pumping test.

R-44 Screen 1 Trial 1

Figure C-8.0-1 shows a semilog plot of the trial 1 drawdown data. The early data showed exaggerated drawdown because the pumping rate was elevated as the drop pipe was being filled for the first time and the pump operated against reduced head.

The middle data on the plot showed drawdown changes associated with erratic pump operation. The generator used for the trials tests on R-44 was defective, showing below normal alternating current output frequency as well as variable current frequency and voltage.

The late data showed drawdown changes associated with discharge rate adjustments made using the flow control valve at the surface. The average discharge rate during trial 1 was 19.2 gpm, while the rate over the last half of the test was 19.5 gpm. The many discharge rate changes during trial 1 precluded analysis of the drawdown data.

Figure C-8.0-2 shows a semilog plot of the trial 1 recovery data. The transmissivity value computed from the early data was 4210 gpd/ft. Based on the screen length of 10 ft, the computed hydraulic conductivity was 421 gpd/ft^2, or 56.3 ft/d.

The slope of the data trace began declining at just a few seconds, and within minutes the slope became essentially flat. Figure C-8.0-3 shows an expanded-scale plot of the late-recovery data.

The flattening of the recovery curve showed the effects of a complex combination of vertical growth of the cone of impression (partial penetration), leakage from below, and delayed drainage of the unconfined aquifer. For illustration purposes, a transmissivity was computed for the late data yielding a value of 270,000 gpd/ft. This was likely not an actual transmissivity but rather an artifact of the delayed yield and leakage. It does suggest, however, the possibility of a large aquifer transmissivity at the R-44 location.

R-44 Screen 1 Trial 2

Figure C-8.0-4 shows a semilog plot of the trial 2 drawdown data. The discharge rate for trial 2 was 20.0 gpm. The transmissivity value computed from the early data was 3550 gpd/ft, making the computed hydraulic conductivity 355 gpd/ft^2, or 47.5 ft/d. Note that the early data showed the effects of a minimal amount of antecedent drainage of the drop pipe through leaky coupling joints.

Later data in Figure C-8.0-4 showed erratic pumping water levels associated with discharge rate fluctuations induced by the inconsistent operation of the electric generator.

Figure C-8.0-5 shows an expanded-scale plot of the trial 2 drawdown data. At this scale, the plot showed more clearly the erratic drawdown induced by the variable generator output. The discharge rate variations precluded analysis of the late data. Nevertheless, the late data showed the effects of the combination of delayed yield and vertical expansion of the cone of depression.

Figure C-8.0-6 shows a semilog plot of the trial 2 recovery data. The transmissivity value computed from the early data was 3350 gpd/ft, making the computed hydraulic conductivity 355 gpd/ft^2, or 47.5 ft/d. The late-recovery data showed flattening associated with a combination of delayed yield, partial penetration and leakage.

Figure C-8.0-7 shows an expanded-scale plot of the late trial 2 recovery data.

The curve appeared to flatten completely (delayed yield) and did not support calculation of a representative transmissivity value. The severe data scatter coupled with the tiny changes in head precluded a rigorous analysis of the late data. The 44-h duration of the recovery period should have been

long enough to exhaust the delayed drainage effect, implying the possibility of a high transmissivity for the regional aquifer at this location.

C-8.1 R-44 Screen 1 24-H Constant-Rate Pumping Test

Figure C-8.1-1 shows a semilog plot of the drawdown data recorded during the 24-h constant-rate pumping test conducted at a discharge rate of 24.2 gpm. The early data showed that some antecedent drainage of the drop pipe had occurred during the background monitoring period. The magnitude of the drawdown spike during the first minute of pumping allowed estimating the early pumping rate before refilling the void in the drop pipe, roughly 28 gpm. Using this discharge rate estimate, the transmissivity computed from the initial drawdown data was 3860 gpd/ft, making the computed hydraulic conductivity 3817 gpd/^{2}, or 42.4 ft/d.

The late data showed a reduction in drawdown over time. There was no obvious explanation for the odd occurrence because the measured discharge rates were constant, especially over the last half day of pumping. It is possible that minor sediment removal with the pumped water could have increased the well efficiency somewhat during the test.

Figure C-8.1-2 shows the recovery data measured following the 24-h constant-rate pumping test. The transmissivity calculated from the early data was 3510 gpd/ft, making the hydraulic conductivity 351 gpd/ft^2, or 46.9 ft/d.

As with all of the data plots, the late-recovery data showed severe flattening associated with delayed yield and vertical expansion of the cone of impression. Figure C-8.1-3 shows an expanded-scale plot of the late-recovery data.

Again, the latest slope in Figure C-8.1-3 did not support calculation of a meaningful transmissivity value because of possible lingering delayed yield effects as well as the broad data scatter. Nevertheless, the data suggested the possibility of a transmissive regional aquifer at the R-44 location.

Packer Deflation

Following the 24-h recovery period, the packer was deflated in preparation for pulling the pump. When this was done, water above the packer that had leaked through coupling joints in the drop pipe bypassed the packer and was delivered to the pressure transducer while the water drained back into the well and formation. This caused a pressure increase that was recorded by the transducer.

Figure C-8.1-4 shows the resulting head buildup and decay that occurred when the packer was deflated. Data were recorded at 1-min intervals so the maximum head buildup was not revealed in the data set. The high specific capacity of R-44 meant that a substantial volume of water could have flowed into the screen zones before the first head measurement in Figure C-8.1-4. The head data confirmed that pipe joints had leaked throughout the R-44 screen 1 pumping tests.

R-44 Screen 1 Specific Capacity Data

Specific capacity data were used along with well geometry to estimate a lower-bound conductivity value for the R-44 screen 1 zone for comparison to the pumping test values. In addition to specific capacity, other input values used in the calculations included the assumed aquifer thickness of 67 ft (from the static water level to the midpoint of the blank pipe section between screens 1 and 2), a storage coefficient of 0.1 and a borehole radius of 0.51 ft. The calculations are somewhat insensitive to the assigned aquifer thickness, as long as the selected value is substantially greater than the screen length.

R-44 screen 1 produced 24.2 gpm with a drawdown of 4.27 ft after 24 h of pumping for a specific capacity of 5.67 gpm/ft. Applying the Brons and Marting method to these inputs yielded a lower-bound hydraulic conductivity value for the screened interval of 432 gpd/ft^2, or 57.7 ft/d. Because the calculation method did not factor in the effects of leakage, it was possible that the computed value could be overestimated. Indeed, the value was somewhat greater than the values obtained from the early pumping test data but similar enough that it was not considered an unreasonable result. Overall, it provided corroboration of the pumping test values and suggested a hydraulically efficient completion.

R-44 Screen 1 Summary

Table 8.1-1 summarizes the hydraulic conductivity values obtained from the R-44 screen 1 pumping test analyses. The average hydraulic conductivity computed from the recovery data was 50.2 ft/d. The recovery average was used because of the effects of antecedent drop pipe drainage on the drawdown data.

The specific capacity obtained from screen 1 suggested a lower-bound hydraulic conductivity of 57.7 ft/d. However, that value did not factor in the effects of leakage that occurred in screen 1 and, thus, was considered consistent with the pumping test values. The results suggested a highly efficient screened interval.

Within seconds of startup or shutdown, vertical expansion of the cone of depression (leakage and partial penetration) and delayed yield affected the pumping and recovery data. The late data suggested an enormous transmissivity for the regional aquifer at the R-44 location, perhaps in excess of 100,000 gpd/ft.

C-9.0 R-44 SCREEN 2 DATA ANALYSIS

This section presents the data obtained from the R-44 screen 2 pumping tests and the results of the analytical interpretations. Data are presented for drawdown and recovery for trials 1 and 2 and the 24-h constant-rate pumping test.

Analysis of the screen 2 data was challenging because of the lack of early data from most of the tests. A programming oversight made in setting up the transducer data collection scheme, coupled with slightly varying clock speeds of the wristwatch used during the tests and the transducers, led to losing the very early data in all but one of the tests.

R-44 Screen 2 Trial 1

Figure C-9.0-1 shows a semilog plot of the drawdown data collected from trial 1 conducted at a discharge rate of 23.9 gpm. The early data showed exaggerated drawdown because the pumping rate was elevated as the drop pipe was being filled for the first time and the pump operated against reduced head.

The varying pumping rate associated with filling the drop pipe precluded analysis of the early drawdown data.

The data following filling of the drop pipe were plotted on an expanded scale as shown in Figure C-9.0-2. The slope of the graph became continuously flatter throughout the trial test. This was caused by a combination of vertical expansion of the cone of depression and leakage from the screen 1 zone. It is also possible that the data included indirect effects of delayed yield of the overlying unconfined screen 1 interval

The latest data on the graph supported a transmissivity calculation of 48,500 gpd/ft. This likely represented the thickness of sediment corresponding to the depth of the cone of depression at that particular time. The total aquifer transmissivity is likely greater than indicated by this calculation because

the cone of depression was probably still expanding vertically and the slope of the graph likely would have continued flattening at later time. Note also that the substantial data scatter added uncertainty to the calculation. In fact, the amount of data scatter exceeded the drawdown change on which the analysis was based.

Figure C-9.0-3 shows the recovery data collected following shutdown of the trail 1 pumping test. The transmissivity computed from the early data on the graph was 3430 gpd/ft. Dividing this value by the screen length of 9.9 ft yielded a hydraulic conductivity estimate of 346 gpd/ft^2, or 46.3 ft/d. However, the earliest recovery data were not collected. Note that the first data point corresponded to a residual drawdown of less than a foot out of more than 18 ft of drawdown at the end of the pumping period. It was suspected that the recovery cone of impression had expanded vertically well beyond the length of the screened interval to some greater effective thickness and that the hydraulic conductivity was likely substantially less than computed from Figure C-9.0-3. Subsequent data, presented below, corroborated this idea.

Figure C-9.0-4 shows an expanded-scale plot of the trial 1 recovery data. The slope of the recovery curve continued to flatten throughout the monitored period. The latest data supported a transmissivity calculation of 124,000 gpd/ft.

There was uncertainty in this transmissivity calculation because of the tiny water-level changes and the substantial data scatter. Furthermore, there was no way to know the height of the cone of impression corresponding to the analysis or whether delayed yield from the upper aquifer zone was affecting the data. The analysis did suggest, however, a large aquifer transmissivity.

R-44 Screen 2 Trial 2

Figure C-9.0-5 shows a semilog plot of the drawdown data collected from trial 2 conducted at a discharge rate of 24.0 gpm. The data from the first few seconds of pumping showed exaggerated drawdown associated with minor antecedent drainage of a portion of the drop pipe through a leaky coupling joint. This precluded capturing the very early data for analysis.

The early data following refilling of the void in the drop pipe were plotted on an expanded scale as shown in Figure C-9.0-6. The transmissivity computed from the graph was 2900 gpd/ft. Diving this value by the screen length of 9.9 ft yielded a hydraulic conductivity estimate of 293 gpd/ft^2, or 39.2 ft/d.

It was likely that the cone of depression had already expanded well beyond the thickness of screened sediment so the hydraulic conductivity values computed based on the screen length of 9.9 ft were considered overestimates of the actual value. Note that the earliest data used in the analysis already showed nearly 16 ft of drawdown. In other words, the snapshot of the early data associated with initial lateral expansion of the cone of depression was masked by the discharge rate fluctuations caused by changing head conditions as the void in the drop pipe refilled. By the time postrefill data were collected, the cone of depression had expanded vertically.

Figure C-9.0-7 shows an expanded-scale plot of the late drawdown data from trial 2. The transmissivity value obtained from the latest slope on the graph was 146,000 gpd/ft. There was uncertainty in the calculated value because of wide data scatter and ongoing vertical expansion of the cone of depression as well as leakage and possible delayed yield effects from the overlying zone.

Figure C-9.0-8 shows the recovery data recorded following the trial 2 test on R-44 screen 2. The data set included earlier data than any other data set obtained in the testing effort, as evidenced by the fact that the residual drawdown was still at about 7 ft when data collection began. This data set allowed obtaining a reasonably representative snapshot of the early-recovery response.

The transmissivity computed from the early-recovery data was 820 gpd/ft, much smaller than previous values. Based on the screen length of 9.9 ft, the computed hydraulic conductivity was 82.8 gpd/^{2}, or 11.1 ft/d. This is likely a good representation of the hydraulic conductivity of the screened sediments. It implied that the larger values obtained previously were biased by vertical expansion of the drawdown or recovery cone.

Figure C-9.0-9 shows an expanded-scale plot of the late trial 2 recovery data. As with previous graphs of late drawdown or recovery data, the slope of the data trace flattened continuously throughout the recovery period, becoming essentially horizontal at the end of the monitoring period.

The continuous flattening resulted from partial penetration effects including both vertical expansion of the cone of impression and leakage from the upper zone, including possible delayed yield effects. No transmissivity value was calculated from the graph in Figure C-9.0-9, as it would have supported computation of any arbitrarily large value, depending on which portion of the curve was used for constructing the line of fit. As stated earlier, the late-time response was consistent with a large transmissivity for the regional aquifer at the R-44 location.

C-9.1 R-44 Screen 2 24-H Constant-Rate Pumping Test

Figure C-9.1-1 shows a semilog plot of the drawdown data recorded during the 24-h constant-rate pumping test conducted at a discharge rate of 23.9 gpm. The early data showed that antecedent drainage of the drop pipe had occurred during the background monitoring period.

The effect of variable discharge rates while filling the void in the drop pipe precluded analysis of the early data from the drawdown curve.

Figure C-9.1-2 shows an expanded-scale plot of the drawdown data following refilling of the drop pipe. The data set was quite noisy and did not support a useful analysis.

The drawdown spike at a time of 3 min was accompanied by a noise at the well head that sounded like air moving through the discharge piping. It was not known if these two events were cause-and-effect or merely coincidental. Generally, air is not entrained in the drop pipe when it drains, because the drained void is typically under vacuum conditions. However, if there were two leaky coupling joints between adjacent check valves, it is possible that water could have drained from the lower one while air was pulled into the upper one.

The abrupt drop in pumping water level that occurred between 600 and 1000 min was caused by temporarily pumping the discharge water to a lower elevation. Against the reduced head, the pumping rate increased by about 1%.

All other perturbations in the drawdown data were caused by uncontrollable discharge rate fluctuations associated with submersible pump and electric generator operation. Such variations in flow rate are not unusual.

Figure C-9.1-3 shows the recovery data measured following the 24-h constant-rate pumping test. The transmissivity calculated from the early data was 1760 gpd/ft, making the computed hydraulic conductivity 178 gpd/ft^2, or 23.8 ft/d.

Because the residual drawdown corresponding to the first data point on Figure C-9.1-3 was only 1.4 ft, most of the recovery had already occurred and it was likely that the earliest data, required to identify the properties of the screened sediments, were not collected. Indeed, the computed hydraulic conductivity was

substantially greater than the value obtained from the trial 2 recovery data. It was likely that the cone of impression had expanded vertically beyond the screened interval before the first data point was recorded.

As with all of the data plots, the late-recovery data showed severe flattening associated with vertical expansion of the cone of impression, leakage and perhaps delayed yield. Figure C-9.1-4 shows an expanded-scale plot of the late-recovery data.

The slope of the data plot decreased continuously, eventually becoming and remaining essentially flat. It was hypothesized that at late time, the water level would eventually reach the initial static level. A line of fit was constructed to pass through the late data and the upper le corner of the graph (corresponding to zero residual drawdown at infinite time). The transmissivity computed from the artificially constructed line of fit was 39,100 gpd/ft.

There was uncertainty in the computed transmissivity value. The scatter in the data set exceeded the magnitude of water-level change on which the analysis was based. Further, any change in the background water level would have meant that targeting zero residual drawdown in the analysis was incorrect.

Regardless of the approach used to analyze the late-recovery data, the flat slope of the late data implied a high transmissivity for the regional aquifer at the R-44 location.

R-44 Screen 2 Specific Capacity Data

Specific capacity data were used along with well geometry to estimate a lower-bound conductivity value for the R-44 screen 2 zone for comparison to the pumping test values. In addition to specific capacity, other input values used in the calculations included the assumed an arbitrarily assigned aquifer thickness of 200 ft, storage coefficient values of 0.01 and 0.001 (for leaky-confined and confined conditions, respectively), and a borehole radius of 0.51 ft.

R-44 screen 2 produced 23.9 gpm with a drawdown of 17.72 ft after 24 h of pumping for a specific capacity of 1.35 gpm/. Applying the Brons and Marting method to these inputs yielded lower-bound hydraulic conductivity values for the screened interval of 111 gpd/^{2}, or 14.9 ft/d, for leaky-confined conditions and 113 ft^2, or 15.1 ft/d, for confined conditions.

These values were greater than the hydraulic conductivity estimate of 11.1 ft/d obtained from the trial 2 recovery data. However, the calculations were based on the assumption of homogeneous conductivity. It was known that the overlying sediments (screen 1) have a hydraulic conductivity around 50 ft/d. In addition, the rapid and severe flattening of all of the screen 2 drawdown and recovery curves was consistent with substantial transmissivity adjacent to the screened horizon. A reasonable explanation of the calculation results was that the screen 2 interval has a lower permeability than the adjacent overlying and/or underlying sediments. The greater permeability of the surrounding sediments (above and/or below the screen 2 interval) enhanced the specific capacity of screen 2. In this light, the computed lower-bound hydraulic conductivity based on the specific capacity performance of screen 2 appeared reasonable and consistent with the trial 2 recovery analysis.

R-44 Screen 2 Summary

Failure to collect very early data from most of the tests on screen 2 made determining formation properties a challenge. The best estimate of the hydraulic conductivity of the screened sediments was 11.1 ft/d from the trial 2 recovery data. The surrounding sediments (above and/or below the screened interval), however, appeared to have a substantially greater conductivity.

The specific capacity obtained from screen 2 suggested a lower-bound hydraulic conductivity of about 15 ft/d. However, that value did not factor in the effects of higher permeability adjacent sediments. In that light, the results were consistent with the estimated hydraulic conductivity of the screened interval. The results also implied an efficient completion.

Within seconds of startup or shutdown, vertical expansion of the cone of depression (leakage and partial penetration) and possibly delayed yield from the upper zone sediments affected the pumping and recovery data. The late data suggested an enormous transmissivity for the regional aquifer at the R-44 location, perhaps in excess of 100,000 gpd/ft.

C-10.0 LEAKANCE/RESISTANCE OF SEDIMENTS BETWEEN SCREENS 1 AND 2

Data from the pumping tests were used to estimate the leakance of the sediments separating R-44 screen 1 from screen 2. Each of the 24-h tests supported estimation of this parameter.

Pumping R-44 screen 1 at 24.2 gpm produced approximately 0.05 ft of drawdown in screen 2, while pumping screen 2 at 23.9 gpm resulted in about the same 0.05 ft of drawdown in screen 1. These responses to pumping were simulated analytically using Equations C-10 and C-11, assuming a uniform vertical anisotropy ratio. For each pumping test, the vertical anisotropy was adjusted until the observed drawdown in the nonpumped zone matched the field observation. The actual sediments are layered, not homogeneous, so the calculations just supported determination of an overall effective vertical resistance to flow.

The following assumptions were used in the calculations:

- aquifer thickness = 300 ft
- hydraulic conductivity = 50 ft/d
- storage coefficient ranged from 0.002 to 0.05.
- pumping rate = 24.2 gpm/23.9 gpm.
- static water level = 879 ft
- screen 1: 895 to 905 ft
- screen 2: 985.3 to 995.2 ft
- pumping time = 1440 min

The assumed hydraulic conductivity value of 50 ft/d matched the value obtained from the screen 1 pumping test. The screen 2 test produced a lower value, but the overall response of screen 2 was consistent with a highly transmissive aquifer. It was possible that screen 2 was set in lower permeability sediments than the aquifer average. Although the accuracy of the estimate was uncertain and the actual aquifer thickness assignment was arbitrary, the calculations were useful to provide a sense of the vertical permeability of the aquifer.

Using the above inputs, Equation C-10 was solved for anisotropy ratio by adjusting the ratio until the drawdown at 1440 min was equal to 0.05 ft. The computations were repeated for a few values of storage coefficient ranging from 0.002 to 0.05. Figure C-10.0-1 shows the computed relationship between storage coefficient and vertical anisotropy ratio. Virtually identical results were obtained for the two pumping tests.

The figure showed that there was insufficient data to determine the vertical anisotropy ratio accurately. Its value varied substantially as a function of storage coefficient and therefore its estimate was only as accurate as the estimate of storage coefficient.

For example, according to Figure C-10.0-1 for an assumed storage coefficient value of 0.01, the computed vertical anisotropy ratio was 0.015. Based on the assumed hydraulic conductivity of 50 ft/d, this made the estimated vertical permeability 0.015 × 50 = 0.75 ft/d. The corresponding leakance of the 80 ft of sediments separating the two screens was 0.75/80 = 0.00938 inverse days and the computed resistance was 1/0.00938 = 107 d. These calculations showed moderate vertical permeability, indicating the absence of a real aquitard. The results suggested moderate vertical movement of groundwater in the vicinity of R-44 screens 1 and 2.

These results implied a fairly conductive separating layer between screen 1 and screen 2, similar to formation characteristics at R-43, but different than what has been observed at other locations on the Plateau where the head separation between the uppermost screens in multi-screened wells is greater than observed here. As a comparison, similar analysis at R-35a and R-35b yielded hydraulic resistance on an order of magnitude greater than computed for R-44, while analysis of R-10 screens 1 and 2 data showed resistance more than two orders of magnitude greater. Note that part of the greater resistance at the other locations is attributable to the greater distance between the well screens. R-44 screens 1 and 2 are 80 ft apart, whereas the separation distance at R-35a/b is about 167 ft (accounting for elevation difference between the two wells) and that at R-10 is about 144 ft. From screen center to screen center, the downward gradients in R-35 a/b and R-10 are 0.031 ft and 0.083 /, respectively, compared with 0.0022 in R-44. Although computations like this have not been made for R-33, it is likely that the hydraulic resistance between screens 1 and 2 at that location is similar to what was determined for R-10 based on the large head difference between the screens in R-33. Thus, compared with other locations on the Plateau, the potential for vertical groundwater movement at R-44 (as well as R-43) is relatively favorable.

C-11.0 SUMMARY

Constant-rate pumping tests were conducted on R-44 screens 1 and 2 in Mortandad Canyon. The tests were conducted to gain an understanding of the hydraulic characteristics of the aquifers in which the screens were installed as well as the intervening sediments between the screens. Additionally, several surrounding wells were monitored to check for hydraulic cross connection to R-44.

Numerous observations and conclusions were drawn for the tests as summarized below.

The static water level in R-44 screen 1 was only 0.2 ft higher than in screen 2, suggesting minimal vertical hydraulic resistance of the intervening sediments. Consistent with this idea, analysis of interference effects between screen 1 and screen 2 (about 0.05 ft after 24 h of pumping 24 gpm) suggested moderate leakance.

All monitored wells and screen zones (R-44 screens 1 and 2, R-45 screens 1 and 2, R-11, R-13, and R-28) showed immediate water-level response to barometric pressure with a barometric efficiency of essentially 100%.

There was no correlation between water levels in any of the monitored wells and cycling of production wells PM-3, PM-5, and O-4. PM-4, on the other hand, which was started up a few days before the test program and ran continuously throughout, induced a small but steady drawdown trend in each of the monitored wells.

In addition to screens 1 and 2 affecting one another when pumping was performed, most (but not all) of the monitored screen zones showed slight pumping response. Table C-11.0-1 summarizes the pumping effects induced by testing R-44 screens 1 and 2, as well as that caused by continuous operation of PM-4.

Leaky threaded joints in the drop pipe used to hang the submersible test pump allowed drainage of a portion of the pipe between pumping events. Pumping against reduced head briefly until the void in the drop pipe was refilled resulted in chaotic discharge rate changes at the onset of pumping, corrupting much of the early drawdown data and rendering it unusable for determining aquifer properties. The early-recovery data, however, were usable. The leaky joints were likely attributable to a combination of worn threads, improperly manufactured threads, and the need to avoid over-tightening the threads to avoid galling.

The pumping test data indicated a hydraulic conductivity for the screen 1 sediments of about 50 ft/d.

Specific capacity analysis showed that screen 1 produced 24.2 gpm with 4.27 ft of drawdown, for a specific capacity of 5.67 gpm/ft. The lower-bound hydraulic conductivity computed from this information was 57.7 ft/d. Considering that this calculation did not consider the effects of leakage and therefore was probably overestimated, it provided reasonable corroboration of the pumping test hydraulic conductivity value.

The pumping test data indicated a hydraulic conductivity for the screen 2 sediments of about 11 ft/d.

Specific capacity analysis showed that screen 2 produced 23.9 gpm with 17.72 ft of drawdown, for a specific capacity of 1.35 gpm/ft. The lower-bound hydraulic conductivity computed from this information was about 15 ft/d. Considering that this calculation was based on homogeneous conditions and did not consider the effects of the greater permeability of adjacent sediments and therefore was probably overestimated, it provided reasonable corroboration of the pumping test hydraulic conductivity value.

All of the pumping tests showed immediate flattening of the drawdown and/or recovery curves. This reflected the effects of a combination of delayed yield and partial penetration (vertical expansion of the cone of depression). The fact that the drawdown and recovery curves remained flat at late time suggested a very large aquifer transmissivity, perhaps as great as 100,000 gpd/ft. At late time, the change in water level was within the “noise” level and accurate quantification of aquifer transmissivity was not possible.

C-12.0 REFERENCES

The following list includes all documents cited in this appendix. Parenthetical information following each reference provides the author(s), publication date, and ER ID. This information is also included in text citations. ER IDs are assigned by the Environmental Programs Directorate’s Records Processing Facility (RPF) and are used to locate the document at the RPF and, where applicable, in the master reference set.

Copies of the master reference set are maintained at the NMED Hazardous Waste Bureau and the Directorate. The set was developed to ensure that the administrative authority has all material needed to review this document, and it is updated with every document submitted to the administrative authority. Documents previously submitted to the administrative authority are not included.

Bradbury, K.R., and E.R. Rothschild, March-April 1985. “A Computerized Technique for Estimating the Hydraulic Conductivity of Aquifers from Specific Capacity Data,” *Ground Water,* Vol. 23, No. 2, pp. 240-246. (Bradbury and Rothschild 1985, 098234)

Brons, F., and V.E. Marting, 1961. “The Effect of Restricted Fluid Entry on Well Productivity,” *Journal of Petroleum Technology,* Vol. 13, No. 2, pp. 172-174. (Brons and Marting 1961, 098235)

Cooper, H.H., Jr., and C.E. Jacob, August 1946. “A Generalized Graphical Method for Evaluating Formation Constants and Summarizing Well-Field History,” *American Geophysical Union Transactions,* Vol. 27, No. 4, pp. 526-534. (Cooper and Jacob 1946, 098236)

Driscoll, F.G., 1986. Excerpted pages from *Groundwater and Wells*, 2nd Ed., Johnson Filtration Systems Inc., St. Paul, Minnesota. (Driscoll 1986, 104226)

Hantush, M.S., July 1961. “Drawdown around a Partially Penetrating Well,” *Journal of the Hydraulics Division, Proceedings of the American Society of Civil Engineers,* Vol. 87, No. HY 4, pp. 83-98. (Hantush 1961, 098237)

Hantush, M.S., September 1961. “Aquifer Tests on Partially Penetrating Wells,” Journal of the Hydraulics Division, Proceedings of the American Society of Civil Engineers, pp. 171–195. (Hantush 1961, 106003)

Schafer, D.C., January-February 1978. "Casing Storage Can Affect Pumping Test Data," *The Johnson Drillers Journal,* pp. 1-6, Johnson Division, UOP, Inc., St. Paul, Minnesota. (Schafer 1978, 098240)

Theis, C.V., 1934-1935. “The Relation Between the Lowering of the Piezometric Surface and the Rate and Duration of Discharge of a Well Using Ground-Water Storage,” *American Geophysical Union Transactions,* Vol. 15-16, pp. 519-524. (Theis 1934-1935, 098241)

Toll, N.J., and T.C. Rasmussen, January–February 2007. “Removal of Barometric Pressure Effects and Earth Tides from Observed Water Levels,” *Ground Water,* Vol. 45, No. 1, pp. 101–105. (Toll and Rasmussen 2007, 104799)

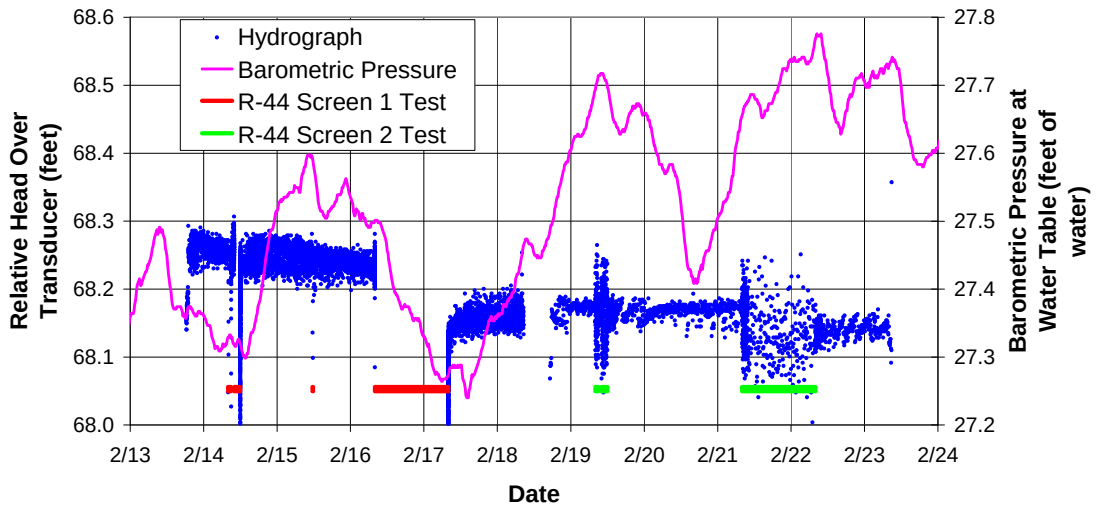

Figure C-7.0-1 R-44 screen 1 apparent hydrograph during R-44 screen 1 and 2 tests

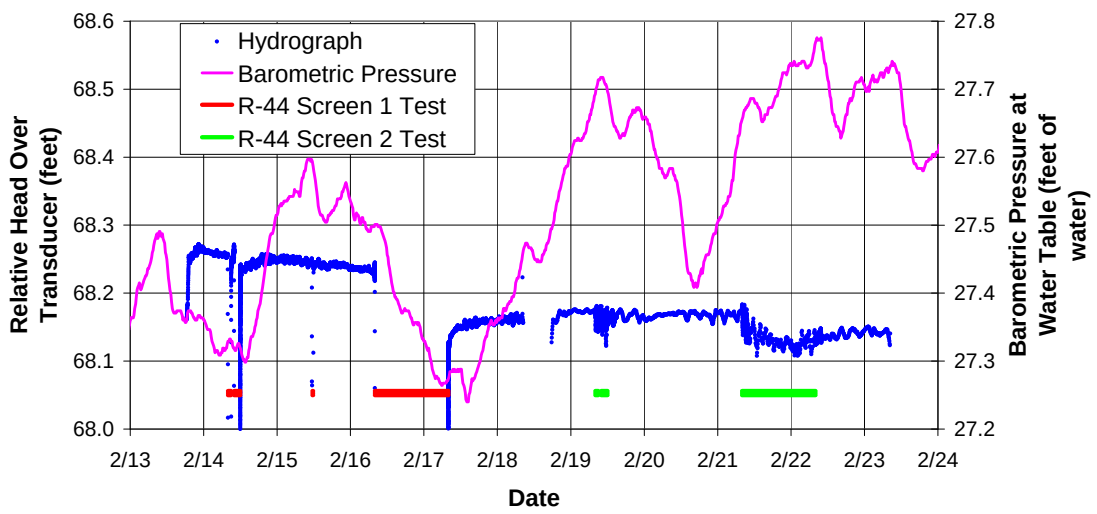

Figure C-7.0-2 R-44 screen 1 rolling apparent hydrograph during R-44 screen 1 and 2 tests

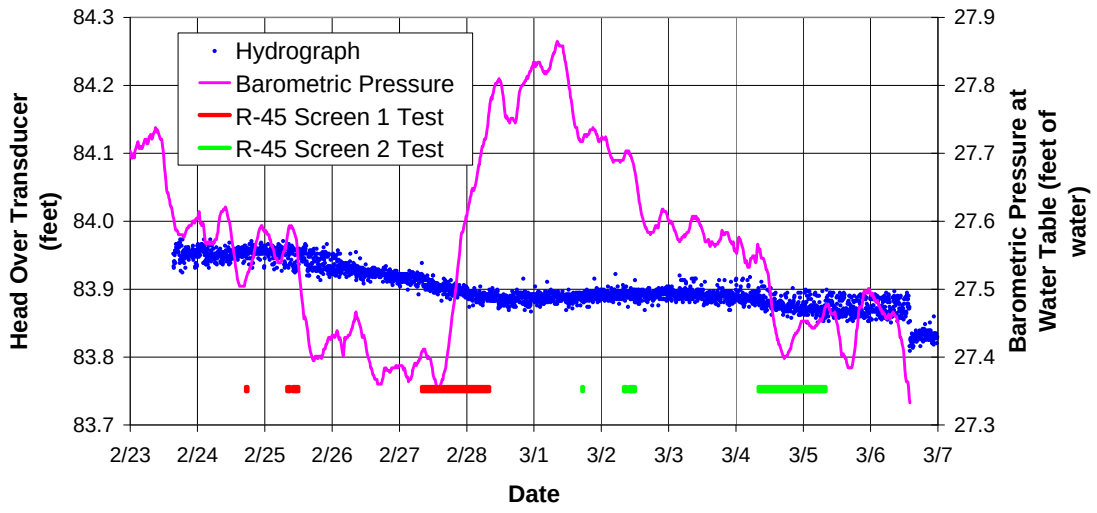

Figure C-7.0-3 R-44 screen 1 apparent hydrograph during R-45 screen 1 and 2 tests

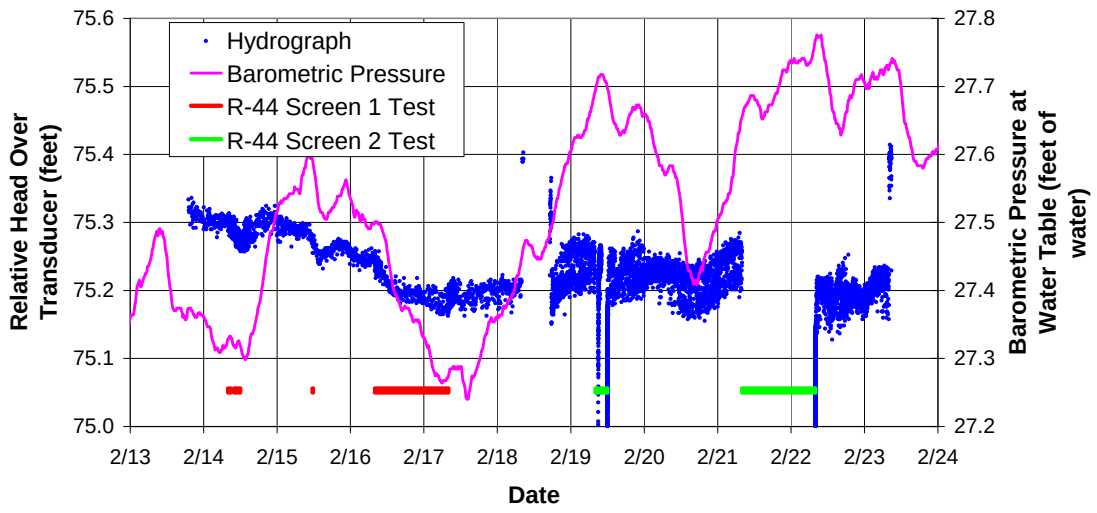

Figure C-7.0-4 R-44 screen 2 apparent hydrograph during R-44 screen 1 and 2 tests

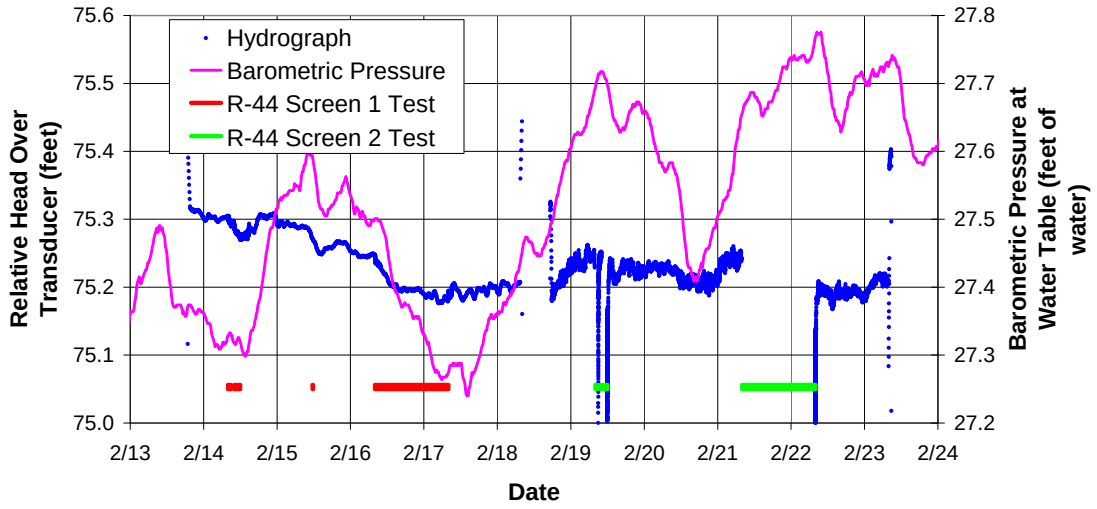

Figure C-7.0-5 **R-44 screen 2 rolling average apparent hydrograph during R-44 screen 1 and 2 tests**

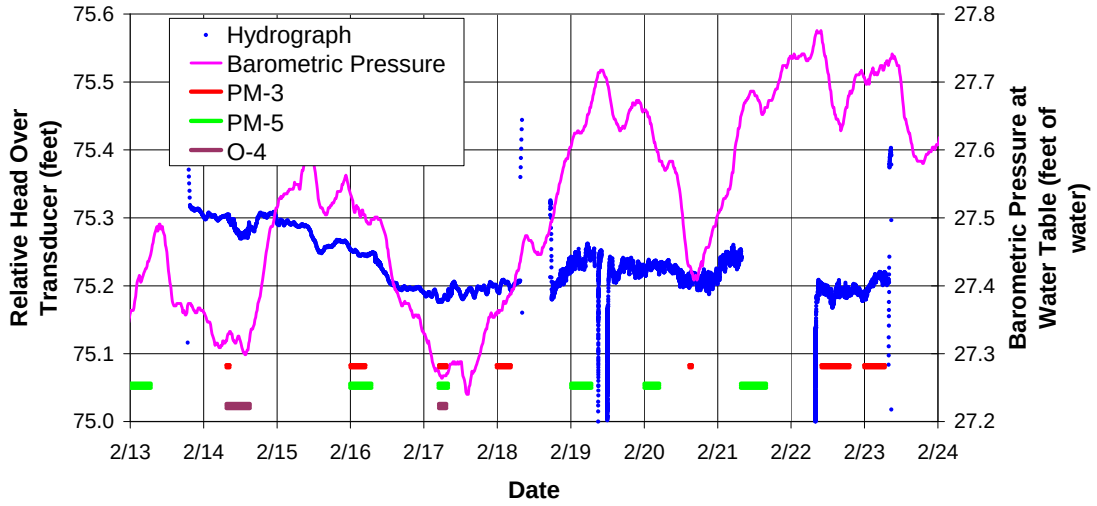

Figure C-7.0-6 **R-44 screen 2 apparent hydrograph during R-44 screen 1 and 2 tests with County well operation**

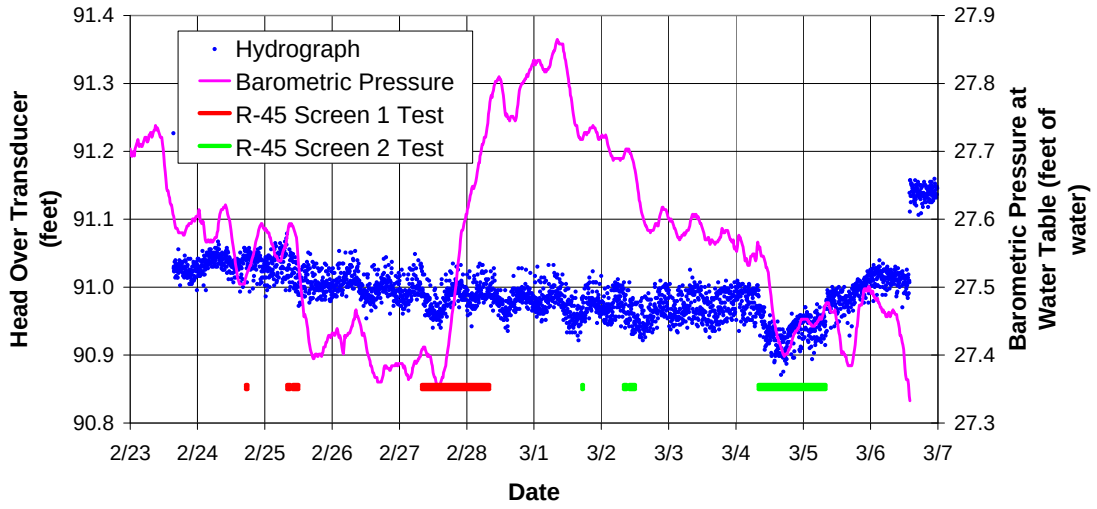

Figure C-7.0-7 R-44 screen 2 apparent hydrograph during R-45 screen 1 and 2 tests

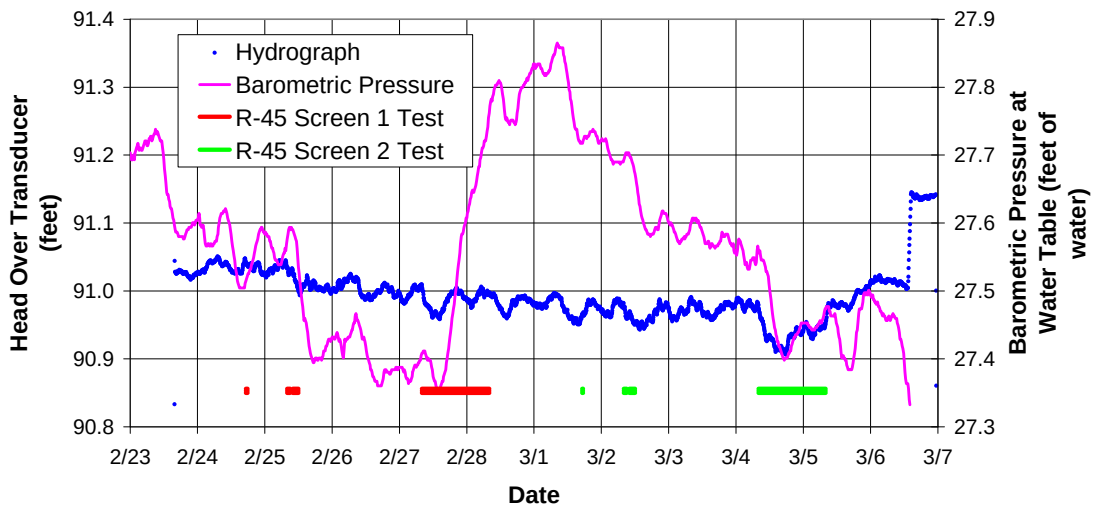

Figure C-7.0-8 R-44 screen 2 rolling average apparent hydrograph during R-45 screen 1 and 2 tests

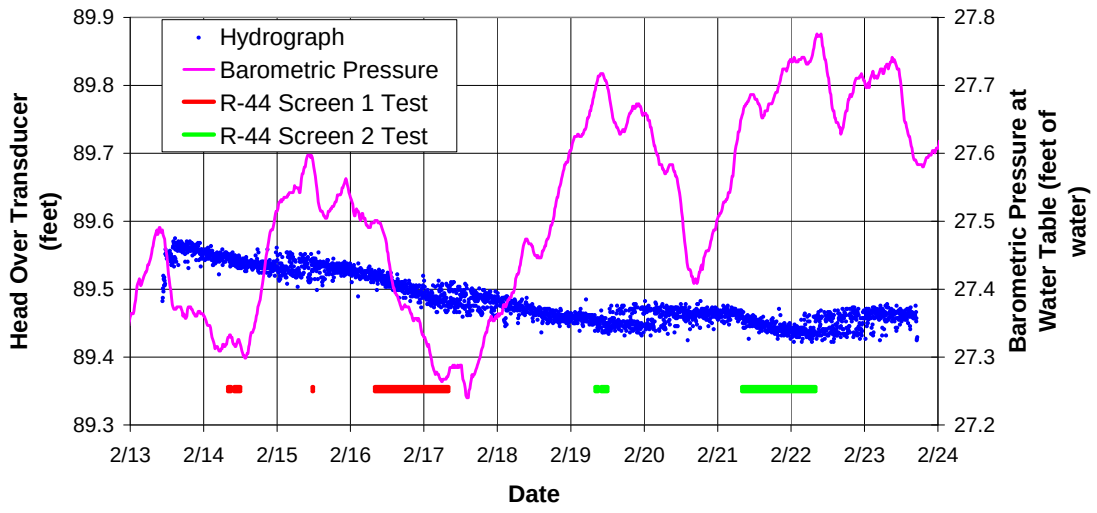

Figure C-7.0-9 R-45 screen 1 apparent hydrograph during R -44 screen 1 and 2 tests

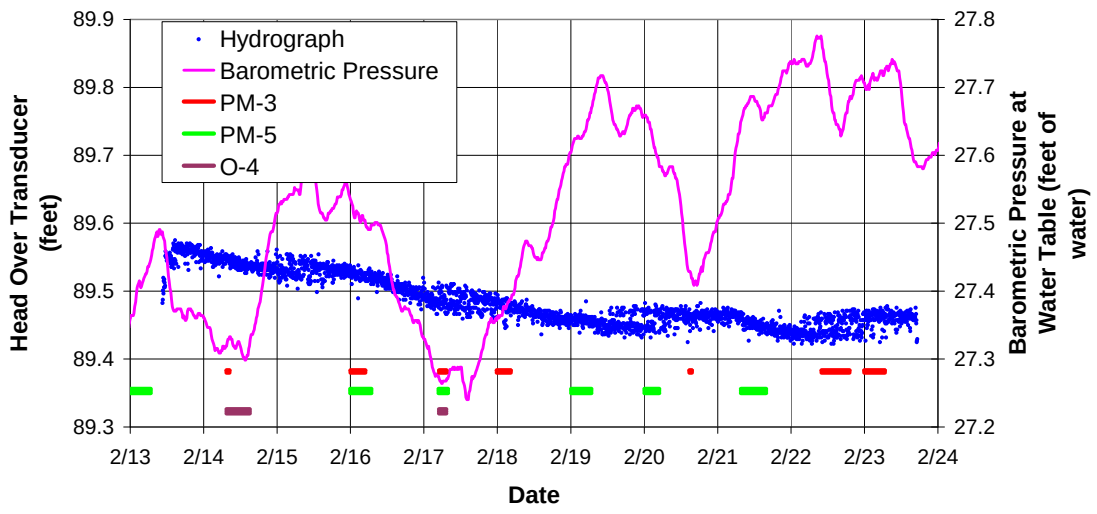

Figure C-7.0-10 R-45 screen 1 apparent hydrograph during R-44 screen 1 and 2 tests with County well operation

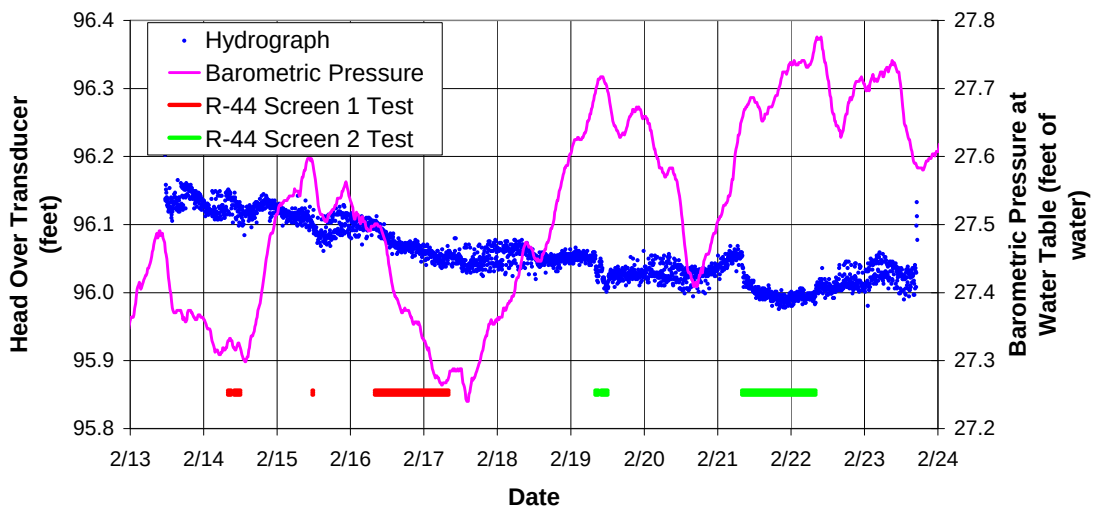

Figure C-7.0-11 R-45 screen 2 apparent hydrograph during R-44 screen 1 and 2 tests

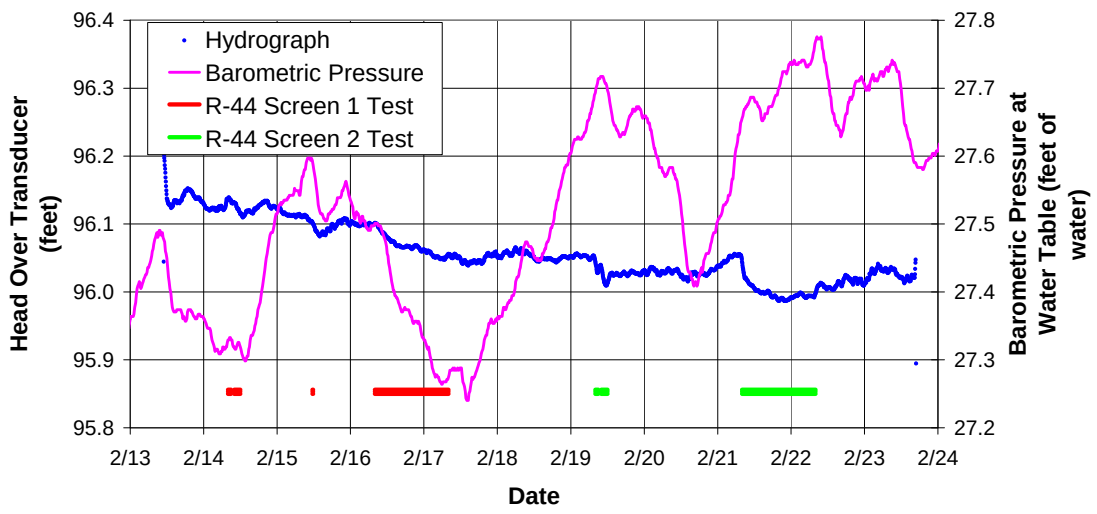

Figure C-7.0-12 R-45 screen 2 rolling average apparent hydrograph during R-44 screen 1 and 2 tests

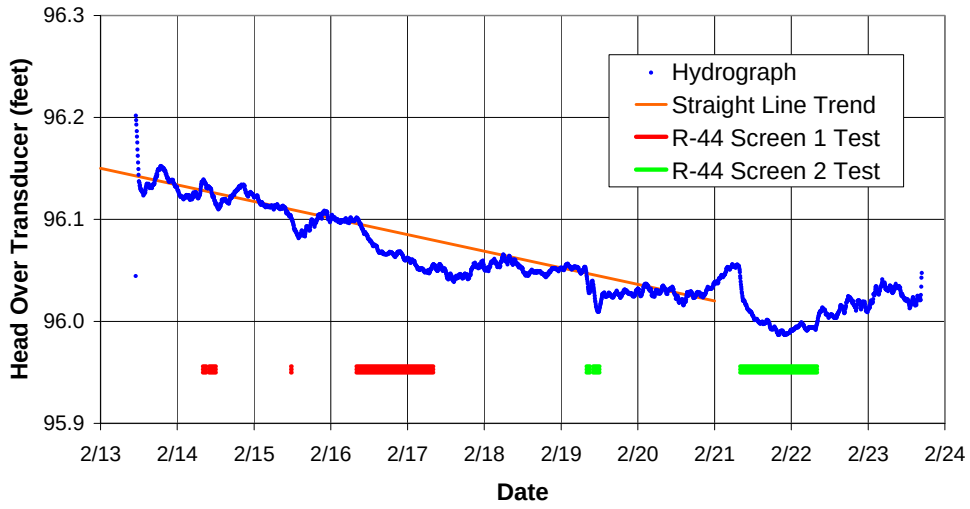

Figure C-7.0-13 R-45 screen 2 apparent hydrograph during R-44 screen 1 and 2 tests—expanded scale

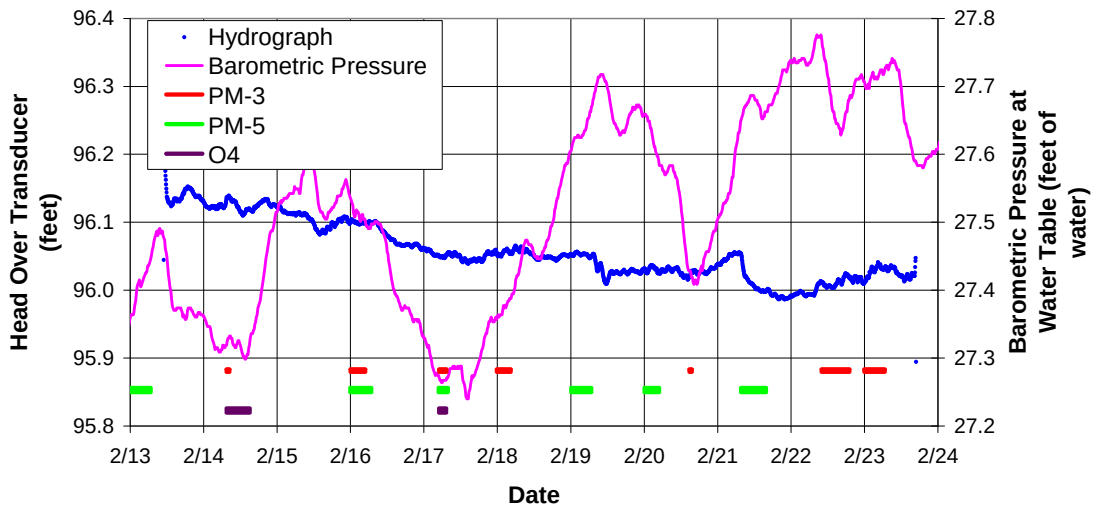

Figure C-7.0-14 R-45 screen 2 apparent hydrograph during R-44 screen 1 and 2 tests with County well operation

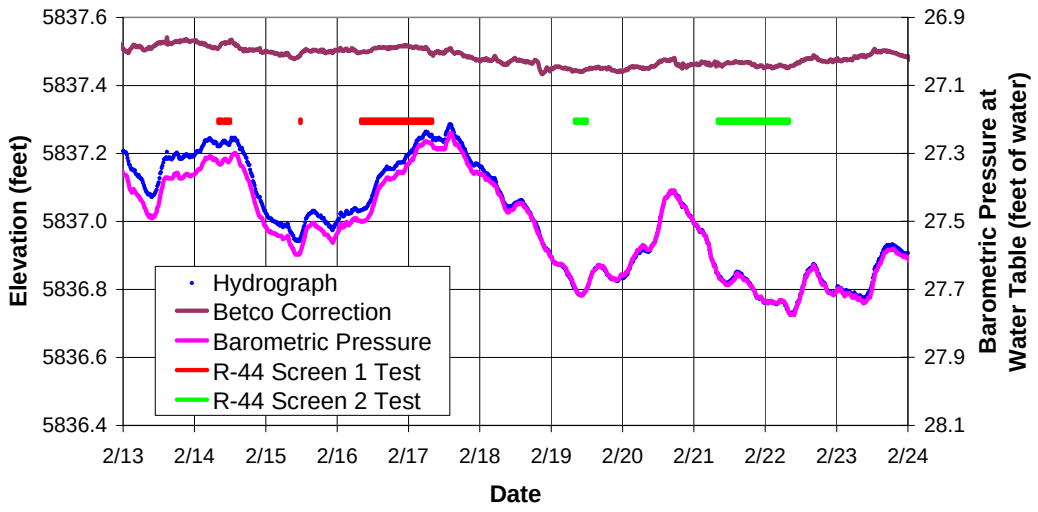

Figure C-7.0-15 R-11 hydrograph during R-44 screen 1 and 2 tests

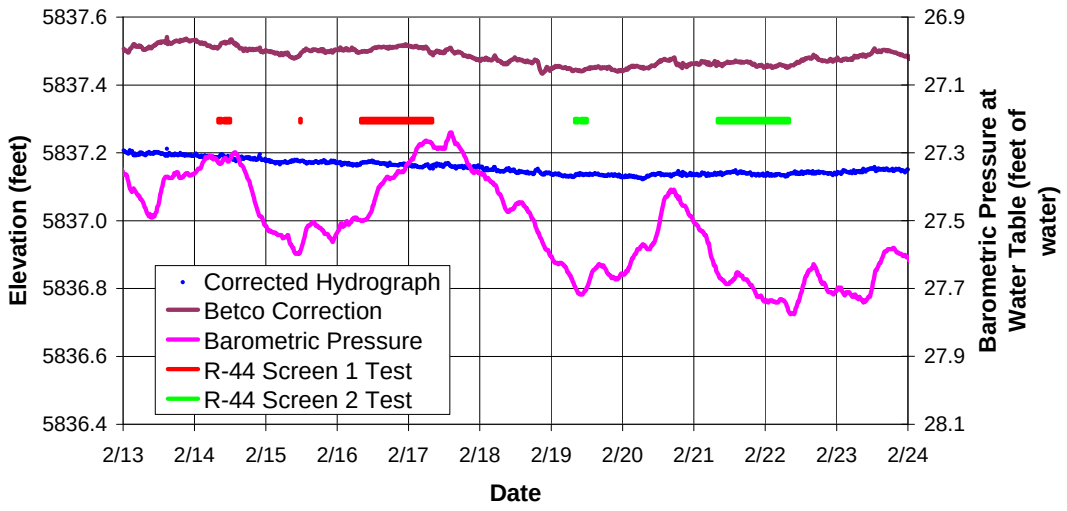

Figure C-7.0-16 R-11 corrected hydrograph during R-44 screen 1 and 2 tests

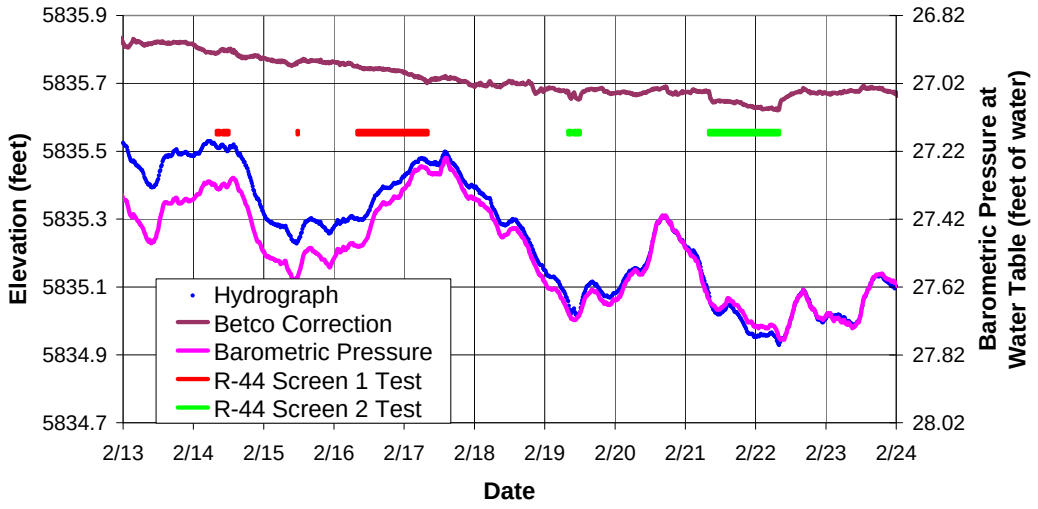

Figure C-7.0-17 R-13 hydrograph during R-44 screen 1 and 2 tests

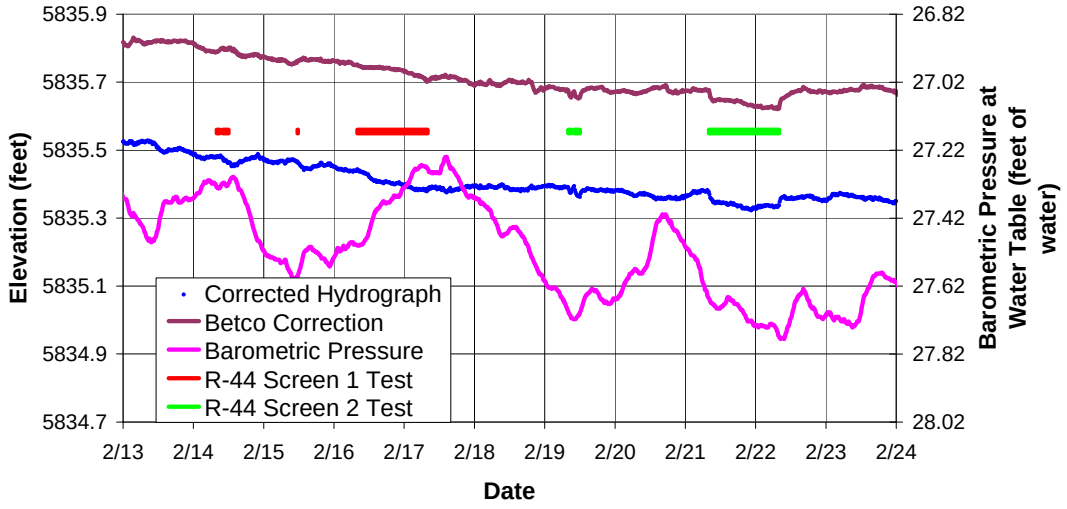

Figure C-7.0-18 R-13 corrected hydrograph during R-44 screen 1 and 2 tests

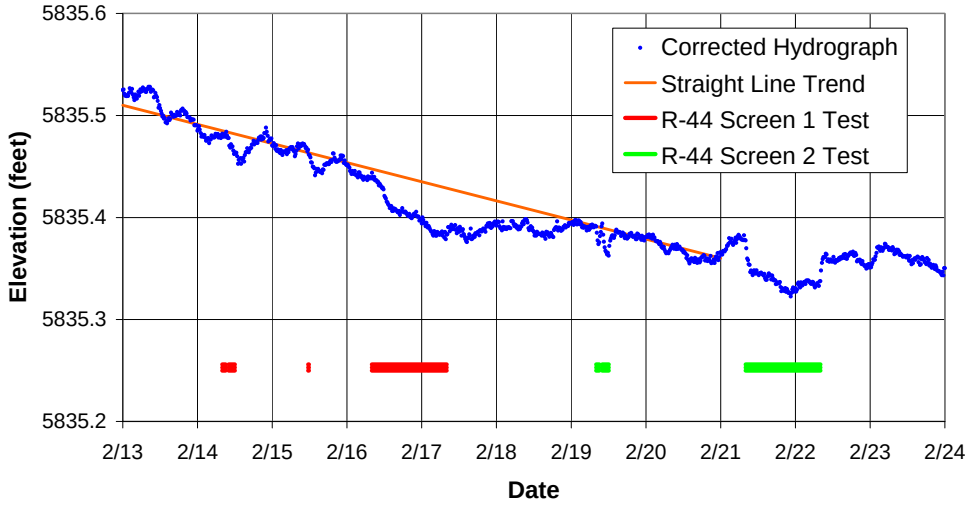

Figure C-7.0-19 R-13 corrected hydrograph during R-44 screen 1 and 2 tests—expanded scale

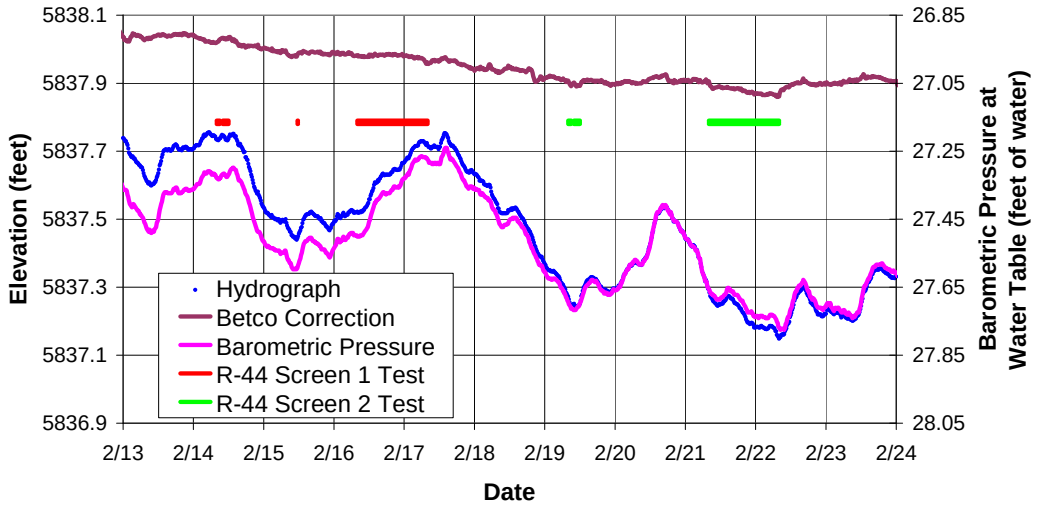

Figure C-7.0-20 R-28 hydrograph during R-44 screen 1 and 2 tests

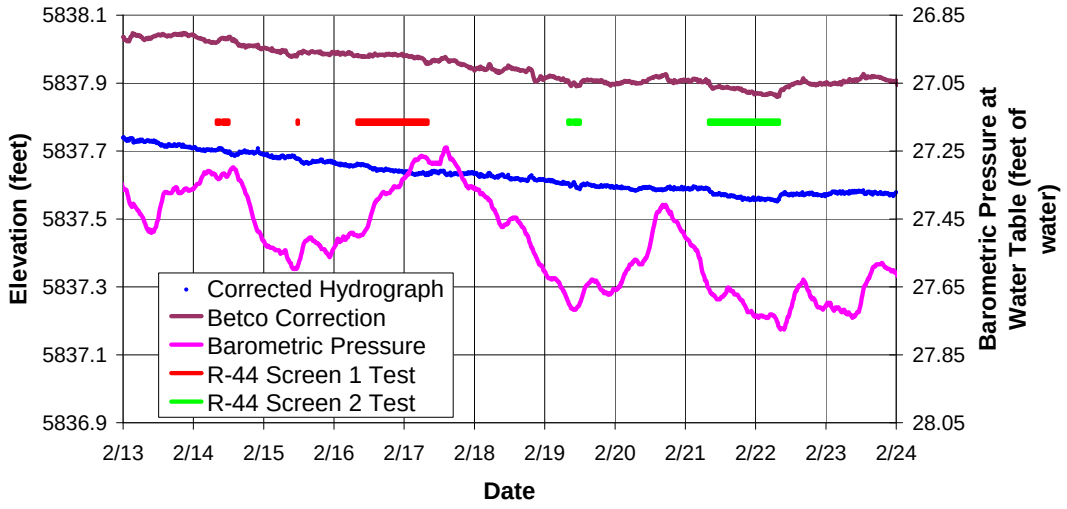

Figure C-7.0-21 R-28 corrected hydrograph during R-44 screen 1 and 2 tests

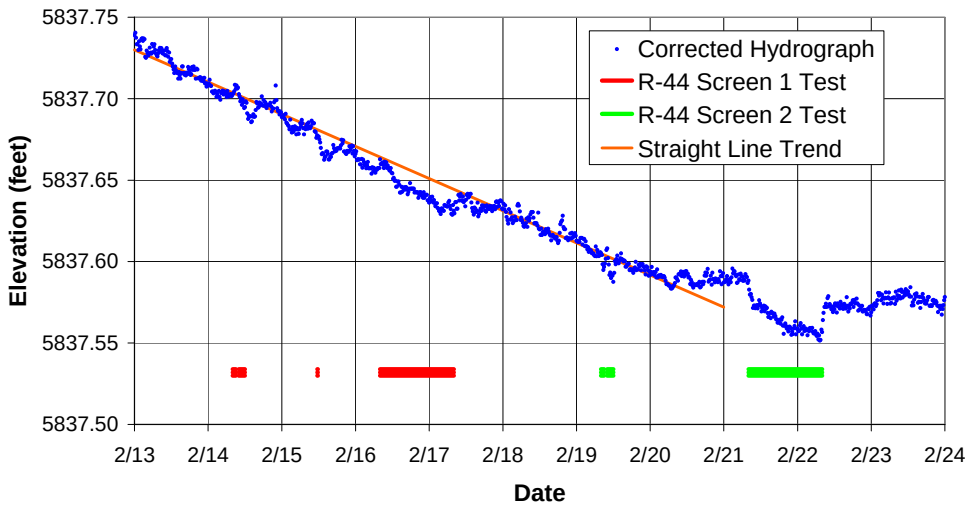

Figure C-7.0-22 R-28 corrected hydrograph during R-44 screen 1 and 2 tests—expanded scale

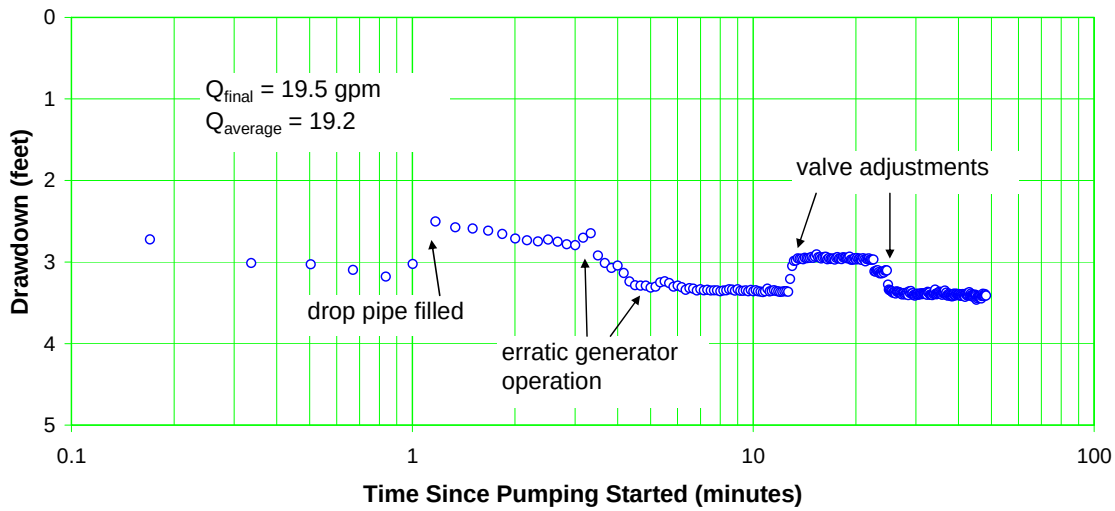

Figure C-8.0-1 Well R-44 screen 1 trail 1 drawdown

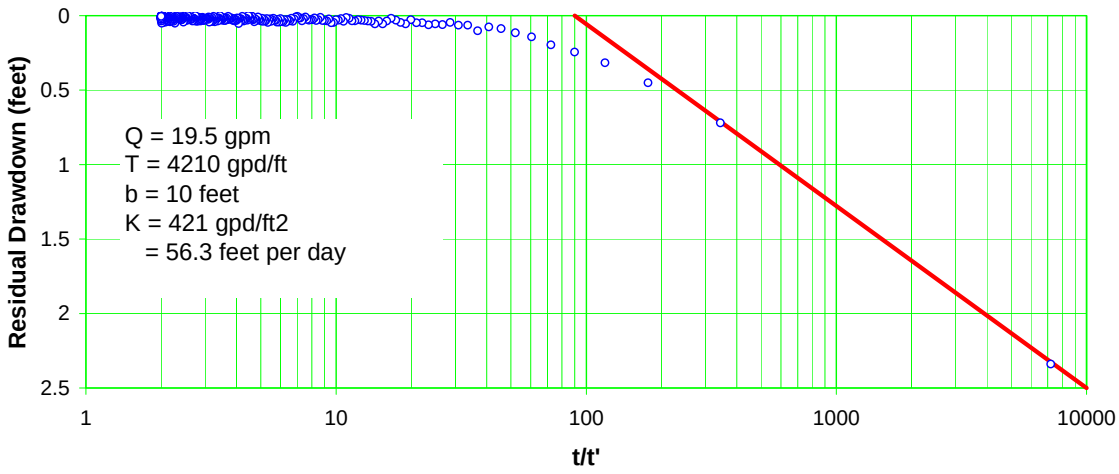

Figure C-8.0-2 Well R-44 screen 1 trail 1 recovery

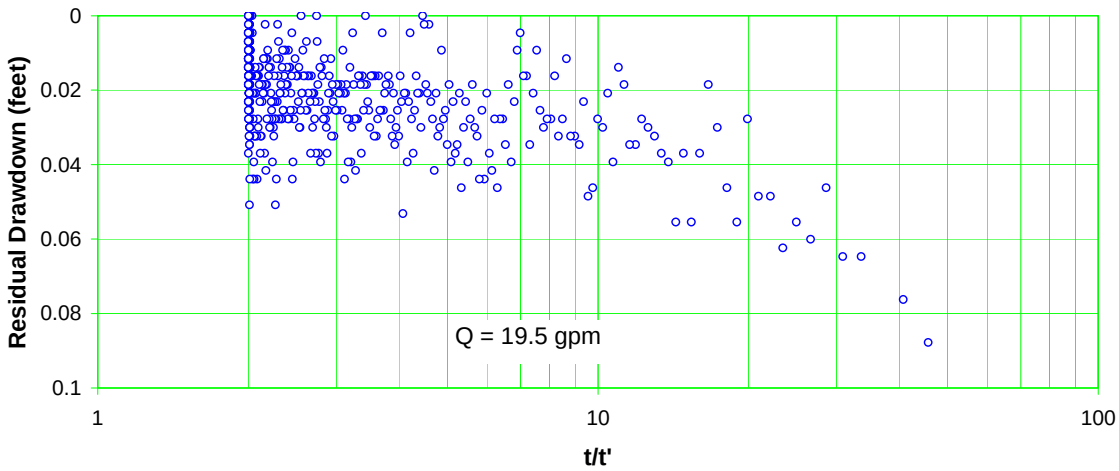

Figure C-8.0-3 Well R-44 screen 1 trail 1 recovery—expanded scale

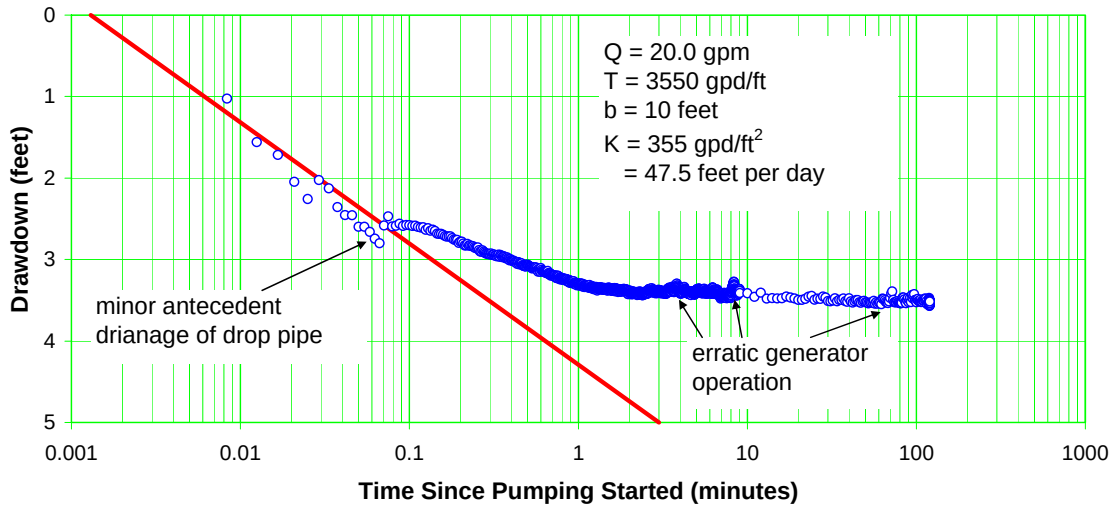

Figure C-8.0-4 Well R-44 screen 1 trail 1 drawdown

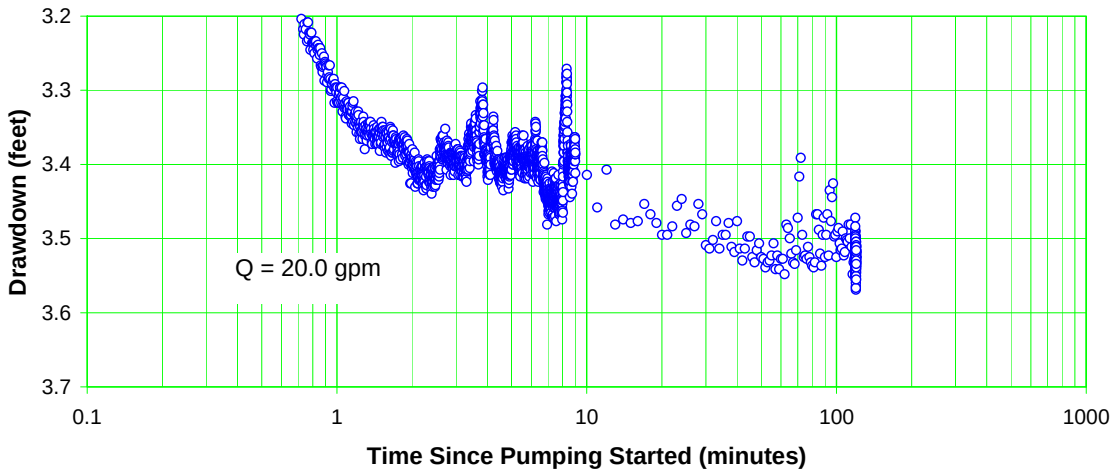

Figure C-8.0-5 Well R-44 screen 1 trail 2 drawdown—expanded scale

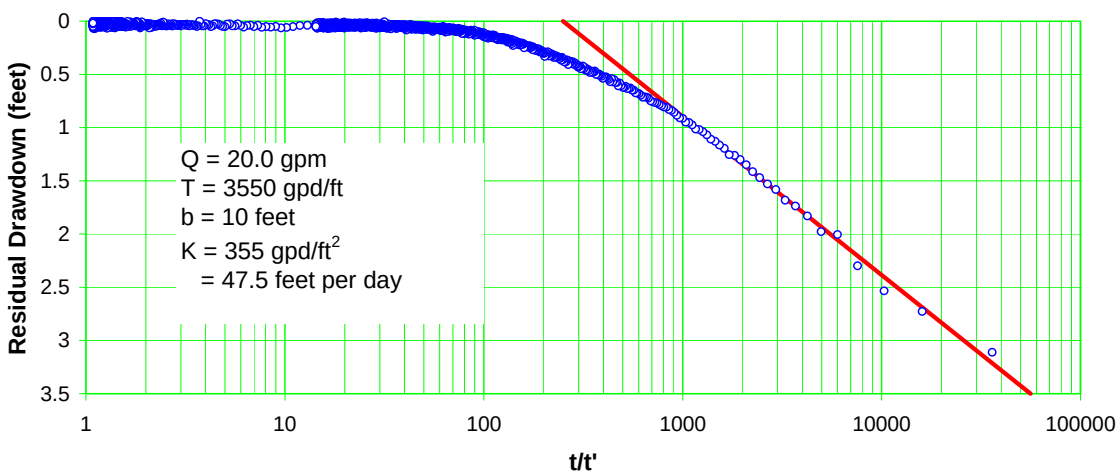

Figure C-8.0-6 Well R-44 screen 1 trail 2 recovery

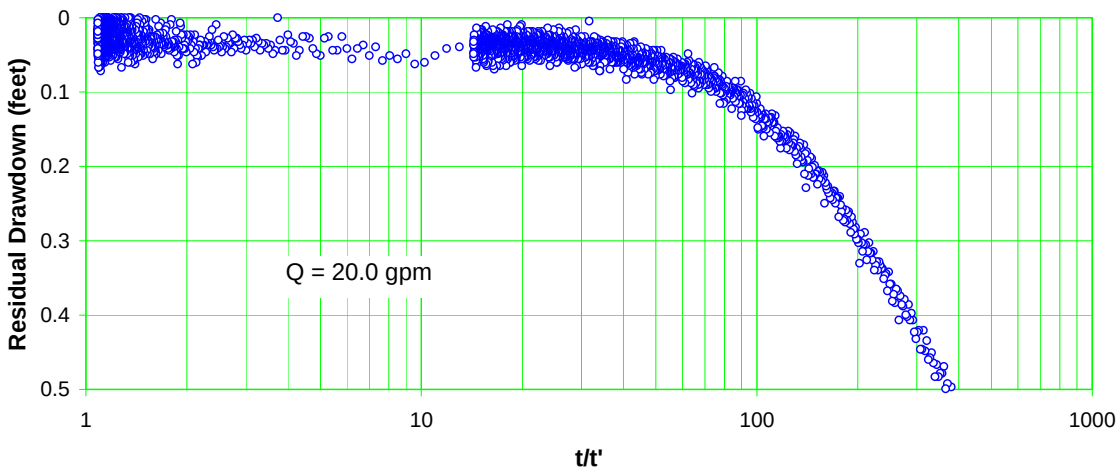

Figure C-8.0-7 Well R-44 screen 1 trail 2 recovery—expanded scale

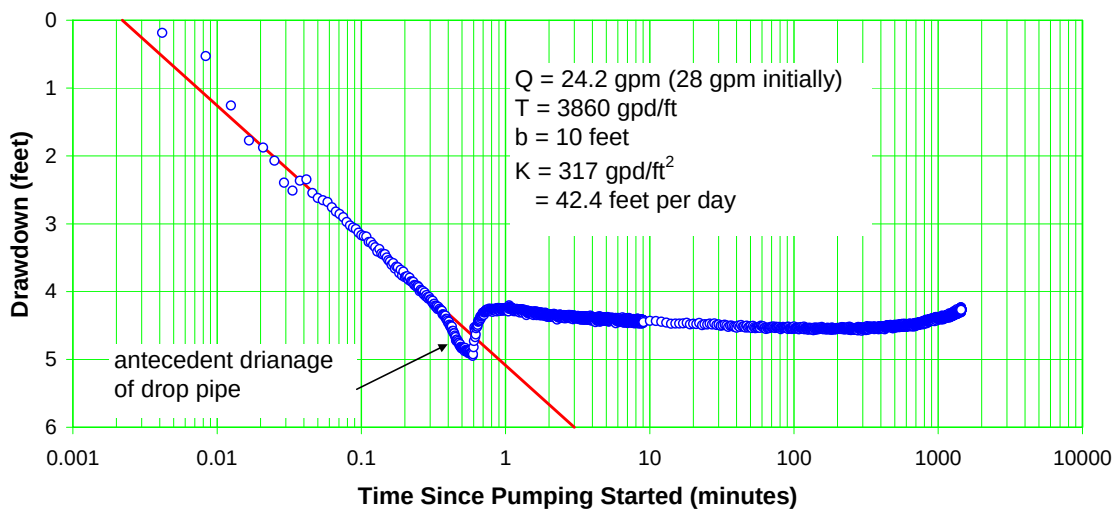

Figure C-8.1-1 Well R-44 screen 1 drawdown

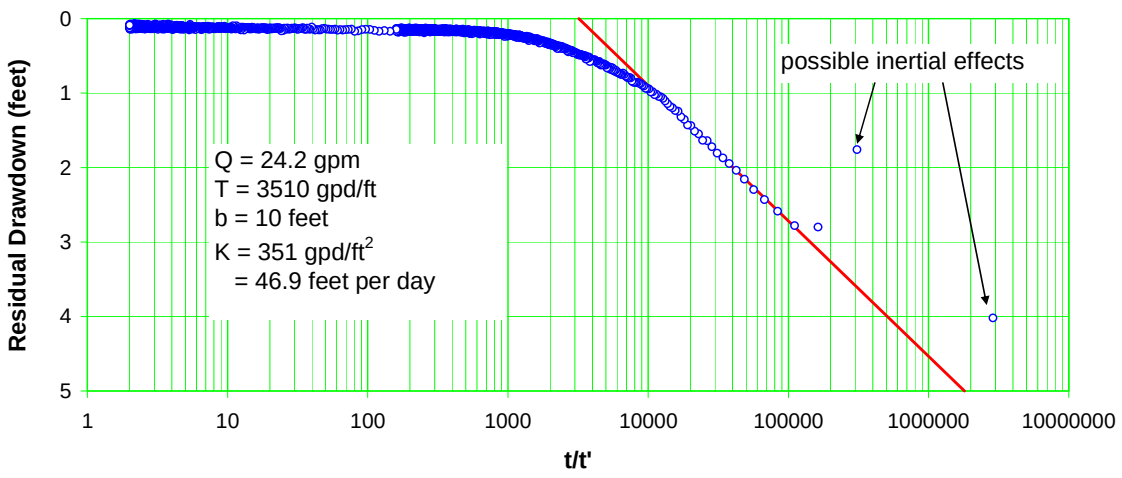

Figure C-8.1-2 Well R-44 screen 1 recovery

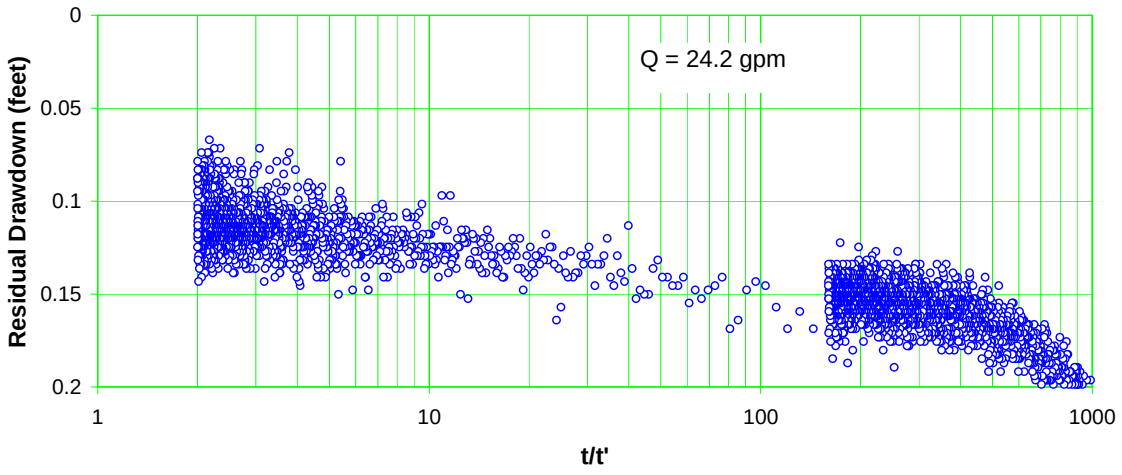

Figure C-8.1-3 Well R-44 screen 1 recovery—expanded scale

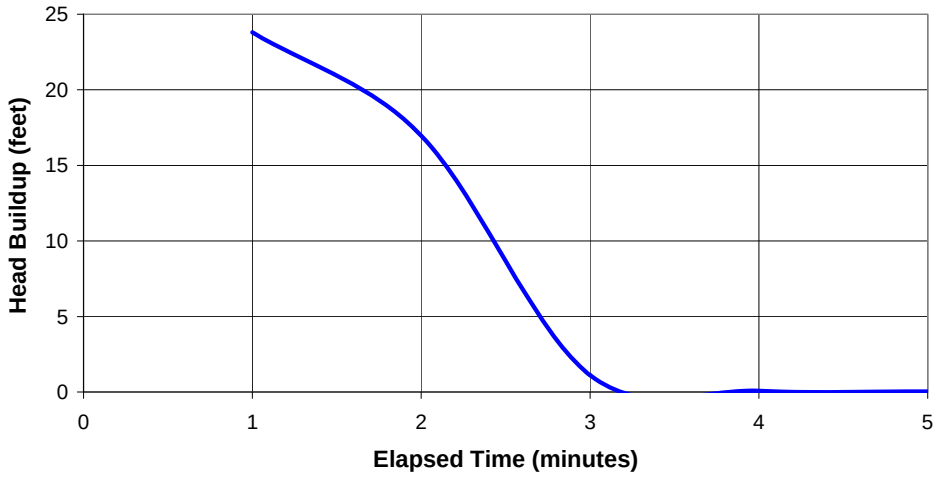

Figure C-8.1-4 Head buildup following packer deflation

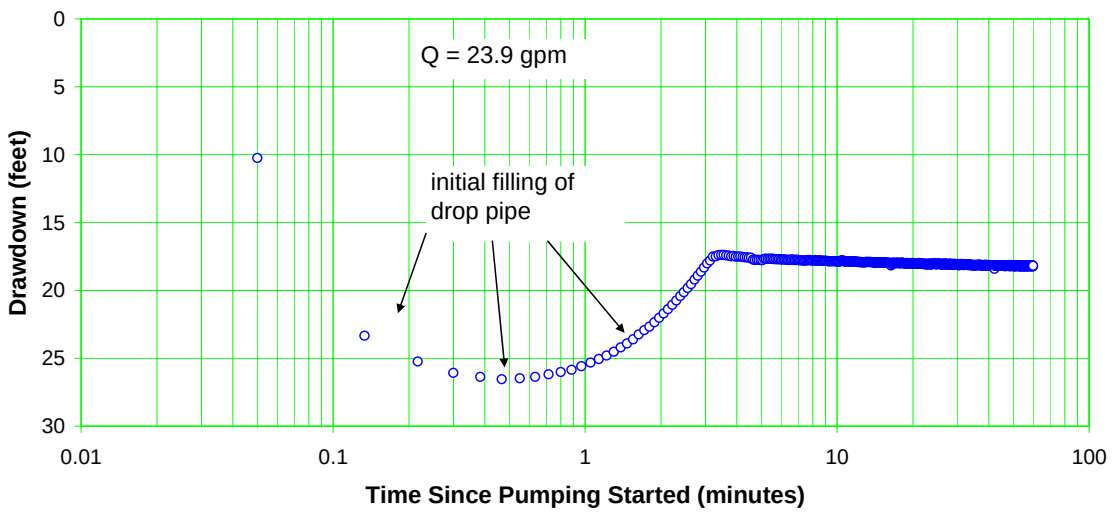

Figure C-9.0-1 Well R-44 screen 2 trail 1 drawdown

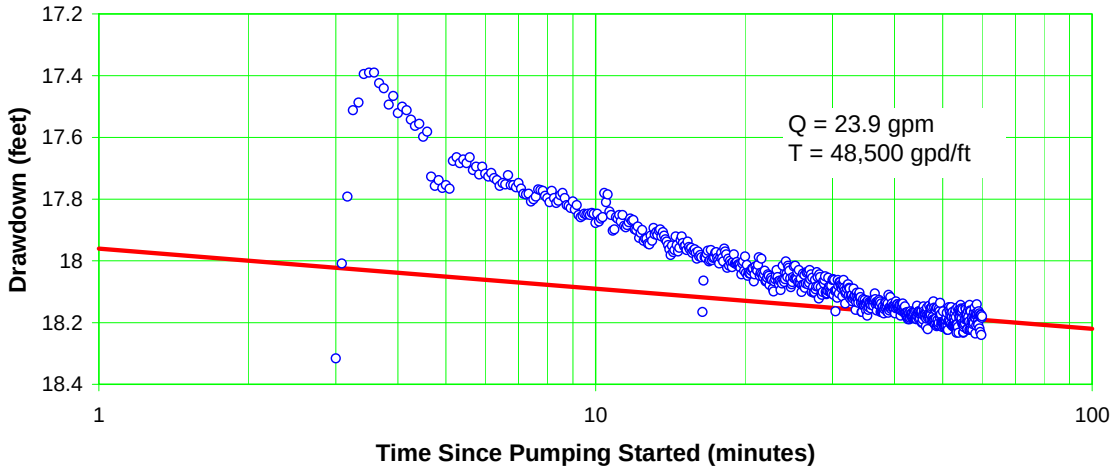

Figure C-9.0-2 Well R-44 screen 2 trial 1 drawdown—expanded scale

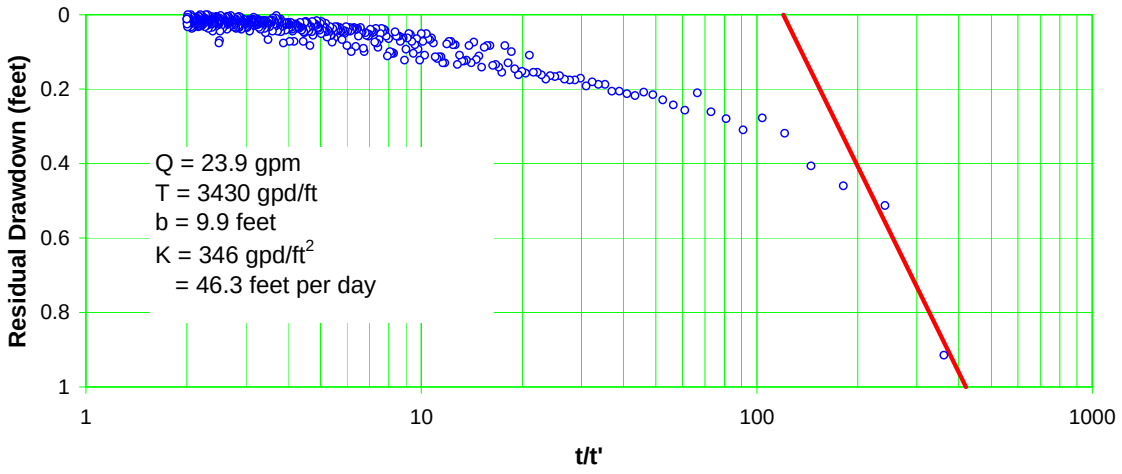

Figure C-9.0-3 Well R-44 screen 2 trial 1 recovery

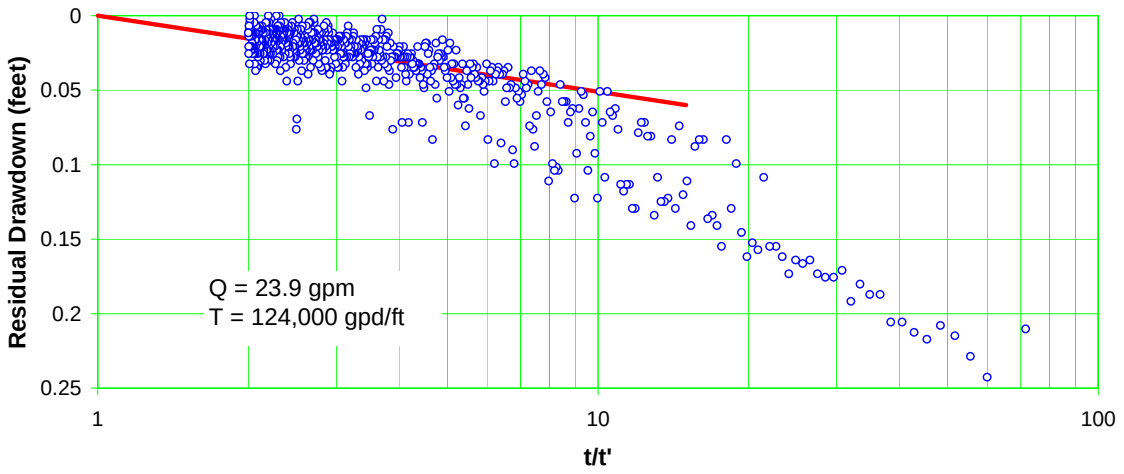

Figure C-9.0-4 Well R-44 screen 2 trial 1 recovery—expanded scale

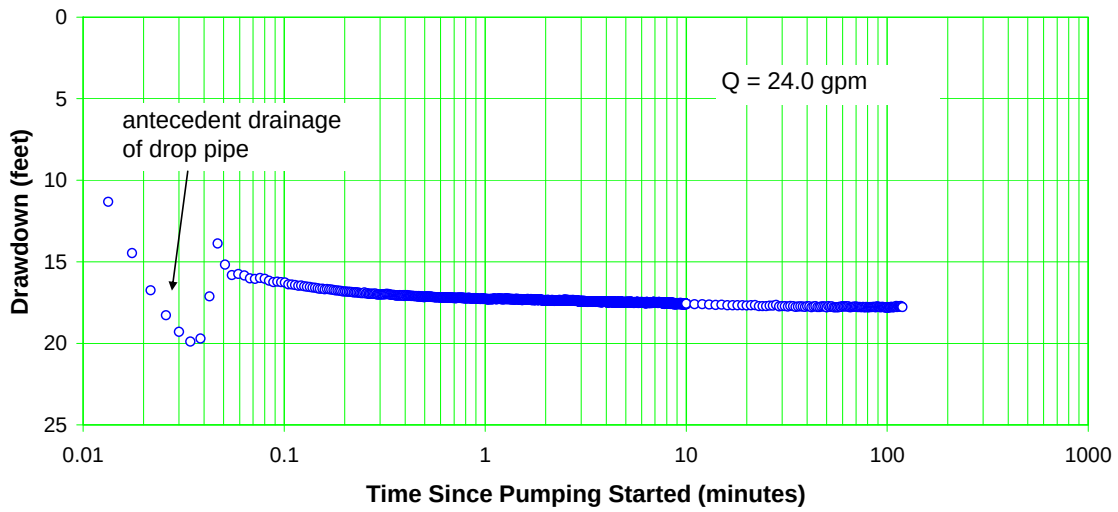

Figure C-9.0-5 Well R-44 screen 2 trial 2 drawdown

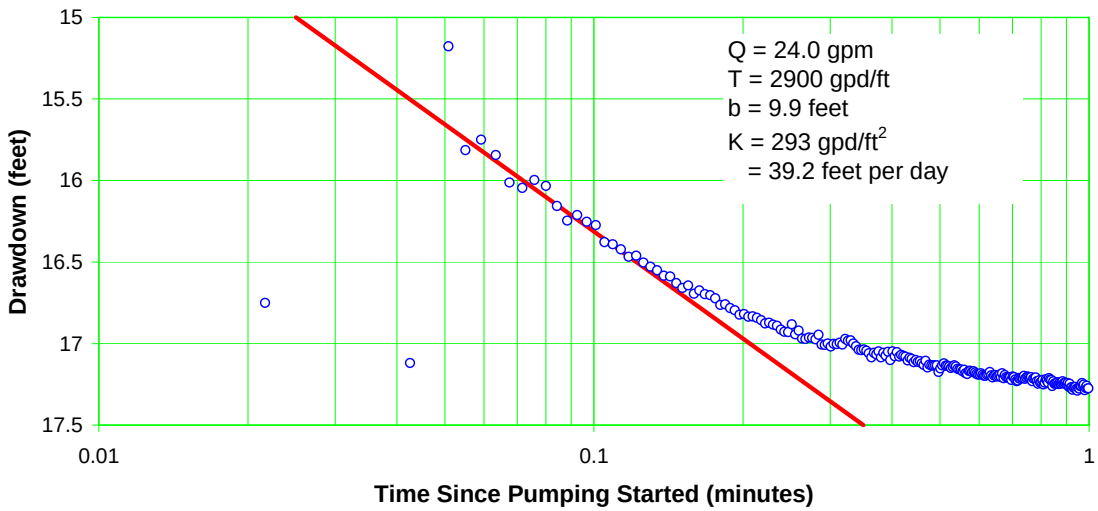

Figure C-9.0-6 Well R-44 screen 2 trial 2 drawdown—early data

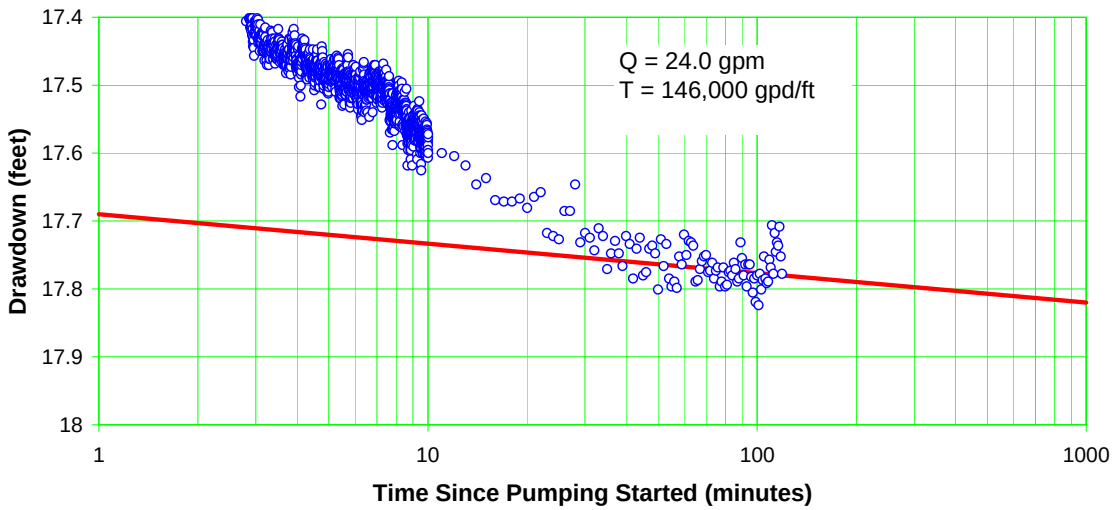

Figure C-9.0-7 Well R-44 screen 2 trial 2 drawdown—late data

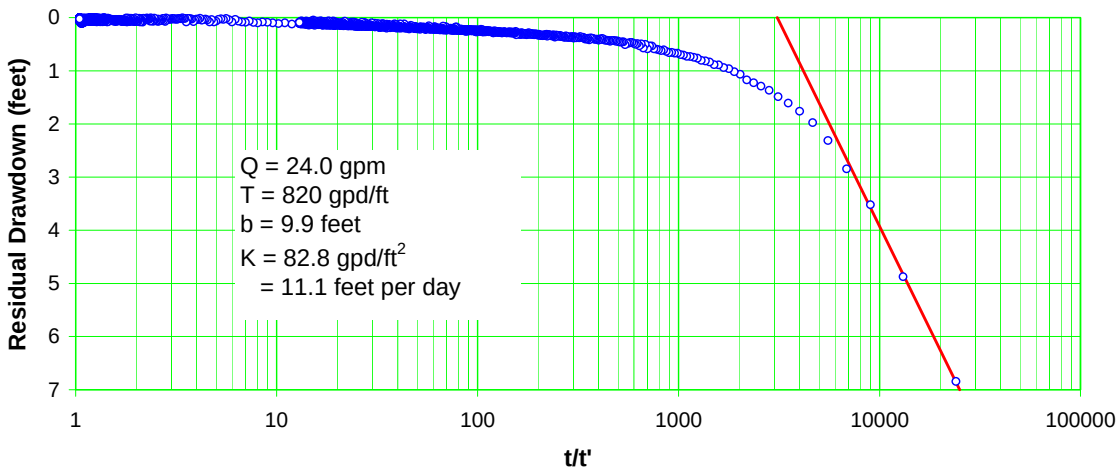

Figure C-9.0-8 Well R-44 screen 2 trial 2 recovery

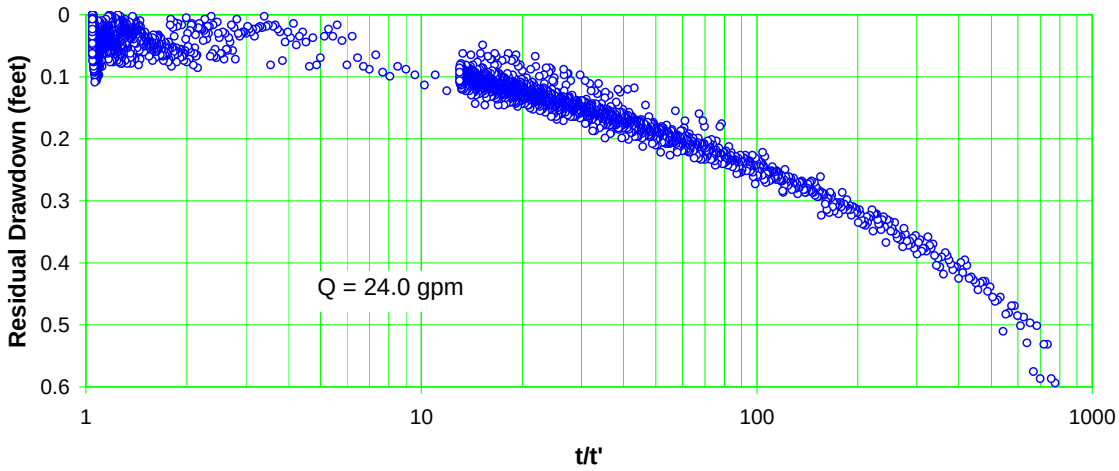

Figure C-9.0-9 Well R-44 screen 2 trial 2 recovery—expanded scale

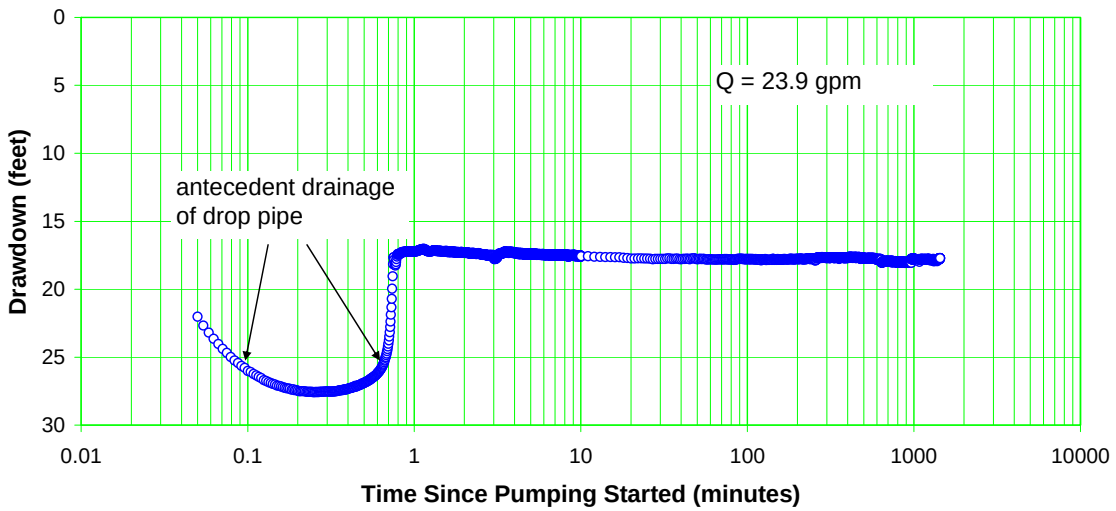

Figure C-9.1-1 Well R-44 screen 2 drawdown

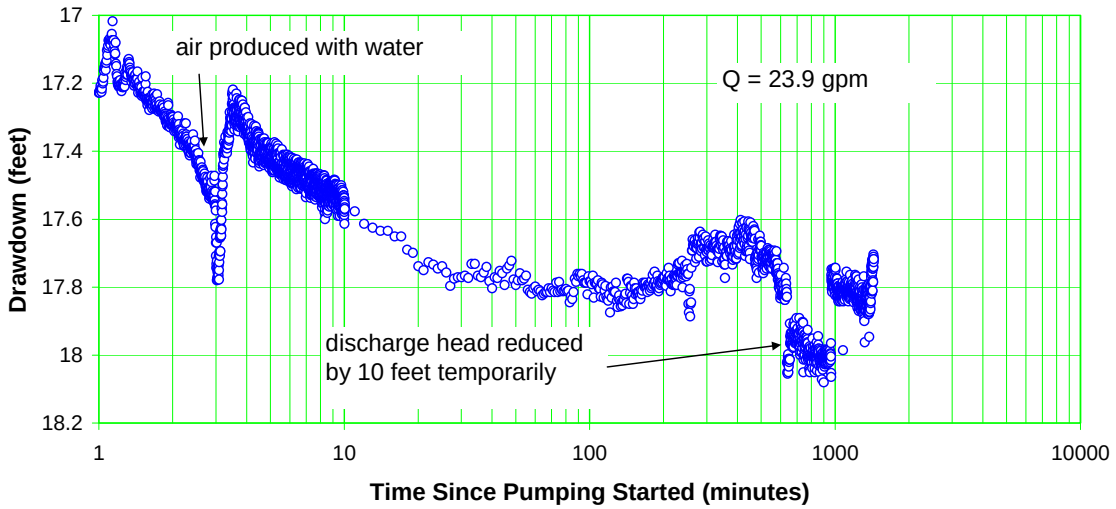

Figure C-9.1-2 Well R-44 screen 2 drawdown—expanded scale

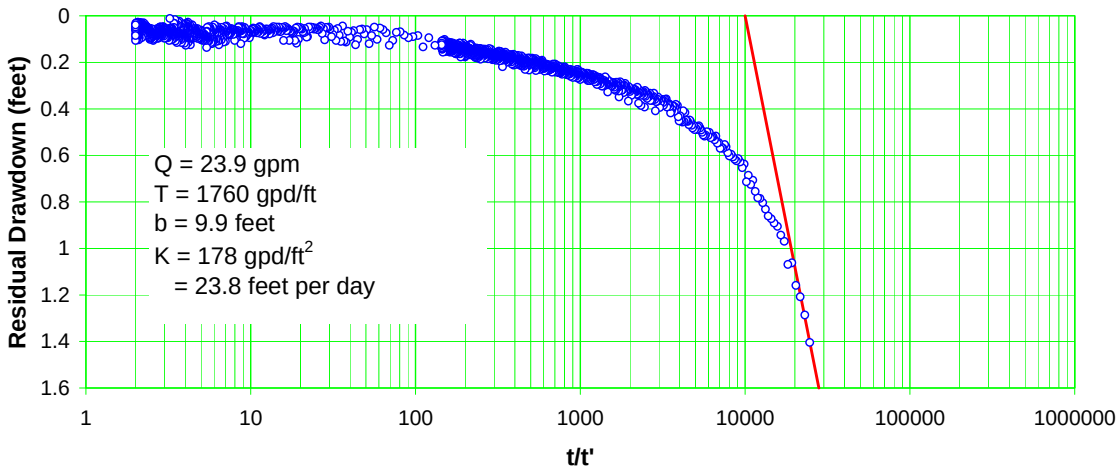

Figure C-9.1-3 Well R-44 screen 2 recovery

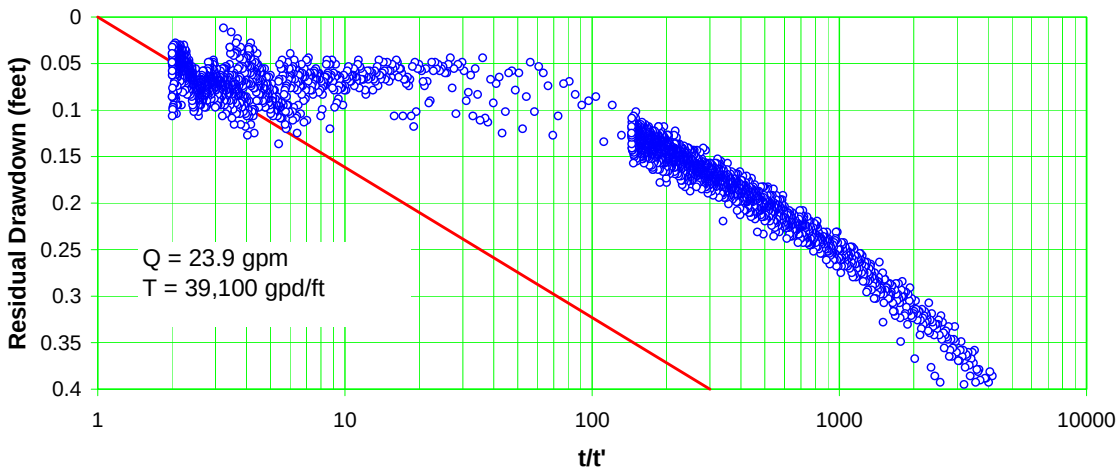

Figure C-9.1-4 Well R-44 screen 2 recovery—expanded scale

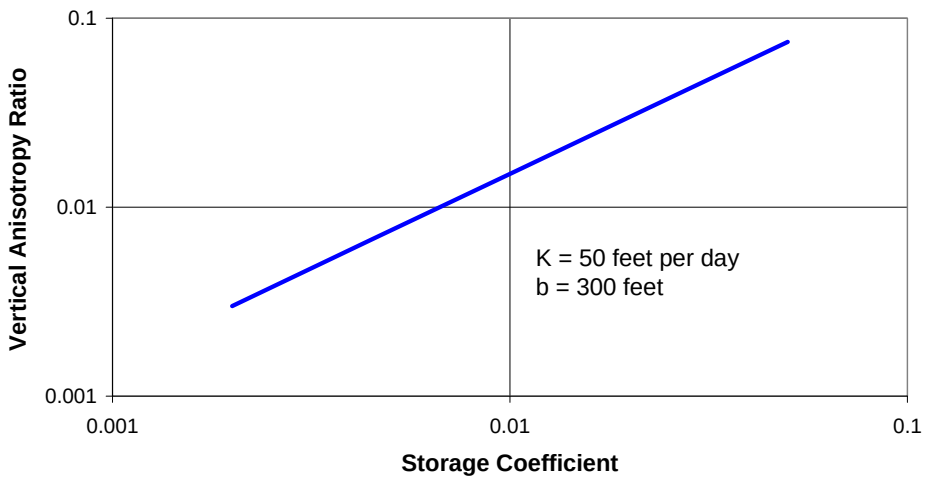

Figure C-10.0-1 Correlation of storage coefficient and anisotropy

Table C-8.1-1
R-44 Screen 1 Pumping Test Results

Analysis	Hydraulic Conductivity (ft/d)
Trial 1 Recovery	56.3
Trial 2 Drawdown	47.5
Trial 2 Recovery	47.5
24-H Drawdown	42.5
24-H Recovery	46.9
Recovery Average	50.2

Table C-11.0-1
R-44 Interference Effects

Drawdown (ft)			
Well Name (Screen ID)	Pump PM-4	Pump R-44 Screen 1	Pump R-44 Screen 2
R-44 Screen 1	0.03 (2.5 d)	n/a[a]	0.05
R-44 Screen 2	0.06 (2.5 d)	0.05	n/a
R-45 Screen 1	0.11 (6 d)	0.00	0.02
R-45 Screen 2	0.04 (3 d)	0.02	0.06
R-11	0.06 (6 d)	0.00	0.00
R-13	0.15 (7 d)	0.03[b]	0.06
R-28	0.14 (7 d)	0.01[b]	0.03

[a] n/a = Not applicable.
[b] Subtle effect.

Appendix D

Borehole Video Logging
(on DVD included with this document)

TO VIEW THE VIDEO THAT ACCOMPANIES THIS DOCUMENT, PLEASE CALL THE HAZARDOUS WASTE BUREAU AT 505-476-6000 TO MAKE AN APPOINTMENT

Appendix E

Schlumberger Geophysical Logging Report
(on CD included with this document)

Schlumberger Geophysical Report

TABLE OF CONTENTS

1.0 SUMMARY 1

2.0 INTRODUCTION 3

3.0 METHODOLOGY 4

3.1 Acquisition Procedure 5
3.2 Log QC and QA 5
3.3 Processing Procedure 6
3.3.1 Environmental Corrections and Raw Measurement Reprocessing 6
3.3.2 Depth-Matching and Reference 7
3.3.3 Integrated Log Analysis 7

4.0 RESULTS 10

4.1 Well Fluid Level 10
4.2 Regional Aquifer 10
4.3 Vadose Zone Perched Water 11
4.4 Geology 11
4.5 Summary Logs 14
4.6 Integrated Log Montage 18
4.6.1 Track 1—Depth 18
4.6.2 Track 2—Basic Logs 18
4.6.3 Track 3—Porosity 18
4.6.4 Track 4—Density 19
4.6.5 Track 5—HNGS Spectral Gamma 19
4.6.6 Tracks 6 to 11—Geochemical Elemental Measurements 19
4.6.7 Track 12—ELAN Mineralogy Model Results (Dry-Weight Fraction) 19
4.6.8 Track 13—ELAN Mineralogy and Pore Space Model Results (Wet Volume Fraction) 20
4.6.9 Track 14—Water Saturation 20
4.6.11 Track 15—Hydraulic Conductivity 21
4.6.12 Track 16—Predicted Flow (Production Potential) Profile 21
4.6.13 Track 17—Summary Logs 22
4.6.14 Track 18—Depth 22

1.0 REFERENCES 22

1.0 SUMMARY

Geophysical logging was performed by Schlumberger in characterization well R-44 in December 2008 before well completion. The logging measurements were acquired from 10 to 1,084 ft below ground surface (bgs), when the borehole contained 12 in. inside diameter (I.D.) freestanding steel casing from ground surface to 1084 ft, drilled with an approximately 12.75-in. diameter bit size.

The primary purpose of the geophysical logging was to characterize the geology and hydrogeology across the depth section where well screens were being considered, with emphasis on determining regional aquifer groundwater level, relative water saturation, depths of porous aquifer zones, and stratigraphy/lithology of geologic units. These objectives were accomplished by measuring, nearly continuously, along the length of the well (1) total water-filled porosity from which, in combination with lithologic composition estimated from the other logs, an indirect estimate of hydraulic conductivity (production capacity) is made; (2) bulk density (sensitive to total water plus air-filled porosity and grain density); (3) neutron-induced gamma ray spectroscopy, providing bulk concentrations of a number of important mineral-forming elements, as well as hydrogen; and (4) spectral natural gamma ray, including potassium, thorium, and uranium concentrations.

The following Schlumberger geophysical logging tools were used in the project (Table 1.1):

- Compensated Thermal/Epithermal Neutron Tool (CNT-G*)
- Triple Detector Litho-Density (TLD*) tool
- Elemental Capture Spectroscopy (ECS*) tool
- Hostile Natural Gamma Spectroscopy (HNGS*) and gamma ray (GR)

Table 1.1
Geophysical Logging Tool, Technology, and Corresponding Measured Properties

Tool	Technology	Properties Measured
Compensated Neutron Tool (CNT-G*)	Epithermal and thermal neutron porosity	Water/moisture content, lithologic variations
Triple Detector Litho-Density (TLD*)	Gamma-gamma bulk density	Bulk density, total porosity, lithology
Elemental Capture Spectroscopy (ECS*)	Neutron induced gamma ray spectroscopy	Formation matrix geochemistry, lithology and mineralogy, formation hydrogen content
Hostile Natural Gamma Spectroscopy (HNGS*) and gamma ray (GR)	Gross and spectral natural gamma ray, including potassium, thorium, and uranium concentrations	Formation matrix geochemistry, lithology and mineralogy

Once the Terranear PMC well drilling project team provided Schlumberger final notification that R-44 was ready for geophysical well logging, the Schlumberger district in Farmington, New Mexico, mobilized a wireline logging truck, the appropriate wireline logging tools and associated equipment, and crew to the job site. Table 1.2 summarizes the geophysical logging runs performed in R-44.

* Mark of Schlumberger.

Table 1.2
Geophysical Logging Services, Their Combined Tool Runs and Intervals Logged, as Performed by Schlumberger in Well R-44

Date of Logging	Run #	Tool 1 (bottom)	Tool 2 (top)	Tool 3	Depth Interval (ft bgs)
9-Dec-2008	1	TLD	GR		22-1084
	2	HNGS			11-1074
	3	CNT-G			80-1079
	4	ECS	GR		12-1078

Preliminary results of these measurements were generated in the logging truck at the time the geophysical services were performed and are documented in field logs provided on-site. However, the measurements presented in the field results are not fully corrected for borehole conditions (particularly casing) and are provided as separate, individual logs. The field results were reprocessed by Schlumberger to (1) correct/improve the measurements, as best as possible, for borehole/formation environmental conditions; (2) perform an integrated analysis of the log measurements so that they are all coherent and provide consistent hydrogeologic and geologic results; and (3) combine the logs in a single presentation, enabling integrated interpretation. The reprocessed log results provide better quantitative property estimates that are consistent for all applicable measurements, as well as estimates of properties that otherwise could not be reliably estimated from the single measurements alone (e.g., total porosity inclusive of all water and air present, water saturation, relative hydraulic conductivity, and lithology).

The geophysical log measurements from well R-44 provide overall, good quality results that are consistent with each other across the logged interval. However, the existence, extent, and effect on the geophysical logs of a water or air-filled annulus between the casing and the borehole wall (voids behind the casing) is difficult to determine and thus there is uncertainty about how well some of the log measurements represent true geologic formation conditions (unaffected by drilling). The distance between the logging tool sensor and formation is unknown and thus difficult to account or correct for. The measurements most affected by voids behind the casing were ones that have a shallow depth of investigation and that require close contact to the uncased borehole wall—the bulk density and the neutron porosity measurements (particularly the former). One indicator that the bulk density is being adversely affected by voids behind the casing is when the computed density porosity is unrealistically high. Where the total porosity estimated from the processed logs reaches above 55%, the bulk density measurement is likely being affected by voids. There are relatively few intervals in R-44 where the density porosity surpasses 55%.

Important results from the processed geophysical logs in R-44 include the following.

1. The well standing water level in R-44 was 880 ft bgs at the time of logging and did not vary much between the different logging runs.
2. The processed logs indicate that the intersected geologic section is fully saturated with water from the bottom of the borehole (1084 ft bgs) to 880 or 878 ft bgs, which lies within alluvium/fanglomerate. Below 878 ft, the log-estimated water content and total porosity are very high (mostly greater than 50% of total rock/sediment volume). Above 878 ft, the water content is much lower, mostly at or below 10%. Total porosity across this same interval mostly ranges from 20% to 40%, resulting in an estimated water saturation that stays below 50% of total pore volume. Based on these results, the depth of the regional aquifer water level (depth at which there is full water saturation) is 878–880 ft, coinciding with the well water level at the time of logging.

3. Above 878 ft bgs, which the processed logs definitely show to be within the vadose zone (above the top of the regional aquifer), the estimated water content varies from less than 5% to 17% of total rock volume, mostly remaining at or below 10%. Estimated water saturation is mostly below 50% of total pore volume (never above 75%) across the entire vadose zone. The highest vadose zone water saturation is in the following zones:
   - 704–708 ft, where water content is 15% and water saturation reaches 60%—located in the bottom part of a likely thick basalt lava sequence that has zones of significantly lower estimated total porosity than the surrounding rock, including the bottom section where this zone is (presumably the basalt is more competent here)
   - 647–652 ft, where water saturation reaches 75%—located in the same basalt lava sequence and low porosity zone
   - 395–397, 467–469, and 500–502 ft, where water saturation reaches between 40% and 62%—located in the same basalt lava sequence in zones where the total porosity is a lot lower than the surrounding rock
   - 314–340 ft, where water saturation reaches 40%—located at the top of the same basalt lava that lies immediately below the Guaje Pumice Bed, where there is higher water content (approximately 15%) and perhaps the basalt is eroded and/or reworked
4. The location of productive zones within the saturated section is difficult to determine because of the adverse cased well conditions. Higher porosity is not necessarily indicative of higher production capacity since fine-grained sediments often have higher porosity and lower productivity than coarser-grained sediments. The highest porosities are likely associated with washouts behind the casing. The predicted relative flow capacity profile generated from the integrated log analysis estimated permeability results suggest that the most productive intervals are 884–893 ft, 897–900 ft, 903–907 ft, 919–922 ft, 924–926 ft, 939–941 ft, 953–954 ft, 964–966 ft, 974–976 ft, 982–995 ft, 1000–1015 ft, 1022–1027 ft, 1042–1048 ft, 1053–1056 ft, and 1072–1074 ft.
5. The geophysical log results clearly delineate that the saturated/water-filled section of the borehole consists of alluvium/fanglomerate that extends well into the unsaturated section up to 709 ft bgs. Above 709 ft bgs, the processed logs strongly indicate a change in the matrix geochemical makeup and lithology to a thick basaltic lava sequence, which extends up to 314 ft (it is possible the top is reworked/altered basalt/tuff). The geophysical log response in the zone 298–314 ft is characteristic of the Guaje Pumice Bed, with very high total porosity and a large increase in thorium and uranium concentrations. The log results corroborate volcanic tuff overlying the pumice bed and extending to the top of the log interval (10 ft bgs), with zonal variations in porosity and geochemical signature, although it is possible the top section is alluvium composed of reworked tufflike material.

2.0 INTRODUCTION

Geophysical logging services were performed in characterization well R-44 by Schlumberger in December 2008 before initial well completion. The purpose of these services was to acquire in situ measurements to help characterize the near-borehole geologic formation environment. The primary objective of the geophysical logging was to provide in situ evaluation of formation properties (hydrogeology and geology) intersected by the well. This information was used by scientists, engineers, and project managers in the Los Alamos Characterization and Monitoring Well Project to help design the well completion, better understand subsurface site conditions, and assist in overall decision-making.

The primary geophysical logging tools used by Schlumberger in well R-44 were the

- CNT-G, which measures, through casing and in water or air-filled hole, volumetric water content of the formation to evaluate moist/porous zones using both epithermal and thermal neutron measurements;
- TLD tool, which measures formation bulk density through casing to estimate total porosity;
- HNGS tool, which measures gross natural gamma and spectral natural gamma ray activity, including potassium, thorium, and uranium concentrations, to evaluate geology/lithology, particularly the amount of thorium and potassium-bearing minerals; and
- ECS tool, which measures neutron-induced spectral gamma ray activity; this determines elemental weight fraction concentrations of a number of key rock-forming elements used to characterize geochemistry, mineralogy, and lithology of the formation, as well as hydrogen content (closely related to water content).

In addition, calibrated gross GR was recorded with every service for the purpose of correlating depths between the different logging runs. Table 2.1 summarizes the geophysical logging runs performed in R-44.

Table 2.1
Geophysical Logging Services, Their Combined Tool Runs and Intervals Logged, as Performed by Schlumberger in Borehole R-44

Date of Logging	Borehole Status	Run #	Tool 1 (bottom)	Tool 2 (top)	Tool 3	Depth Interval (ft bgs)
9-Dec-2009	Steel freestanding casing from surface to bottom. Single string of 12- in I.D. casing from surface to the bottom of the borehole at 1018 ft, with bit size of ~12.75 in.	1	TLD	GR		22–1084
	Same	2	HNGS			11–1074
	Same	3	CNT-G			80–1079
	Same	4	ECS	GR		12–1078

A more detailed description of these geophysical logging tools can be found on the Schlumberger website (http://www.slb.com/content/services/evaluation/index.asp?).

3.0 METHODOLOGY

This section describes the methods Schlumberger employed for geophysical logging of well R-44, including the following stages/tasks:

- measurement acquisition at the well site
- quality assessment of logs
- reprocessing of field data

3.1 Acquisition Procedure

Once the well drilling project team notified Schlumberger that R-44 was ready for geophysical well logging, the Schlumberger district in Farmington, New Mexico, mobilized a wireline logging truck, the appropriate wireline logging tools and associated equipment, and crew to the job site. Upon arriving at the Los Alamos National Laboratory site, the crew completed site-entry paperwork and received a site-specific safety briefing.

After arriving at the well site, the crew proceeded to rig up the wireline logging system, including

- parking and stabilizing the logging truck in a position relative to the borehole that is best for performing the surveys,
- setting up a lower and an upper sheave wheel (the latter attached to, and hanging above, the borehole from the drilling rig/mast truck),
- threading the wireline cable through the sheaves, and
- attaching to the end of the cable the appropriate sonde(s) for the first run.

Next, prelogging checks and any required calibrations were performed on the logging sondes, and the tool string was lowered into the borehole. If any of the tools required active radioactive sources (in this case, a neutron and gamma source for the ECS/CNT-G and TLD, respectively), the sources were taken out of their carrying shields and placed in the appropriate tool source-holding locations using special source-handling tools just before lowering the tool string. The tool string was lowered to the bottom of the borehole and brought up at the appropriate logging speed as measurements were made. At least two logging runs (one main and one repeat) were made with each tool string.

Upon reaching the surface, any radioactive sources were removed from the tools and were returned to their appropriate storage shields, thus eliminating any radiation hazards. Any postlogging measurement checks were performed as part of log quality control (QC) and quality assurance (QA). The tool string was cleaned as it was pulled out of the hole, separated, and disconnected.

The second tool string was attached to the cable for another logging run, followed by subsequent tool strings and logging runs. After the final logging run was completed, the cable and sheave wheels were rigged down.

Before departure, the logging engineer printed field logs and created a compact disc containing the field log data for on-site distribution and sent the data via satellite to the Schlumberger data storage center. The Schlumberger Water Services data processing center was alerted that the data were ready for postacquisition processing.

3.2 Log QC and QA

Schlumberger has a thorough set of procedures and protocols for ensuring that the geophysical logging measurements are of very high quality. This includes full calibration of tools when they are first built, regular recalibrations and tool measurement/maintenance checks, and real-time monitoring of log quality as measurements are made. Indeed, one of the primary responsibilities of the logging engineer is to ensure, before and during acquisition, that the log measurements meet prescribed quality criteria.

A tool-specific base calibration that directly relates the tool response to the physical measurement using the designed measurement principle is performed on all Schlumberger logging tools when first assembled in the engineering production centers. This is accomplished through a combination of computer modeling and controlled measurements in calibration models with known chemical and physical properties.

The base calibration for most Schlumberger tools is augmented through regular “master calibrations” typically performed every 1 to 6 mo in local Schlumberger shops (such as Farmington, New Mexico), depending on tool design. Master calibrations consist of controlled measurements using specially designed calibration tanks/jigs and internal calibration devices that are built into the tools, both with known physical properties. The measurements are used to fine-tune the tool’s calibration parameters and to verify that the measurements are valid.

In addition, on every logging job, before and after on-site “calibrations” are executed for most Schlumberger tools directly before/after lowering/removing the tool string from the borehole. For most tools, these represent a measurement verification instead of an actual calibration used to confirm the validity of the measurements directly before acquisition and to ensure that they have not drifted or been corrupted during the logging job.

All Schlumberger logging measurements have a number of associated depth-dependent QC logs and flags to assist with identifying and determining the magnitude of log quality problems. These QC logs are monitored in real-time by the logging engineer during acquisition and are used in the postacquisition processing of the logs to determine the best processing approach for optimizing the overall validity of the property estimates derived from the logs.

Additional information on specific tool calibration procedures can be found on the Schlumberger website (http://www.slb.com/content/services/evaluation/index.asp).

3.3 Processing Procedure

After the geophysical logging job was completed in the field and the data was archived, the data were downloaded to the Schlumberger processing center. There the data were processed in the following sequence: (1) the measurements were corrected for near-wellbore environmental conditions, and the measurement field processing for certain tools (in this case, the TLD and ECS) were redone using better processing algorithms and parameters; (2) the log curves from different logging runs were depth-matched and spliced, if required; and (3) the near-wellbore substrate lithology/mineralogy and pore fluids were modeled through integrated log analysis. Afterwards, an integrated log montage was built to combine and compile all the processed log results.

3.3.1 Environmental Corrections and Raw Measurement Reprocessing

If required, the field log measurements were processed to correct for conditions in the well, including fluid type (water or air), presence of steel casing, and (to a much lesser extent) pressure, temperature, and fluid salinity. Basically, these environmental corrections entail subtracting from the measurement response the known influences of the set of prescribed borehole conditions. In R-44, the log measurements requiring these corrections are the CNT porosity, TLD bulk formation density, ECS elemental concentrations, and HNGS spectral gamma ray logs.

Two neutron porosity measurements are available from the CNT tool: one that measures thermal ("slow") neutrons and one that measures epithermal ("fast") neutrons. Measurement of epithermal neutrons is required to make neutron porosity measurements in air-filled holes. In water/mud-filled holes, both the epithermal and thermal neutron measurements are valid. Both measurements can be environmentally corrected for a single string of steel-casing. The CNT measurements were reprocessed for casing, borehole fluid type (air versus water), and other environmental conditions. For further processing and analysis (e.g., integrated log analysis), the reprocessed neutron porosity was used.

The raw ECS elemental yield measurements include the contribution of iron from steel casing and hydrogen from fluid in the borehole. The processing consists of subtracting this unwanted contribution from the raw normalized yield, then performing the normal elemental yields-to-weight fraction processing. The contribution to subtract is a constant baseline amount (or zoned constant values if there are bit/casing size changes), usually determined by comparing the normalized raw yields in zones directly below/above the borehole casing/fluid change. Casing corrections were applied to the ECS logs across the entire log interval, attempting to account for one string of steel casing throughout. At the time of the ECS logging in R-44, the borehole contained water from bottom to 880 ft; no hydrogen correction was required in the air-filled section above 880 ft, and the difference between the hydrogen yield above and below this depth was used to determine the baseline borehole hydrogen correction to apply below.

The HNGS spectral gamma ray is affected by the material (fluid, air, and casing) in the borehole because different types and amounts of these materials have different gamma ray shielding properties; the HNGS measures incoming gamma rays emitted by radioactive elements in the formation surrounding the borehole. The processing algorithms try to correct for the damping influence of the borehole material. The HNGS logs from R-44 were reprocessed to account for, as best as possible, the environmental effects of the casing, borehole fluid (water below 880 ft and air above), and hole size.

The measurements cannot be fully corrected for borehole washouts or rugosity since the specific characteristics (e.g., geometry) of these features are unknown (especially in this scenario where they hidden by casing) and their effects on the measurements are often too significant to account for. Thus, the compromising effects of these conditions on the measurements should be accounted for in the interpretation of the log results.

3.3.2 Depth-Matching and Reference

Once the logs were environmentally corrected for the conditions in the borehole and the raw measurement reprocessing was completed, the logs from different tool runs were depth-matched to each, as needed, using the gross gamma ray log, acquired in all the logging runs, for depth correlation, or other logs that are well correlated (e.g., porosity). The depth reference for all field prints and processed logs, including those presented in this report, is ground surface.

3.3.3 Integrated Log Analysis

An integrated log analysis, using as many of the processed logs as possible, was performed to model the near-wellbore substrate lithology/mineralogy and pore fluids. This analysis was performed using the Elemental Log Analysis (ELAN*) program (Mayer and Sibbit 1980, 103867; Quirein et al. 1986, 098043)—a petrophysical interpretation program designed for depth-by-depth quantitative formation evaluation from borehole geophysical logs. ELAN estimates the volumetric fractions of user-defined rock

*Mark of Schlumberger.

matrix and pore constituents at each depth based on the known log measurement responses to each individual constituent by itself[1]. ELAN requires an a priori specification of the volume components present within the formation, i.e., fluids, minerals, and rocks. For each component, the relevant response parameters for each measurement are also required. For example, if one assumes that quartz is a volume component within the formation and the bulk density tool is used, then the bulk density parameter for this mineral is well known to be 2.65 g/cc.

The logging tool measurements, volume components, and measurement response parameters used in the ELAN analysis for R-44 are provided in Table 3.1. The final results of the analysis – an optimized mineral-fluid volume model – are shown on the integrated log montage (see Attachment 1), 6th track from the right (inclusive of the depth track). In addition, the ELAN program provides a direct comparison of the modeled versus the actual measured geophysical logs, as well as a composite log of all of the key ELAN-derived results, including geologic/hydrogeologic properties computed from the mineral-fluid volume model (see Attachment 2). To make best use of all the measurement data and to perform the analysis across as much of the well interval as possible (22 to 1084 ft bgs), as many as possible of the processed logs were included in the analysis, with less weighting applied to less robust logs. Not all of the tool measurements shown in Table 3.1 and the ELAN modeled versus measured log display are used for the entire interval analyzed, as not all the measurements are available, or of good quality, across certain sections of the borehole. To accommodate fewer tool measurements, certain model constituents are removed from the analysis in some intervals.

The ELAN analysis was performed with as few constraints or prior assumptions as possible. A considerable effort was made to choose a set of minerals or mineral types for the model that is representative of Los Alamos area geology and its volcanic origins. For the ELAN analysis, the log interval from 22 to 314 ft bgs was assumed to be volcanic tuff or pumice, and a mineral suite considered representative of this volcanic tuff, based on Laboratory cuttings mineral analysis, was used (primary “minerals” silica glass/cristobalite/tridymite [indistinguishable from the log measurements], quartz, potassium feldspar, and augite, with accessory minerals calcite and pyrite). The results of laboratory analyses of Bandelier Tuff and Puye Formation samples from around the Laboratory site were also used to constrain the proportion of quartz versus the combination of glass/cristobalite/tridymite in the ELAN analysis. The log interval 314 to 709 ft bgs was assumed to be basaltic lava flows/material with a possible mineral suite of plagioclase and potassium feldspar, quartz, augite, hypersthene, heavy mafic minerals (such as magnetite), montmorillinite, and pyrite. The log interval 709 to 1084 ft bgs was assumed to be the Puye Formation, or fanglomerate/alluvium with similar composition, and a mineral suite considered representative of this geology, based on Laboratory cuttings mineral analysis, was used (primary “minerals” silica glass/cristobalite/tridymite [indistinguishable from the log measurements], plagioclase and potassium feldspar; quartz at a defined small fraction of the silica glass content; montmorillinite clay; with possible accessory/trace minerals biotite, hematite, augite, hypersthene, heavy mafic minerals, and pyrite).

No prior assumption is made about water saturation—where the boundary between saturated and unsaturated zones lies (e.g., the depth to the top of the regional aquifer or perched zones). Thus, the presence and amount of air in the pore space is unconstrained. Total porosity and water-filled porosity are also left unconstrained throughout the analysis interval, despite the obvious influence on the log response of borehole washouts and annular voids behind the casing. There is no way to objectively correct for the adverse effect on the log measurements from these borehole conditions; therefore, the

[1]Mathematically, this corresponds to an inverse problem—solving for constituent volume fractions from an (over)determined system of equations relating the measured log results to combinations of the tool measurement response to individual constituents.

decision was made to perform the ELAN analysis so as to honor the log measurements. Accordingly, interpretations should be made from the ELAN results with the understanding that the mineral-fluid model represents a mathematically optimized solution that is not necessarily a physically accurate representation of the native geologic formation. Within this context, the ELAN model is a robust estimate of the bulk mineral-fluid composition that accounts for the combined response from all the geophysical measurements.

Table 3.1
Tool Measurements, Volumes, and Respective Parameters Used in the R-44 ELAN Analysis

Volume Tool Measurement	Air	Water	Hypersthene	Hematite	Labradorite	Silica Glass, Cristo., Tridy.	Heavy Mafic Minerals	Augite	Montmorillinite	Biotite	Pyrite	Orthoclase	Calcite	Quartz
Bulk density (g/cc)	–0.19	1.00	3.55	5.161	2.68	2.33	5.08	3.08	2.02	3.04	4.99	2.54	2.71	2.64
Thermal neutron poro. (nonlinear) (ft^3/ft^3)	0	1.00	0.036	0.126	-0.01	-0.03	0.07	0.015	0.65	0.15	0.01	-0.01	0.0	-0.07
Epithermal neutron poro. (ft^3/ft^3)	0	1.00	0.012	0.0556	-0.01	0.0	0.022	-0.01	0.6	0.14	0.165	-0.01	0.0	-0.05
Dry weight silicon (lbf/lbf)[a]	0.0	0.0	0.24	0.0	0.247	0.468	0.184	0.225	0.242	0.178	0.0	0.3	0.0	0.468
Dry weight calcium (lbf/lbf)	0.0	0.0	0.0	0.0	0.09	0.0	0.0	0.10	0.012	0.007	0.0	0.0	0.405	0.0
Dry weight iron (lbf/lbf)	0.0	0.0	0.20	0.699	0.023	0.0	0.22	0.112	0.02	0.199	0.466	0.015	0.0	0.0
Dry weight aluminum (lbf/lbf)	0.0	0.0	0.0	0.0	0.162	0.0	0.0	0.018	0.103	0.081	0.0	0.104	0.0	0.0
Dry weight sulfur (lbf/lbf)	0.0	0.0	0.0	0.0	0.0	0.0	0.0	0.0	0.0	0.0	0.535	0.0	0.0	0.0
Dry weight titanium (lbf/lbf)	0.0	0.0	0.01	0.01	0.0	0.0	0.0	0.048	0.001	0.016	0.0	0.0	0.0	0.0
Wet weight potassium (lbf/lbf)	0.0	0.0	0.0	0.0	0.0	0.0	0.0	0.003	0.004	0.070	0.0	0.12	0.0	0.0
Weight hydrogen (lbf/lbf)	0.0	0.111	0.0	0.0	0.0	0.01	0.0	0.0	0.022	0.003	0.0	0.0	0.0	0.0
Wet weight thorium (ppm)	0	0	13.5	0	1.75	2	4	13.5	24	25	0	5	0	0
Neutron capture unit (cu)b cross-section)	0	22.21	18.9	101.4	7.87	4	103	25.66	20	54.1	90	15.82	7.4	4.7

[a] lbf = Pound force.

[b] cu = Capture unit.

4.0 RESULTS

Preliminary results from the wireline geophysical logging measurements acquired by Schlumberger in R-44 were generated in the logging truck at the time the geophysical services were performed and were documented in the field logs provided on site. However, the measurements presented in the field results are not fully corrected for undesirable influence (from a measurement standpoint) of borehole and geologic conditions and are provided as separate, individual logs. The field log results have been processed to (1) correct/improve the measurements, as best as possible, for borehole/formation environmental conditions, and (2) ensure that all the logs from different tool runs are on depth. Additional logs were generated from integrated analysis of processed measured logs, providing valuable estimates of key geologic and hydrologic properties.

The processed log results are presented as continuous curves of the processed measurement versus depth and are displayed as (1) a one-page, compressed summary log display for selected directly related sets of measurements (see Figures 4.1, 4.2, and 4.3); and (2) an integrated log montage that contains all the key processed log curves, on depth and side by side (see Attachment 1). The summary log displays address specific characterization needs, such as porosity, production capacity, moisture content, water saturation, and lithologic changes. The purpose of the integrated log montage is to present, side by side, all the most salient processed logs and log-derived models, depth-matched to each other, so that correlations and relationships between the logs can be identified.

Important results from the processed geophysical logs in R-44 are described below.

4.1 Well Fluid Level

The standing water level in R-44 (within the freestanding 12-in. I.D. casing) was stable during the December 9, 2008, logging, residing at 880 ft bgs. The various measurements from all four logging runs concurred on this well water level.

4.2 Regional Aquifer

The processed geophysical logs definitively indicate that the intersected geologic section is fully saturated with water from the bottom of the borehole (1,084 ft bgs) to 880 or 878 ft bgs, which lies within alluvium/fanglomerate (see porosity summary display in Figure 4.1 or integrated log montage in Attachment 1). Below 878 ft the log estimated water content and total porosity are very high (mostly greater than 50% of total rock/sediment volume), resulting in an estimated pore volume water saturation (fraction of the total pore volume containing water) greater than 75% (90 to 100% through much of the interval). Above 878 ft the water content is much lower, mostly at or below 10%. Total porosity across this same interval mostly ranges from 20% to 40%, resulting in an estimated water saturation that stays below 50% of total pore volume.

Conclusions that can be drawn from these geophysical log results are that the regional aquifer water level (depth at which there is full water saturation) is 878 to 880 ft, coinciding with the well water level at the time of logging.

The location of productive zones within the saturated section is difficult to determine because of the adverse cased well conditions. Higher porosity is not necessarily indicative of higher production capacity since fine-grained sediments often have higher porosity and lower productivity than coarser-grained sediments. The highest porosities are likely associated with washouts behind the casing. The predicted relative flow capacity profile generated from the integrated log analysis estimated permeability results

suggest that the most productive intervals are 884–893 ft, 897–900 ft, 903–907 ft, 919–922 ft, 924–926 ft, 939–941 ft, 953–954 ft, 964–966 ft, 974–976 ft, 982–995 ft, 1000–1015 ft, 1022–1027 ft, 1042–1048 ft, 1053–1056 ft, and 1072–1074 ft (see porosity summary display in Figure 4.1 or integrated log montage in Attachment 1).

4.3 Vadose Zone Perched Water

As mentioned above, the depth to the top of the regional aquifer and, thus, the extent of the vadose zone definitely extends above 878 ft bgs. Above 878 ft bgs, the estimated water content varies from less than 5% to 17% of total rock volume, mostly remaining at or below 10% (see porosity summary display in Figure 4.1 or integrated log montage in Attachment 1). Estimated water saturation is mostly below 50% of total pore volume (never above 75%) across the entire vadose zone. The highest vadose zone water saturation is in the following zones (although not high enough to suggest 100% saturation and significant perched water:

- 704–708 ft, where water content is 15% and water saturation reaches 60%—located in the bottom part of a likely thick basalt lava sequence that has zones of significantly lower estimated total porosity than the surrounding rock, including the bottom section where this zone is (presumably the basalt is more competent here)
- 647–652 ft, where water saturation reaches 75%—located in the same basalt lava sequence and low porosity zone
- 395–397, 467–469, and 500–502 ft, where water saturation reaches between 40% and 62%—located in the same basalt lava sequence in zones where the total porosity is a lot lower than the surrounding rock
- 314–340 ft, where water saturation reaches 40%—located at the top of the same basalt lava that lies immediately below the Guaje Pumice Bed, where there is higher water content (approximately 15%) and perhaps the basalt is eroded and/or reworked

4.4 Geology

The processed geophysical log results, particularly the matrix geochemistry logs, provide information on lithology and potential formation contacts intersected by R-44 across the log interval (from 22 to 1084 ft bgs). The generalized geologic stratigraphy observed from the logs across the measured interval is as follows (depth below ground surface):

- **<u>22–75 ft bgs</u>: High porosity silicon- and thorium-rich volcanic tuff or alluvium—** characterized by high, varying total porosity (30%–50% of total rock volume); high silica glass/tridymite/cristobalite content; moderate potassium feldspar content; varying minor to moderate amounts of quartz and augite (or similar minerals); and trace amounts of pyrite (or other sulfur-bearing minerals) and calcite (or other calcium-bearing minerals)
- **<u>75–94 ft bgs (top of processed log interval)</u>: High porosity silicon-rich volcanic tuff—** characterized by high total porosity (35%–58% of total rock volume); high silica glass/tridymite/cristobalite content; moderate potassium feldspar content; varying minor to moderate amounts of quartz and augite (or similar minerals); and trace amounts of pyrite (or other sulfur-bearing minerals) and calcite (or other calcium-bearing minerals)
- **<u>94–150 ft bgs</u>: High porosity silicon- and thorium-rich volcanic tuff—**characterized by consistently high total porosity (40–45% of total rock volume); high silica

glass/tridymite/cristobalite content; moderate potassium feldspar content; varying minor to moderate amounts of quartz and augite (or similar minerals); and trace amounts of pyrite (or other sulfur-bearing minerals) and calcite (or other calcium-bearing minerals)

- **150–200 ft bgs: Moderate porosity silicon- and thorium-rich volcanic tuff—** characterized by consistently moderate total porosity (30–35% of total rock volume); high silica glass/tridymite/cristobalite content; moderate potassium feldspar content; varying minor to moderate amounts of quartz and augite (or similar minerals); and trace amounts of pyrite (or other sulfur-bearing minerals) and calcite (or other calcium-bearing minerals)
- **200–230 ft bgs: Very high porosity silicon-rich volcanic tuff—**characterized by very high total porosity (30–50% of total rock volume); high silica glass/tridymite/cristobalite content; moderate potassium feldspar content; varying minor to moderate amounts of quartz, augite (or similar minerals), and calcite (or other calcium-bearing minerals); and trace amounts of pyrite (or other sulfur-bearing minerals)
- **230–250 ft bgs: Moderate porosity silicon- and thorium-rich volcanic tuff—** characterized by consistently moderate total porosity (35% of total rock volume); high silica glass/tridymite/cristobalite content; moderate potassium feldspar content; varying minor to moderate amounts of quartz and augite (or similar minerals); and trace amounts of pyrite (or other sulfur-bearing minerals) and calcite (or other calcium-bearing minerals)
- **250–280 ft bgs: High porosity silicon and thorium rich volcanic tuff—**characterized by consistently high total porosity (40% of total rock volume); high silica glass/tridymite/cristobalite content; moderate potassium feldspar content; varying minor to moderate amounts of quartz and augite (or similar minerals); and trace amounts of pyrite (or other sulfur-bearing minerals) and calcite (or other calcium-bearing minerals)
- **280–298 ft bgs: Very high porosity silicon- and thorium-rich volcanic tuff—** characterized by very high total porosity (45%–50% of total rock volume); high silica glass/tridymite/cristobalite content; moderate potassium feldspar content; varying minor to moderate amounts of quartz and augite (or similar minerals); and trace amounts of pyrite (or other sulfur-bearing minerals) and calcite (or other calcium-bearing minerals)
- **298–314 ft bgs: Very high porosity silicon-, thorium-, and uranium-rich volcanic tuff/pumice—**characterized by very high total porosity (45%–48% of total rock volume); high silica glass/tridymite/cristobalite content; moderate potassium feldspar content; varying minor to moderate amounts of quartz and augite (or similar minerals); and trace amounts of pyrite (or other sulfur-bearing minerals) and calcite (or other calcium-bearing minerals)
- **314–347 ft bgs: High porosity iron-rich volcanics (likely basalt)**—characterized by potentially high total porosity (35%–42%); high quartz and augite (or similar minerals) content; variably minor to moderate hypersthene (or similar minerals) and alkali feldspars content; and variably trace to small amounts of pyrite
- **347–390 ft bgs: Extremely high porosity (likely washouts) calcium- and titanium-rich volcanics (likely basalt)—**characterized by unrealistically high total porosity (greater than 50%, the highest likely elevated because of voids behind the casing); high quartz augite (or similar mineral) content; varying moderate to high plagioclase feldspar content; minor alkali feldspar content; and variably trace to small amounts of pyrite

- **<u>390–406 ft bgs</u>: Low to moderate porosity calcium- and titanium-rich volcanics (likely basalt**)—characterized by low to moderate total porosity (16%–40%); high quartz augite (or similar mineral) content; varying moderate to high plagioclase feldspar content; minor alkali feldspar content; and variably trace to small amounts of pyrite
- **<u>406–450 ft bgs</u>: Very high porosity calcium- and titanium-rich volcanics (likely basalt)—**characterized by very high to unrealistically high total porosity (30% to greater than 50%, the highest likely elevated because of voids behind the casing); high quartz augite (or similar mineral) content; varying moderate to high plagioclase feldspar content; minor alkali feldspar content; and variably trace to small amounts of pyrite
- **<u>450–505 ft bgs</u>: Low to moderate porosity calcium- and titanium-rich volcanics (likely basalt)—**characterized by low to moderate total porosity (16%–32%, except for a spurious peak); high quartz augite (or similar mineral) content; varying moderate to high plagioclase feldspar content; minor alkali feldspar content; and variably trace to small amounts of pyrite
- **<u>505–618 ft bgs</u>: Very high porosity calcium- and titanium-rich volcanics (likely basalt)—**characterized by very high to unrealistically high total porosity (30% to greater than 60%, the highest likely elevated because of voids behind the casing); high quartz augite (or similar mineral) content; varying moderate to high plagioclase feldspar content; minor alkali feldspar content; and variably trace to small amounts of pyrite
- **<u>618–709 ft bgs</u>: Low to moderate porosity calcium- and titanium-rich volcanics (likely basalt)—**characterized by low to moderate total porosity (10%–30%, average of about 20%, except for a spurious peak); high quartz augite (or similar mineral) content; varying moderate to high plagioclase feldspar content; minor alkali feldspar content; and variably trace to small amounts of pyrite
- **<u>709–752 ft bgs</u>: Extremely high porosity (likely washouts), silicon-rich and iron-deficient alluvium/fanglomerate—**characterized by unrealistically high total porosity (40% to well over than 60%, likely elevated because of voids behind the casing); high silica glass/tridymite/cristobalite or quartz content; moderate potassium feldspar content; varying minor to moderate amounts of montmorillinite, plagioclase and/or augite (or similar minerals); variably trace to minor amounts of calcite and/or pyrite
- **<u>752–880 ft bgs</u>: Low to moderate porosity, silicon-rich and iron-deficient alluvium/fanglomerate—**characterized by low to moderate total porosity (18%–30% with spurious peaks); high silica glass/tridymite/cristobalite or quartz content; moderate potassium feldspar content; varying minor amounts of montmorillinite, plagioclase and/or augite (or similar minerals); variably trace to minor amounts of calcite and/or pyrite
- **<u>880–982 ft bgs</u>: Very high porosity, silicon-rich and iron-deficient alluvium/fanglomerate—**characterized by very high total porosity (35% to over 60%, likely elevated because of voids behind the casing); high silica glass/tridymite/cristobalite or quartz content; minor potassium feldspar content; varying minor to moderate amounts of montmorillinite, plagioclase and/or augite (or similar minerals); variably trace to minor amounts of calcite and/or pyrite
- **<u>982–1084 ft bgs (bottom of log interval)</u>: High porosity, silicon-rich and iron-deficient alluvium/fanglomerate—**characterized by high total porosity (23%–54%); high silica glass/tridymite/cristobalite or quartz content; moderate potassium feldspar content; varying minor to moderate amounts of montmorillinite, plagioclase and/or augite (or similar minerals); variably trace to minor amounts of calcite and/or pyrite

4.5 Summary Logs

Three summary log displays have been generated for R-44 to highlight the key hydrogeologic and geologic information provided by the processed geophysical log results:

- Porosity and hydrogeologic properties summary log showing continuous hydrogeologic property logs, including total porosity (water and air), water-filled porosity, water saturation, estimated hydraulic conductivity, transmissivity, and relative producibility (production capacity); highlights key derived hydrologic information obtained from the integrated log results (Figure 4.1)
- Density and clay content summary showing a continuous logs of formation bulk density and estimated grain density, as well as estimated clay volume, highlights key geologic rock matrix information obtained from the log results (Figure 4.2)
- Spectral natural gamma ray and lithology summary showing a high vertical resolution, continuous volumetric analysis of formation mineral and pore fluid composition (based on an integrated analysis of the logs), and key lithologic/stratigraphic correlation logs from the spectral gamma ray measurement (concentrations of gamma-emitting elements); highlights the geologic lithology, stratigraphy, and correlation information obtained from the log results (Figure 4.3)

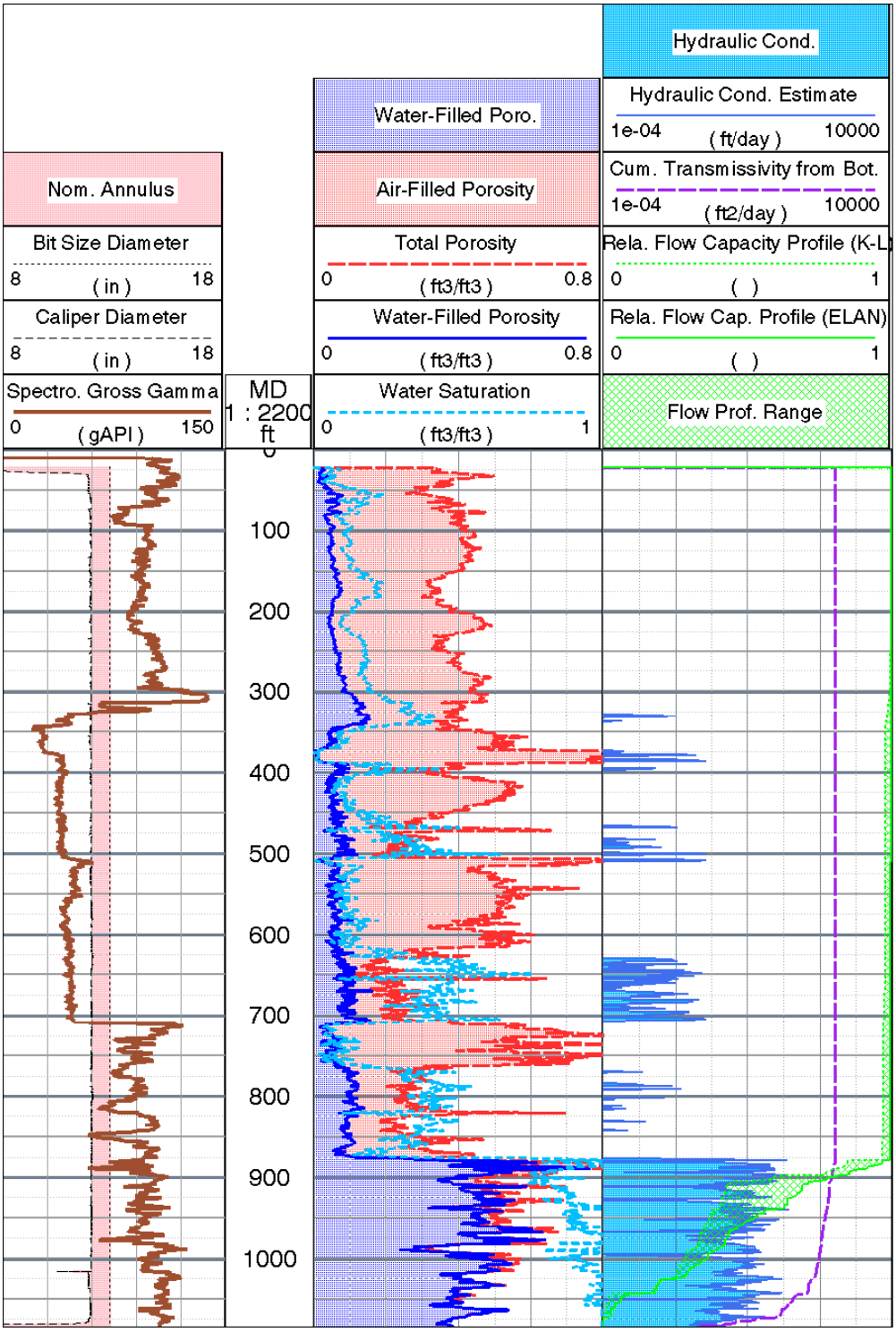

Figure 4.1 **Summary of porosity logs in R-44 borehole from processed geophysical logs, interval of 23 to 1084 ft bgs, with caliper, gross gamma, water saturation, estimated relative flow capacity profile, hydraulic conductivity, and transmissivity logs also displayed. Porosity, water saturation, and hydraulic conductivity logs are derived from the ELAN-integrated log analysis.**

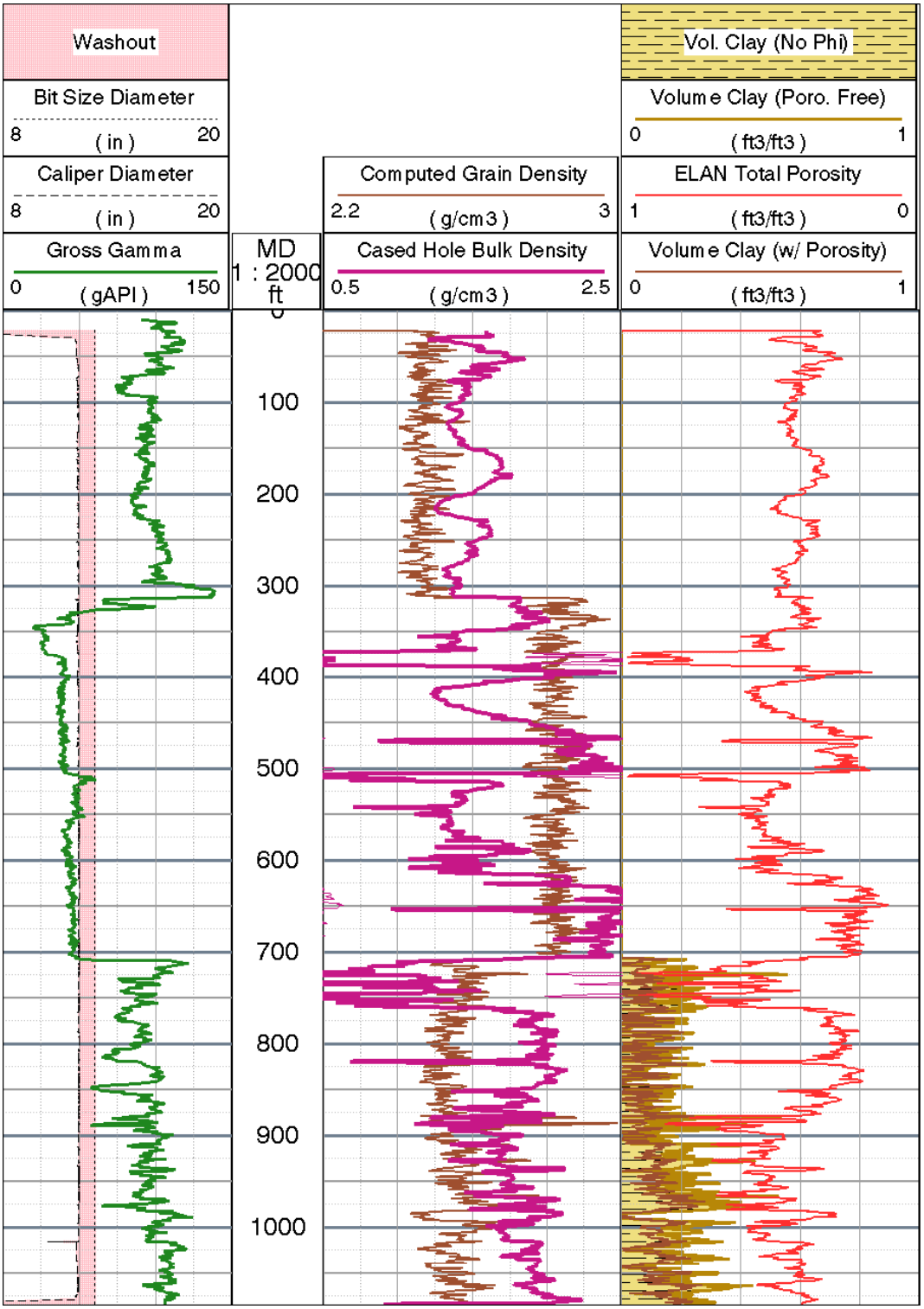

Figure 4.2 Summary of bulk density and apparent grain density logs in R-44 borehole from processed geophysical logs, interval of 23 to 1084 ft bgs. Also shown are caliper, gross gamma, volume of clay, and total porosity logs. (The latter two were derived from the ELAN analysis. Note that clay was not solved for above 708 ft).

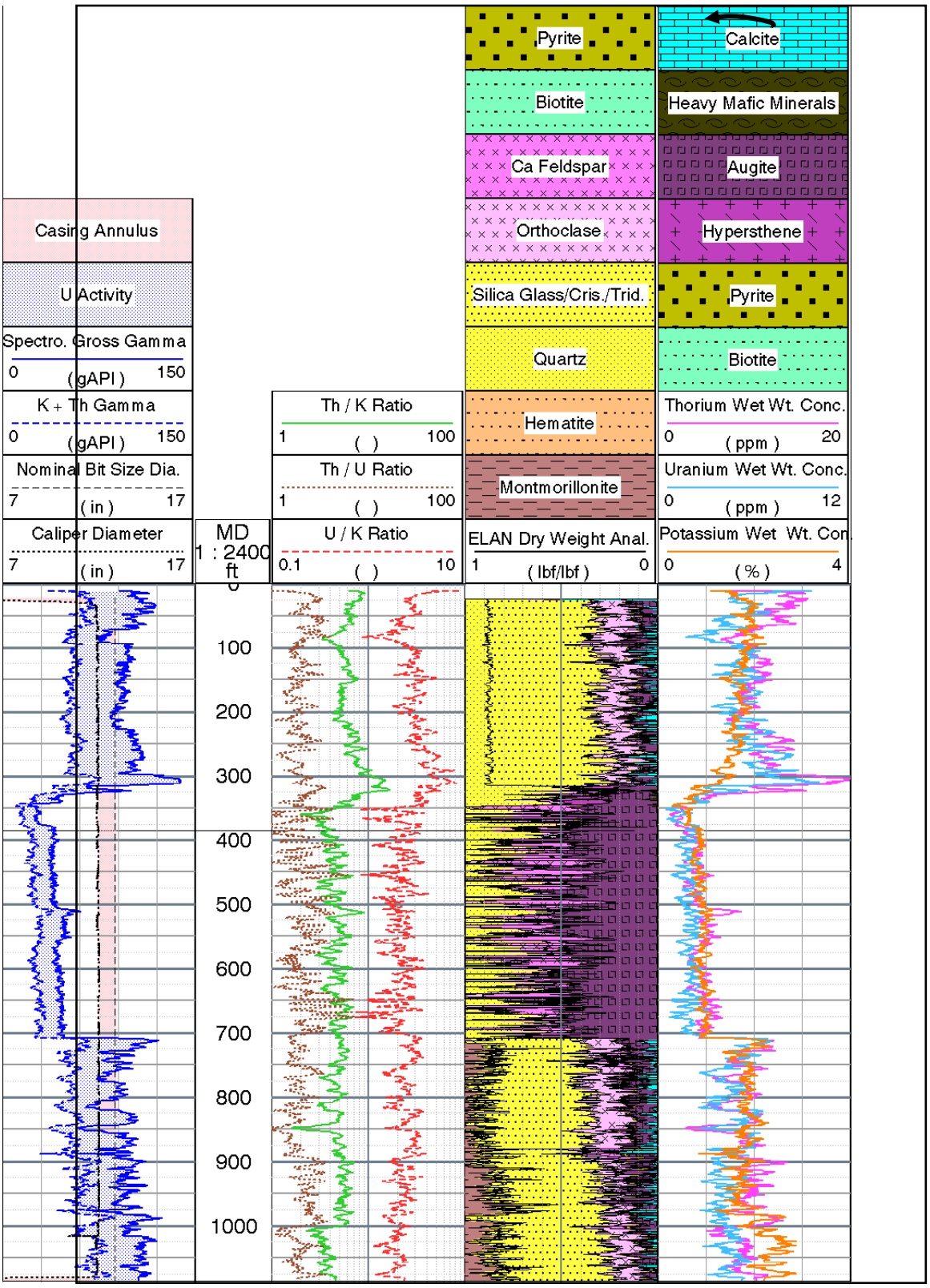

Figure 4.3 Summary of spectral natural gamma ray logs and ELAN mineralogy/lithology and pore fluid model volumes derived from the ELAN-integrated log analysis for R-44 borehole, interval 23 to 1084 ft bgs. Caliper log is also shown.

4.6 Integrated Log Montage

This section summarizes the integrated geophysical log montage for R-44. The montage is provided in Appendix 1. A description of each log curve in the montage follows, organized under the heading of each track, starting from track 1 on the left-hand side of the montage. Note that the descriptions in this section focus on what the curves are and how they are displayed; the specific characteristics and interpretations of the R-44 geophysical logs are provided in the previous section

4.6.1 Track 1—Depth

The first track on the left contains the depth below ground surface in units of feet, as measured by the geophysical logging system during the CNT-G logging run. All the geophysical logs are depth-matched to the gross gamma log acquired with this logging run.

4.6.2 Track 2—Basic Logs

The second track on the left (inclusive of the depth track) presents basic curves:

- gamma ray (thick black), recorded in American Petroleum Institute gamma ray (gAPI) standard units and displayed on a scale of 0 to 150 gAPI units
- single arm caliper from the TLD (thin solid pink) with nominal bit size as a reference (dashed-dotted black) to show nominal annular distance between inside of inner casing to borehole wall (pink shading), recorded as hole diameter in inches and displayed on a scale of 8 to 18 in.
- cable tension (dashed-dotted dark red) recorded at logging truck and displayed to indicate tool pickup at bottom on a scale of 0 to 1000 lbf

Two gamma ray curves from the HNGS are displayed:

- total gross gamma (thick solid black curve with thinner dashed black curve as backup representing the uncorrected SGT gamma ray displayed on a scale to match the corrected HNGS gamma)
- gross gamma minus the contribution of uranium (dotted black)
- yellow shading between the two curves to show uranium contribution to the total gamma ray response.

4.6.3 Track 3—Porosity

The third track displays the primary porosity log results. All the porosity logs are recorded in units of volumetric fraction and are displayed on a linear scale of 0.75 (left side) to -0.1 (right side). Specifically, these logs consist of

- CNT epithermal neutron porosity (bold solid light blue curve)—processed for zoned air-filled and water-filled cased hole;
- CNT water-filled resolution enhanced thermal neutron porosity (solid dark blue curve)—thermal neutron porosity valid only in the fluid-filled borehole;

- ECS bulk volumetric water content derived from hydrogen weight concentration measurement, corrected for water in casing and converted to volume fraction (short-dashed sky blue);
- total porosity derived from bulk density and ELAN water-filled porosity using a grain density of 2.45/2.65/2.55 g/cc (dashed red curve), 2.55/2.75/2.65 g/cc (long-dashed red curve), and 2.65/2.85/2.75 g/cc (dotted red curve)–with red shading between the 2.45/2.65/2.55 g/cc and 2.65/2.85/2.75 g/cc porosity curves to show the range (the lowest-grain density range used across the tuff/pumice interval [22–314 ft], the highest-grain density range used across the basalt interval [314–709 ft]),and middle-grain density range used across the alluvium/fanglomerate interval (709–1084 ft)]; and
- ELAN water-filled porosity (bold dashed-dotted cyan with dark blue shading to right)–derived from the ELAN-integrated analysis of all log curves to estimate optimized matrix and pore volume constituents.

4.6.4 Track 4—Density

The fourth track displays the

- bulk density, corrected for single string of steel casing (thick solid maroon curve) on a wrapping scale of 1 to 3 g/cc; and
- apparent grain density (dashed brown curve), derived from the ELAN analysis, on a scale of 2.4 to 3.2 g/cc.

4.6.5 Track 5—HNGS Spectral Gamma

The fifth track from the left displays the spectral components of the HNGS measurement results as wet weight concentrations, corrected as best as possible for casing and borehole size and fluid:

- potassium (solid green curve) in units of percent weight fraction and on a scale of–5% to 5%;
- thorium (dashed brown) in units of parts per million and on a scale of 25 to–25 ppm; and
- uranium (dotted blue) in units of parts per million and on a scale of 20 to 0 ppm.

4.6.6 Tracks 6 to 11—Geochemical Elemental Measurements

The narrow tracks 6 to 11 present the geochemical measurements, along with their estimated one standard deviation uncertainty range: iron (Fe) and silicon (Si), sulfur (S) and calcium (Ca), estimated aluminum (Al) and potassium (K), titanium (Ti) and gadolinium (Gd), hydrogen (H) and apparent relative bulk chlorinity (Rela. Cl), and uranium (U) and carbon yield (C Yield)—from left to right respectively, in units of dry matrix weight fraction (except K and H in wet-weight fraction, Rela. Cl in ppk, U in wet-weight ppm, and C Yield in relative yield units).

4.6.7 Track 12—ELAN Mineralogy Model Results (Dry-Weight Fraction)

Track 12 displays the results from the ELAN-integrated log analysis (the matrix portion)–presented as dry-weight fraction of mineral types chosen in the model:

- montmorillinite clay (brown/tan)
- hematite (orange with small black dots)

- quartz (yellow with closely spaced small black dots)
- combined silica glass, tridymite, and cristobalite (yellow with widely spaced large black dots)
- orthoclase or other potassium feldspar (lavender)
- labradorite or similar plagioclase feldspar (pink)
- biotite (light green)
- pyrite (orange-tan with black squares)
- hypersthene (purple)
- augite (maroon)
- heavy mafic/ultramafic minerals, such as magnetite or olivine (dark green)
- calcite (cyan)

4.6.8 Track 13—ELAN Mineralogy and Pore Space Model Results (Wet Volume Fraction)

Track 13 displays the results from the ELAN-integrated log analysis–presented as wet mineral and pore fluid volume fractions:

- montmorillinite clay (brown/tan)
- hematite (orange with small black dots)
- quartz (yellow with closely spaced small black dots)
- combined silica glass, tridymite, and cristobalite (yellow with widely spaced large black dots)
- orthoclase or other potassium feldspar (lavender)
- labradorite or similar plagioclase feldspar (pink)
- biotite (light green)
- pyrite (orange-tan with black squares)
- hypersthene (purple)
- augite (maroon)
- heavy mafic/ultramafic minerals, such as magnetite or olivine (dark green)
- calcite (cyan)
- air (red)
- water (white)
- moved air (orange)
- moved water (blue)

4.6.9 Track 14—Water Saturation

Track 14 displays the continuous-in-depth water saturation logs estimated from the processed logs, recorded in units of volumetric fraction of pore space filled with water (ratio of cubic feet per cubic feet) and presented on a scale of 0 to 1 ft3/ft3 (left to right.

- optimized estimate of water saturation (volumetric fraction of pore space filled with water) from the ELAN analysis (bold dashed-dotted purple curve with blue shading to the right and red shading to the left, corresponding to water-filled and air-filled pore space, respectively); and
- water saturation as calculated directly from the bulk density and ELAN-estimated porosity using a grain density of 2.45/2.65/2.55 g/cc (dashed red curve), 2.55/2.75/2.65 g/cc (long-dashed red curve), and 2.65/2.85/2.75 g/cc (dotted red curve)–with red shading between the 2.45/2.65/2.55 g/cc and 2.65/2.85/2.75 g/cc porosity curves to show the range (the lowest-grain density range used across the tuff/pumice interval [22–314 ft], the highest-grain density range used across the basalt interval [314–709 ft]),and middle-grain density range used across the alluvium/fanglomerate interval (709–1084 ft).

4.6.11 Track 15—Hydraulic Conductivity

Track 15 displays several estimates of hydraulic conductivity (K) derived from the ELAN-integrated log analysis (sensitive to the estimated porosities and mineral composition), presented on a logarithmic scale of 10-5 to 105 ft/d:

- a K-versus-depth estimate derived from using the ELAN permeability equation with water-filled porosity and matrix mineral weight fraction values derived from the ELAN analysis, converted to hydraulic conductivity (bold solid blue curve with gradational coloring to represent the range of hydraulic conductivity relative to standard unconsolidated clastic sediments);
- a K-versus-depth estimate derived from using the k-Lambda permeability equation with water-filled porosity and matrix mineral weight fraction values derived from the ELAN analysis, converted to hydraulic conductivity (long-dashed sky blue curve); and
- an intrinsic K-versus-depth estimate (assuming full saturation) using the ELAN total porosity and mineral-based permeability equation with total porosity and matrix mineral weight fraction values derived from the ELAN analysis, converted to hydraulic conductivity (dotted purple).

In addition, an estimate of cumulative transmissivity from the bottom of the log interval is displayed for the ELAN mineral-based estimator (bold dashed-dotted bright green curve), computed by integrating from bottom to top the hydraulic conductivity estimates, presented on a logarithmic scale of 10–5 to 105 ft2/d.

4.6.12 Track 16—Predicted Flow (Production Potential) Profile

Track 16 displays the integrated predicted relative flow (production potential) profile from the permeability (hydraulic conductivity) logs that mimics a flow meter (spinner) acquired under flowing conditions:

- predicted relative water flow profile derived from the k-Lambda water permeability log (long-dashed blue), displayed on a unitless linear scale of 0 to 1 relative volumetric flow rate (ratio of flow rate to flow rate);
- predicted relative water flow profile derived from the ELAN water permeability log (bold solid blue curve), displayed on a unitless linear scale of 0 to 1 relative volumetric flow rate;
- relative integrated intrinsic permeability profile derived by integrating the k-Lambda intrinsic permeability log (dashed-dotted red), displayed on a unitless linear scale of 0 to 1;
- relative integrated intrinsic permeability profile derived by integrating the ELAN intrinsic permeability log (dashed red), displayed on a unitless linear scale of 0 to 1; and

- predicted hypothetical well water flow versus depth profile for the entire log interval (dotted green), assuming a well radius of 4 in., entirely open to flow, and pumping is occurring under steady state conditions with a drawdown of 25 ft (incremental flow computed using the Thiem steady state flow equation), derived from the k-Lambda water permeability log (bold solid blue), displayed on a scale of 0 to 100,000 gallons per day (gal/day).

4.6.13 Track 17—Summary Logs

Track 18, the second track from the right, displays several summary logs that describe the fluid and air-filled volume measured by the geophysical tools:

- optimized estimate of total volume fraction water from the ELAN analysis (solid blue curve and blue plus cyan area shading);
- optimized estimate of volume fraction moveable water (non-clay bound moveable water-filled porosity) from the ELAN analysis (dashed cyan curve and cyan area shading);
- optimized estimate of total volume fraction of air-filled porosity from the ELAN analysis (solid red curve and dotted red area shading);and
- estimate of bulk volumetric water content from the ECS tool (thin dashed dark blue curve).

The porosity and volumetric water content scales are from 0 to 0.6 total volume fraction, left to right.

4.6.14 Track 18—Depth

The final track on the right, the same as the first track on the left, displays the depth below ground surface in units of feet, as measured by the geophysical logging system during the HNGS logging run.

1.0 REFERENCES

The following list includes all documents cited in this report. Parenthetical information following each reference provides the author(s), publication date, and ER ID. This information is also included in text citations. ER IDs are assigned by the Environmental Programs Directorate's Records Processing Facility (RPF) and are used to locate the document at the RPF and, where applicable, in the master reference set.

Copies of the master reference set are maintained at the NMED Hazardous Waste Bureau and the Directorate. The set was developed to ensure that the administrative authority has all material needed to review this document, and it is updated with every document submitted to the administrative authority. Documents previously submitted to the administrative authority are not included

Mayer, C., and A. Sibbit, September 21–24, 1980. "Global, A New Approach to Computer-Processed Log Interpretation," 55th Annual Fall Technical Conference and Exhibition of the Society of Petroleum Engineers of AIME, September 21–24, 1980, Dallas, Texas. (Mayer and Sibbit 1980, 103867)

Quirein, J., S. Kimminau, J. LaVigne, J. Singer, and F. Wendel, June 9–13, 1986. "A Coherent Framework for Developing and Applying Multiple Formation Evaluation Models," SPWLA 27th Annual Logging Symposium, June 9–13, 1986, Schlumberger Well Services, Houston, Texas. (Quirein et al. 1986, 098043)

Integrated Wireline Log Well Montage

Processed Advanced Cased Hole Geophysical Logs

Using the following logs: TLD*, CNT-G* HNGS* ECS* SGT*

COMPANY: Tetramer PMC (drilling contractor for LANL)
WELL: TA-49-1
FIELD: LANL
STATE/PROV: NEW MEXICO
COUNTRY: USA
Date Logged: 9-Dec-2008
Date Processed: May-2009
Elevations: K.B. NA D.F. NA G.L. NA
API Number:
Job Number:
Well Location:

GEOLOPAME PROCESSED INTERPRETATION

FOLD HERE The well name, location and borehole reference data were furnished by the customer

All interpretations or opinions based on inferences from electrical or other measurements and we cannot, and do not guarantee the accuracy or correctness of any interpretations, and we do not, except in the case gross or wilful misconduct on our part, be liable or responsible for any loss, costs, damages or expenses incurred or sustained by anyone resulting from any interpretations made by any of our officers, agents or employees. These interpretations are also subject to Clause 4 of our General Terms and Conditions as set out in our Price Schedule.

GP Vers.: 17C0-154 Process Date: May-2009 Center: SWS Sacramento Baseline: GF4.2 Log Analyst: N. CLAYTON

Mud and Borehole Measurements:

Rm @ Measured Temperature: NA	BHT: NA	Bitsize: 12.75 in	
Rmf @ Measured Temperature: NA	Type Fluid in Hole: AirWater	FGM:	
Rmc @ Measured Temperature: NA	Mud density: 0/8.34 lbm/gal	FGM:	

Remarks:

Depth reference is ground surface.
Well contained one or more strings of casing (casing advance) during logging.
Well water level at around 880' at time of logging.
ELANP performed without porosity or water saturation constraints.
Interpretation should account for well conditions.

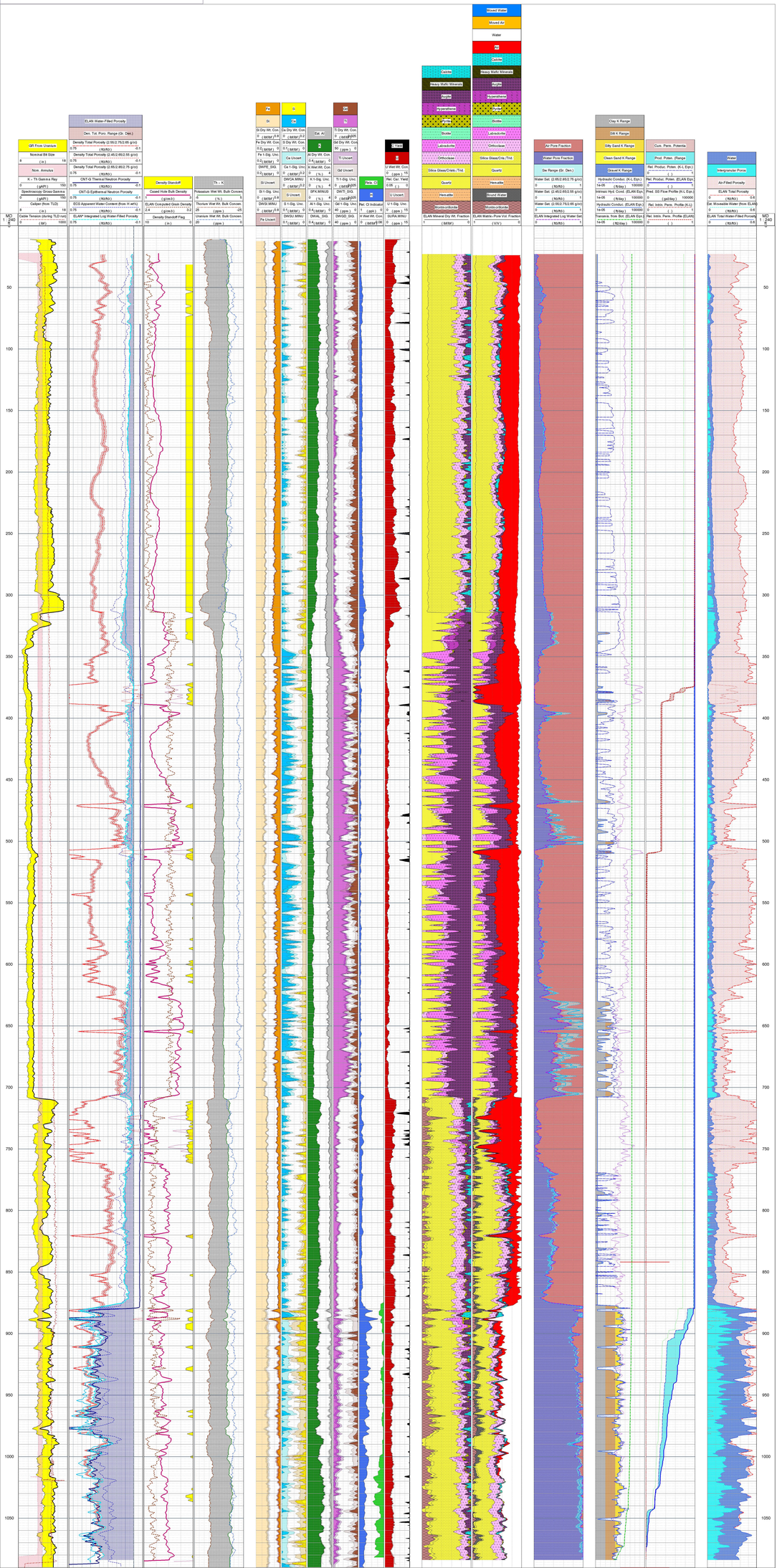

Schlumberger

ELAN^Ø Geophysical Log Integrated Analysis

Optimized Interval + Know Volume Model

COMPANY	TEXACO EXPTNC		
WELL	Fr-44		
FIELD	LUNA		
State	NEW MEXICO		
COUNTRY			
Date Processed	May 2009	Date Logged	9-Dec-2008
Job Number	Processed at	SWS Beaumont	
Well Location			
Latitude	Longitude		
Elevations: KB	DF	GL	

Depth of signature shifting: Real-time shifts applied to raw data operations

FIELD HERE

The well heavy borehole and borehole alliance data are furnished by the curtesy of.

All interpretations are opinions based on inferences from electrical or other measurements and we cannot, and do not guarantee the accuracy or correctness of any interpretation, and we shall not be liable or responsible for any loss or gains or actual negligence on our part, but liable or responsible only for any loss, costs, damages or expense incurred or sustained by anyone resulting from any interpretation made by any of our officers, agents or employees. These interpretations are subject to our standard terms and conditions as set out in our current Price Schedule.

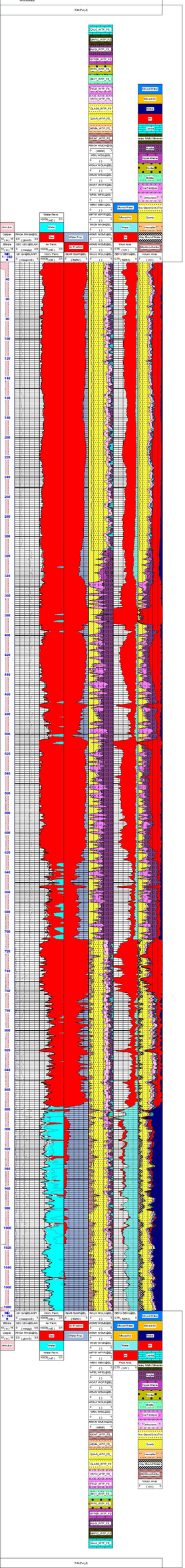
PHIPLIS
CALC_WTSP_P2
WBRC_WTSP_P2
ROX_WTSP_P2
PHIEW_WTSP_P2
PHIEW_WTSP_P2
PHIEW